Reactions of Tri-tert-Butylphosphatetrahedrane as a Spring-Loaded Phosphinidene Synthon Featuring Nickel-Catalyzed Transfer to Unactivated Alkenes

Martin-Louis Y. Riu, André K. Eckhardt, and Christopher C. Cummins*

Department of Chemistry, Massachusetts Institute of Technology, Cambridge, MA 02139, USA

E-mail: ccummins@mit.edu

Table of Contents

S.1 Synthetic Details **S.3**

S.1.1 General Information S.3

S.1.2 Synthesis of **3** from **1** and $PhC(N^tBu)_2SiN(SiMe_3)_2$ S.4

S.1.3 Synthesis of **5** from **1** and Ph_3PCH_2 . . . . . S.7

S.1.3.1 Generation and NMR Characterization of Phosphaalkene **4** S.10

S.1.3.2 Treatment of **1** with $Ph_3P{=}CMe_2$ S.15

S.1.4 Synthesis of **6**-Ph from **1**, $Ni(COD)_2$, $^iPr_3P$, and Styrene S.16

S.1.4.1 Ligand Screening S.18

S.1.4.2 Quantification of Conversion using an Internal Standard S.24

S.1.4.3 Catalysis using Ni($^{4\text{-tBu}}$stb)$_3$ as the Ni(0) Source S.25
S.1.4.4 Monitoring Phosphinidene Transfer by Low Temperature NMR Spectroscopy S.27
S.1.4.5 Treatment of **1** with ^{i}Pr$_3$P, and Styrene S.29
S.1.4.6 *cis*-β-Deuterostyrene as a Substrate in Catalysis S.29
S.1.5 Synthesis of **6**-H from **1**, Ni(COD)$_2$, ^{i}Pr$_3$P, and Ethylene S.32
S.1.6 Synthesis of **6**-^{t}Bu from **1**, Ni(COD)$_2$, ^{i}Pr$_3$P, and Neohexene S.35
S.1.7 Synthesis of **7** from **1**, Ni(COD)$_2$, ^{i}Pr$_3$P, and 1,3-Cyclohexadiene S.42
S.1.7.1 Thermal Stability of **7** in Mesitylene S.45
S.1.8 Attempted Phosphinidene Transfer to Benzene S.46
S.1.9 Attempted Phosphinidene Transfer to Ferrocene S.47
S.1.10 Attempted Phosphinidene Transfer to 1,1-Difluoro-2-vinyl-cyclopropane (Radical Clock) S.48
S.1.11 Generation of Phosphirane and Isolation of **8**·W(CO)$_5$ S.50
S.1.11.1 Preparation of (THF)W(CO)$_5$ S.54
S.1.11.2 Quantification of Conversion to **8** using an Internal Standard S.54
S.1.12 Treatment of **6**-Ph with HOTf S.57
S.1.13 Synthesis of [^{t}Bu$_3$C$_3$]OTf S.59

S.2 X-Ray Diffraction Studies **S.61**

S.3 Computational Details **S.65**
S.3.1 Bonding Analysis for **3** S.65
S.3.2 Mechanism for the Formation of **6**-H S.66

References **S.68**

S.1 Synthetic Details

S.1.1 General Information

Except as otherwise noted, all manipulations were performed in a Vacuum Atmospheres model MO-40M glovebox under an inert atmosphere of purified N_2. All solvents were obtained anhydrous and oxygen-free by bubble degassing (Ar), purified by passage through columns of alumina using a solvent purification system (Pure Process Technology, Nashua, NH),[1] and stored over 4 Å molecular sieves.[2] Deuterated solvents were purchased from Cambridge Isotope Labs, then degassed and stored over 4 Å molecular sieves for at least 48 h prior to use. Charcoal, Celite (EM Science), and 4 Å molecular sieves were dried by heating above 200 °C under dynamic vacuum for at least 48 h prior to use. All glassware was dried in an oven for at least two hours at temperatures greater than 150 °C. (^{t}BuC)$_3$P (**1**),[3] *cis*-β-deuterostyrene,[9] $Ph_3P{=}CMe_2$,[4] PhC(N^{t}Bu)$_2$SiN(SiMe$_3$)$_2$ (**2**),[5] Ph_3PCH_2,[6] 1,3-bis(2,6-bis(diphenylmethyl)-4-methylphenyl)imidazolium chloride (IPr*·HCl),[7] and 1,3-bis(2,6-bis(diphenylmethyl)-4-methylphenyl)imidazo-2-ylidene (IPr*)[8] were prepared according to literature procedures. Prior to use, styrene (Sigma-Aldrich) was degassed and purified according to a literature procedure.[9] Neohexene (Sigma-Aldrich), 1,3-cyclohexadiene (Sigma-Aldrich), and 1,1-difluoro-2-vinylcyclopropane (Sigma-Aldrich) were degassed by three freeze-pump-thaw cycles and stored over 4 Å molecular sieves for at least 48 h and ferrocene (Strem) was sublimed prior to use. Triisopropylphosphine (Strem), bis(cyclooctadiene)nickel(0) (Strem), tris(*trans*-1,2-bis(4-*tert*-butylphenyl)ethene)nickel(0) (Ni($^{4\text{-tBu}}$stb)$_3$, Strem), triflic acid (Strem), tungsten hexacarbonyl (Strem), trimethylsilyl triflate (Sigma-Aldrich), ethylene (Airgas), tricyclohexylphosphine (Sigma-Aldrich), triethylphosphine (Sigma-Aldrich), (±)-2,2'-bis(diphenylphosphino)-1,1'-binaphthyl (Strem), tri-*tert*-butylphosphine (Sigma-Aldrich), triphenylphosphine (Sigma-Aldrich), 1,2-bis(diphenylphosphino)ethane (Strem), and 1,2-bis(dicyclohexylphosphino)ethane (Strem) were used as received.

NMR spectra were obtained on a Bruker Avance-III HD Nanobay spectrometer operating at 400.09 MHz equipped with a 5mm liquid-nitrogen cooled Prodigy broad band observe cryoprobe or on a Bruker Avance Neo spectrometer operating at 500.34 MHz equipped with a 5mm liquid-nitrogen cooled Prodigy broad band observe cryoprobe. ^{1}H and ^{13}C NMR spectra were referenced internally to residual solvent signals.[10] ^{31}P NMR spectra were externally referenced to 85% H_3PO_4 (0 ppm). Elemental combustion analyses were performed by Midwest Micro Laboratories (Indianapolis, IN, USA).

High resolution mass spectral (HRMS) data were collected using a Jeol AccuTOF 4G LC-Plus mass spectrometer equipped with an Ion-Sense DART source. Data were calibrated to a sample of PEG-600 and were collected in positive-ion mode. Samples were prepared in THF or benzene (ca. 10 μM concentration) and were briefly exposed to air (<5 s) before being placed in front of the DART source.

Photochemical reactions were performed using a Rayonet photochemical reactor RPR-200 (Southern New England Ultra Violet Company) loaded with 16 RPR-2537A lamps, each emitting ca. 35 W at 253.7 nm.

S.1.2 Synthesis of 3 from 1 and $PhC(N^tBu)_2SiN(SiMe_3)_2$

To a stirring solution of **1** (35 mg, 0.15 mmol, 1.0 equiv) in benzene (1 mL) was added $PhC(N^tBu)_2SiN(SiMe_3)_2$ (**2**, 63 mg, 0.15 mmol, 1.0 equiv) portionwise. After 24 h, all volatile materials were removed under reduced pressure and the resulting red solids were taken up in pentane (ca. 2 mL). The solution was filtered through a pipette containing a plug of glass microfiber filter paper. After the filtrate was concentrated to ca. 0.5 mL under reduced pressure, it was placed in a −30 °C freezer for crystallization. Phosphasilene **3** was isolated as a red, crystalline solid (71 mg, 0.11 mmol, 72%). Melting point: 154-156 °C. Elem. Anal. Calc'd(found) for $C_{36}H_{68}N_3PSi_3$: C 65.69(65.80), H 10.41(10.38), N 6.38(6.38). ^{1}H NMR (500 MHz, benzene-d_6, 25 °C, Fig. S.1) δ 7.47 (d, J = 8.5 Hz, 1H), 7.44 (d, J = 7.7 Hz, 1H), 7.06-6.97 (m, 2H), 6.94 (t, J = 7.2 Hz, 1H), 1.55 (s, 18H), 1.36 (s, 27H), 0.95

(d, $^{4}J_{\mathrm{PH}}$ = 3.5 Hz, 9H), 0.51 (s, 9H) ppm. ^{13}C{^{1}H} NMR (126 MHz, benzene-d_6, 25 °C, Fig. S.2 and S.3) δ 172.4, 131.9 (d, $^{2}J_{\mathrm{PC}}$ = 8.1 Hz), 131.7, 130.3, 128.4, 128.4, 55.2, 48.0 (d, $^{1}J_{\mathrm{PC}}$ = 85.3 Hz), 38.8 (d, $^{2}J_{\mathrm{PC}}$ = 2.6 Hz), 32.6, 32.4, 31.7 (d, $^{3}J_{\mathrm{PC}}$ = 2.8 Hz), 31.5, 9.8 (d, $^{4}J_{\mathrm{PC}}$ = 23.4 Hz, $^{1}J_{\mathrm{SiC}}$ = 82.3 Hz), 7.4 ($^{1}J_{\mathrm{SiC}}$ = 56.4 Hz) ppm. ^{31}P{^{1}H} NMR (203 MHz, benzene-d_6, 25 °C, Fig. S.4) δ −182.3 ($^{1}J_{\mathrm{PSi}}$ = 240.4 Hz) ppm.

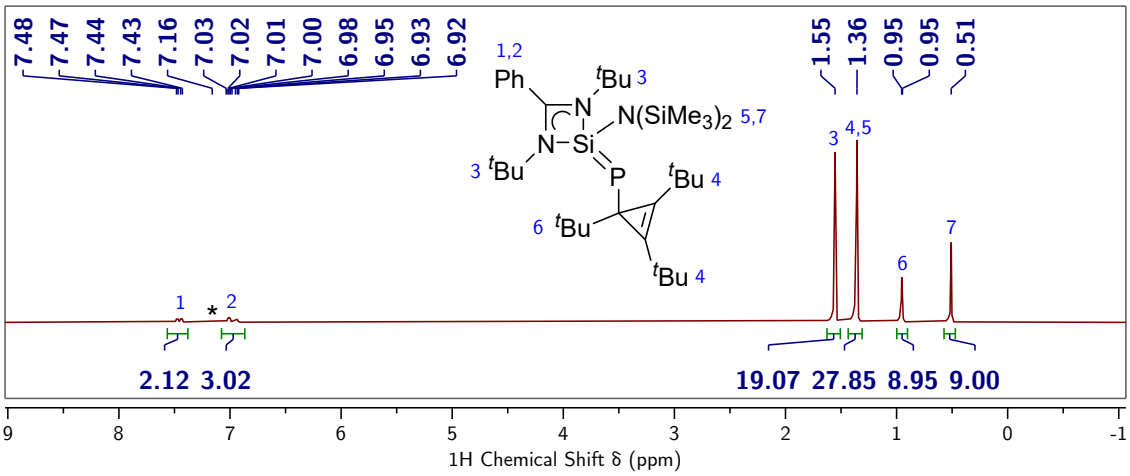

Figure S.1: ^{1}H NMR (500 MHz, benzene-d_6, 25 °C) spectrum of **3**. * marks benzene-d_6.

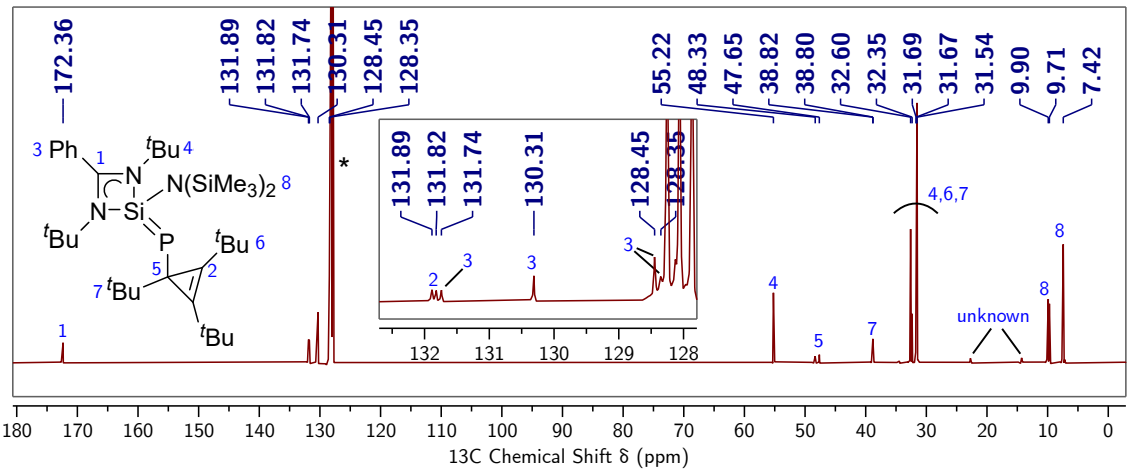

Figure S.2: ^{13}C{^{1}H} NMR (126 MHz, benzene-d_6, 25 °C) spectrum of **3**. Inset shows a zoomed-in region of the NMR spectrum. * marks benzene-d_6.

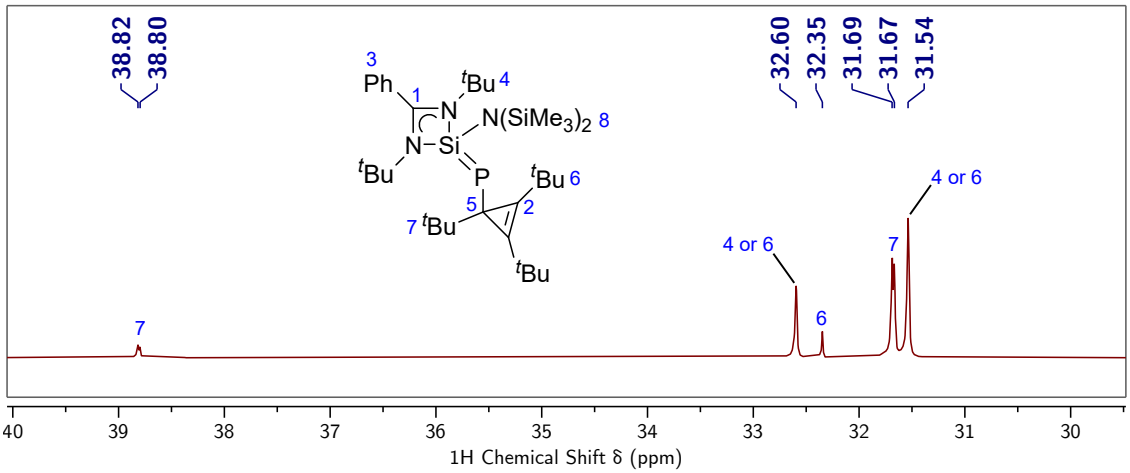

Figure S.3: $^{13}C\{^1H\}$ NMR (126 MHz, benzene-d_6, 25 °C) spectrum of **3**.

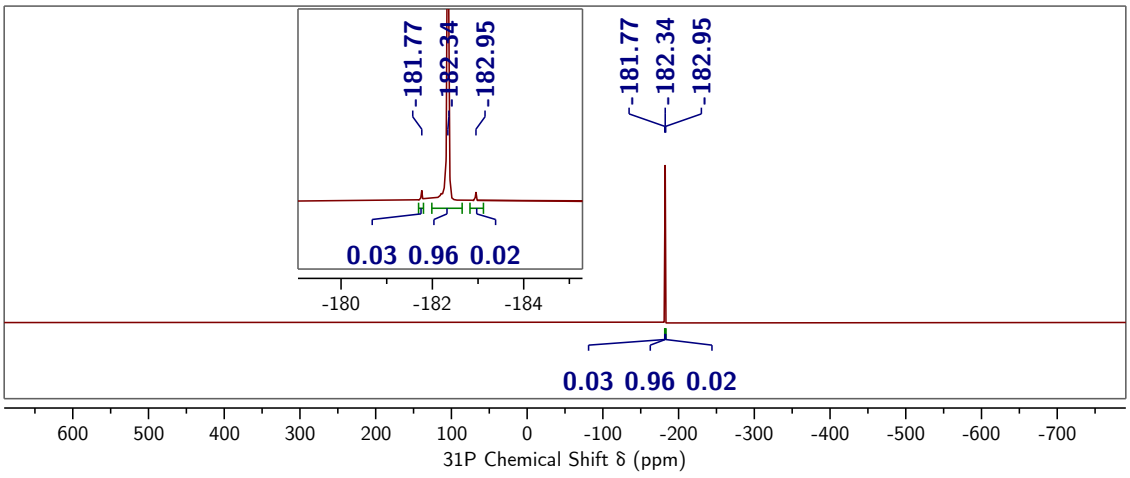

Figure S.4: $^{31}P\{^1H\}$ NMR (203 MHz, benzene-d_6, 25 °C) spectrum of **3**. Inset shows a zoomed-in region of the NMR spectrum.

S.1.3 Synthesis of 5 from 1 and Ph_3PCH_2

Compound **1** (0.100 g, 0.420 mmol, 2.0 equiv) and Ph_3PCH_2 (0.058 g, 0.21 mmol, 1.0 equiv) were dissolved in THF (5 mL) and the resulting solution was transferred to a Schlenk tube (10 mL) containing a stir bar. The tube was sealed, removed from the glovebox, and placed in a preheated 80 °C oil bath for 48 h. The orange solution was brought into the glovebox where all volatile materials were removed under reduced pressure. Pentane (2 mL) was added to the resulting orange residue and the solution was passed through a medium sintered frit (15 mL) containing a one-inch plug of silica. The plug was washed with additional pentane (4 mL) and the combined colorless filtrates were brought to constant mass under reduced pressure. Diphosphirane **5** was isolated as a colorless solid (0.052 g, 0.11 mmol, 50%). The NMR assignments for **5** were made using 2D NMR techniques ^{1}H,^{13}C HSQC and ^{1}H,^{13}C HMBC (Fig. S.8 and S.9, respectively). While **5** was not detected, $[^t Bu_3C_3]^+$ ($[M]^+$ Calc'd for $[C_{15}H_{27}]^+$ 207.211276; Found 207.20860) was observed by DART HRMS. Crystals for elemental analysis were grown from tetramethylsilane. Elem. Anal. Calc'd(found) for $C_{31}H_{56}P_2$: C 75.87(75.43), H 11.50(11.49). ^{1}H NMR (400 MHz, benzene-d_6, 25 °C, Fig. S.5) δ 1.30 (s, 18H), 1.25 (s, 18H), 1.17 (s, 18H), 0.64 (dd, $^2J_{PH}$ = 12.6, 10.0 Hz, 2H) ppm. ^{13}C{^{1}H} NMR (101 MHz, benzene-d_6, 25 °C, Fig. S.6) δ 125.91 (t, J_{PC} = 3.3 Hz), 125.32, 44.65 (t, J_{PC} = 3.3 Hz), 37.41 (t, J_{PC} = 16.4 Hz), 31.26, 30.62 (t, J_{PC} = 3.8 Hz), 30.27, 29.98, 8.33 (t, $^1J_{PC}$ = 48.3 Hz) ppm. ^{31}P{^{1}H} NMR (162 MHz, benzene-d_6, 25 °C, Fig. S.7) δ −175.2 ppm.

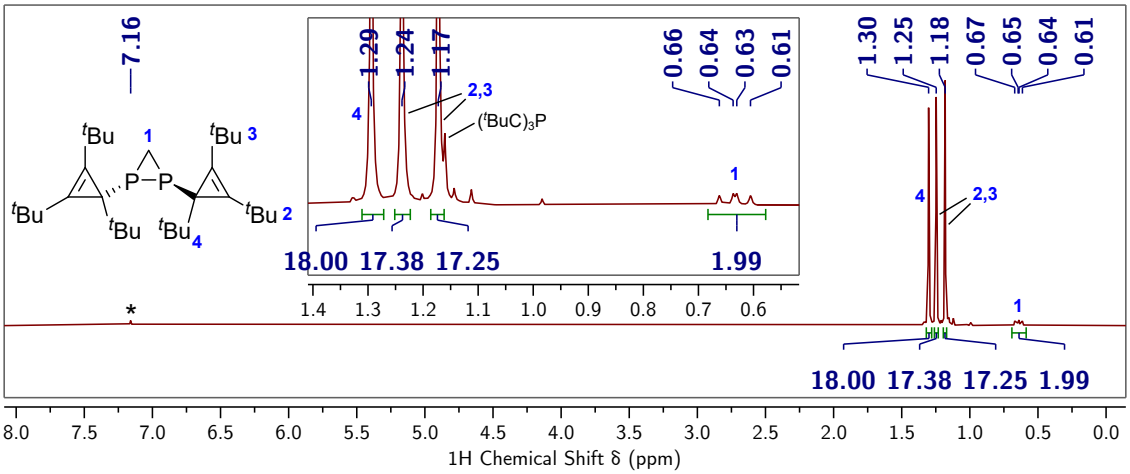

Figure S.5: ^{1}H NMR (400 MHz, benzene-d_6, 25 °C) spectrum of **5** and trace **1**. Inset shows a zoomed-in region of the NMR spectrum. * marks benzene-d_6.

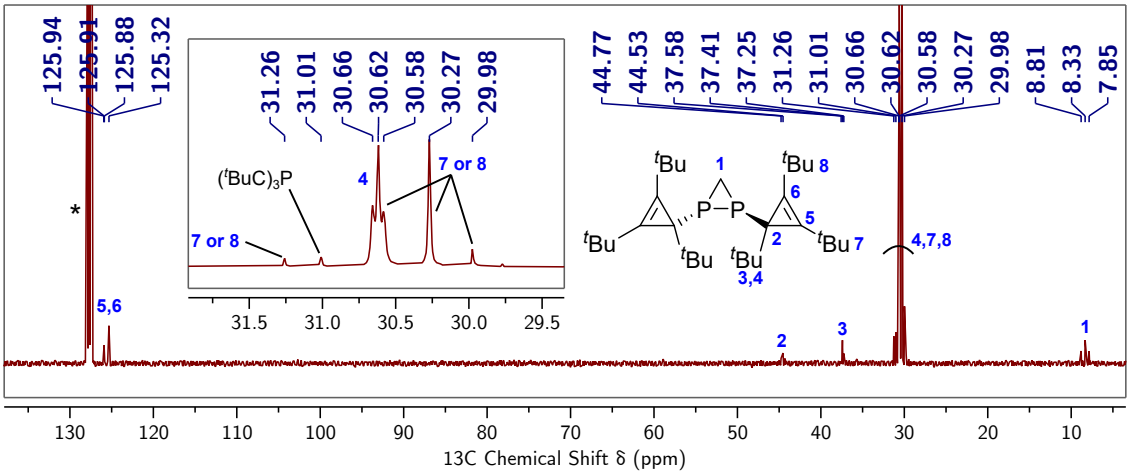

Figure S.6: ^{13}C{^{1}H} NMR (101 MHz, benzene-d_6, 25 °C) spectrum of **5** and trace **1**. Inset shows a zoomed-in region of the NMR spectrum. * marks benzene-d_6.

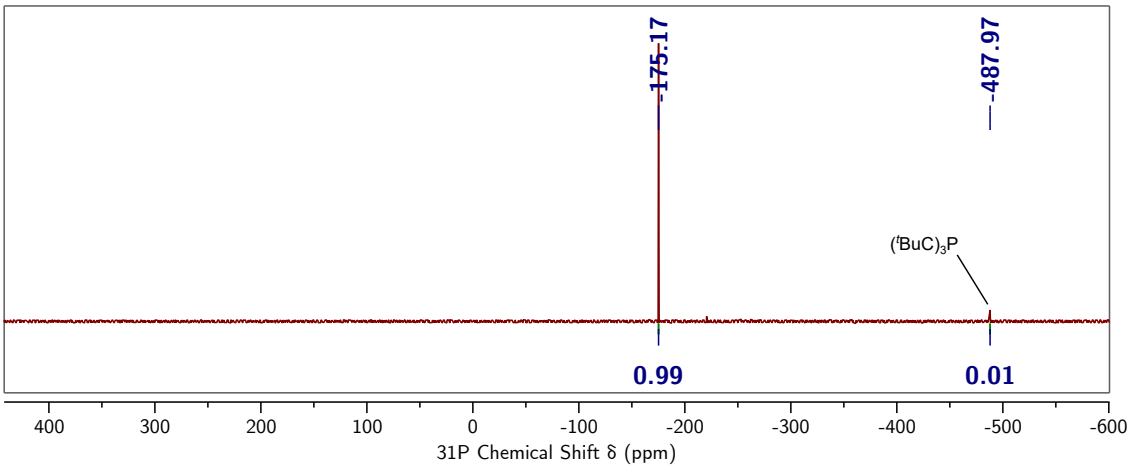

Figure S.7: ^{31}P{^{1}H} NMR (162 MHz, benzene-d_6, 25 °C) spectrum of **5** and trace **1**.

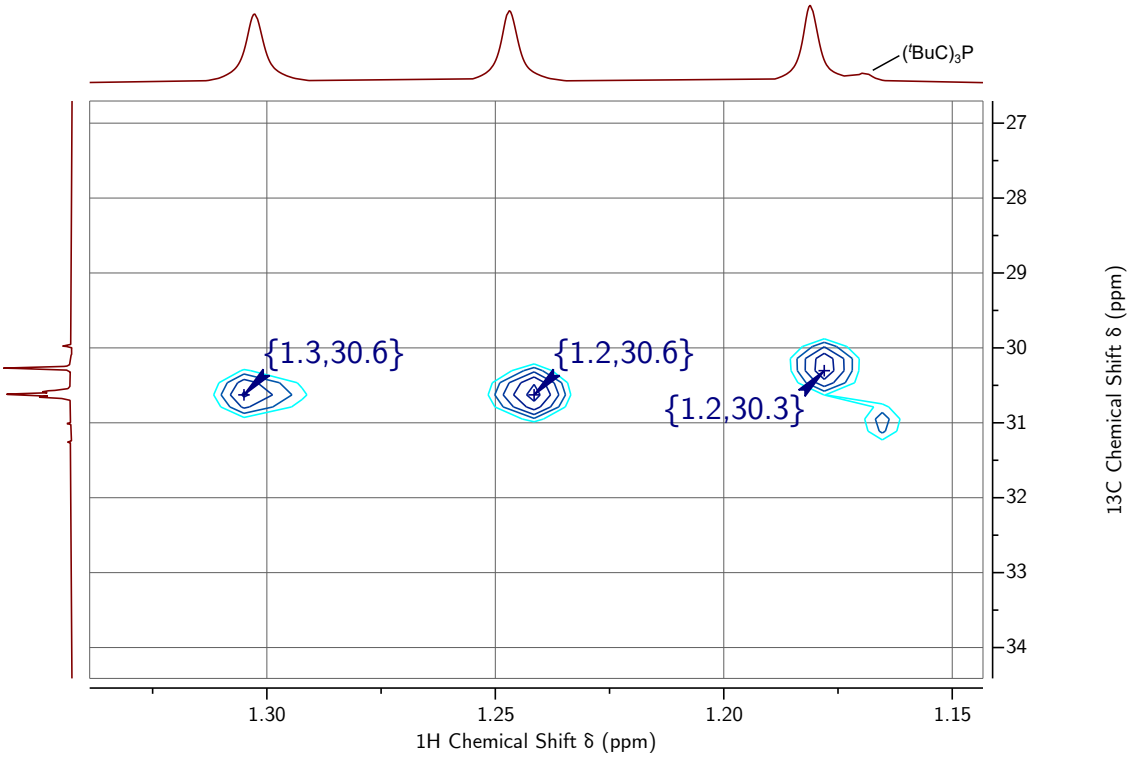

Figure S.8: ^{1}H, ^{13}C-HSQC NMR (400 MHz, benzene-d_6, 25 °C) spectrum of **5**.

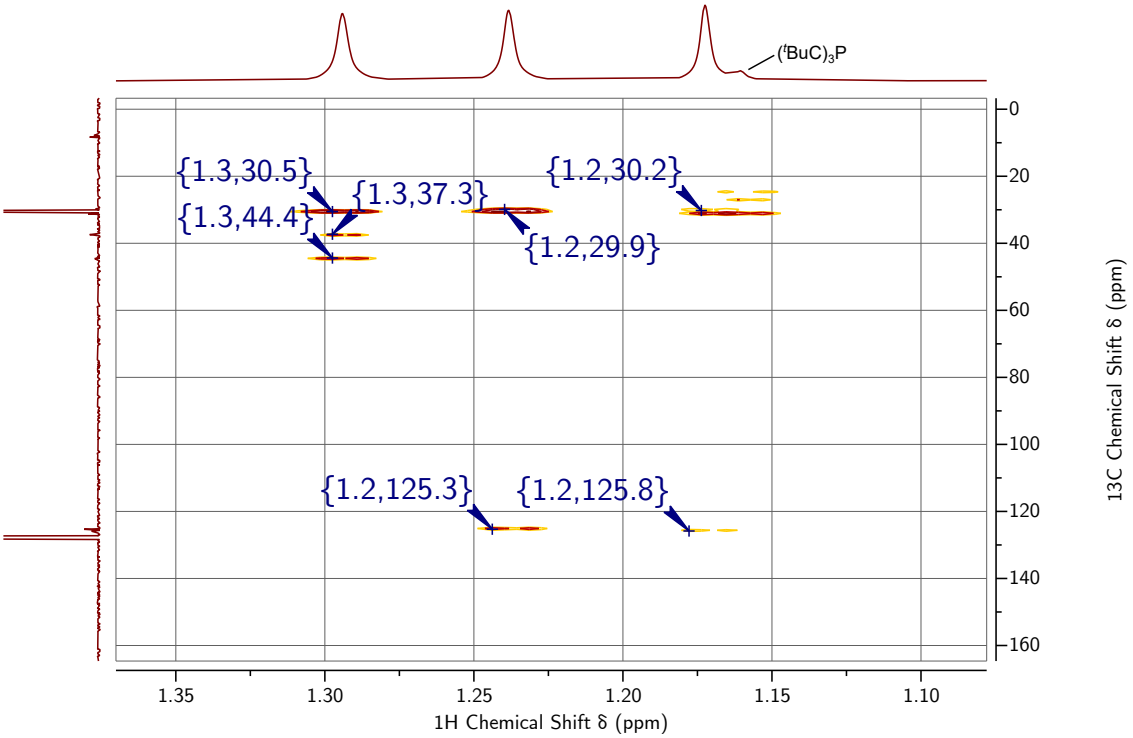

Figure S.9: ^{1}H, ^{13}C-HMBC NMR (400 MHz, benzene-d_6, 25 °C) spectrum of **5**.

S.1.3.1 Generation and NMR Characterization of Phosphaalkene 4

Compound **1** (0.017 g, 0.072 mmol, 2.0 equiv) and Ph_3PCH_2 (0.010 g, 0.036 mmol, 1.0 equiv) were dissolved in benzene-d_6 (0.7 mL) and the resulting solution was transferred to a J Young tube. The tube was removed from the glovebox and placed in a preheated 80 °C oil bath for 45 min. NMR analysis of the resulting orange solution revealed a mixture of **4**, **5**, **1**, and unidentified byproducts (Fig. S.10-S.13). NMR assignments for **4** were made using 2D NMR techniques ^{1}H,^{31}P-HMQC, ^{1}H,^{13}C HSQC, and ^{1}H,^{13}C HMBC (Fig. S.14-S.17). ^{1}H NMR (500 MHz, benzene-d_6, 25 °C, Fig. S.10) δ 7.66 (dd, J = 28.2, 5.0 Hz, 1H), 7.44 (d, J = 31.8, 5.1 Hz, 1H), 1.23 (s, 9H), 1.14 (s, 18H) ppm. ^{13}C{^{1}H} NMR (126 MHz, benzene-d_6, 25 °C, Fig. S.11 and S.12) δ 154.94 (d, $^1J_{PC}$ = 34.8 Hz), 121.63 (d, $^2J_{PC}$ = 34.8 Hz), 50.38 (d, $^1J_{PC}$ = 56.6 Hz), 36.22 (d, $^2J_{PC}$ = 29.4 Hz), 31.72 (d, $^3J_{PC}$ = 17.8 Hz), 31.53, 30.37 (d, $^3J_{PC}$ = 1.7 Hz). ^{31}P{^{1}H} NMR (203 MHz, benzene-d_6, 25 °C, Fig. S.13) δ 343.15 (dd, $^2J_{PH}$ = 31.8, 28.2 Hz) ppm.

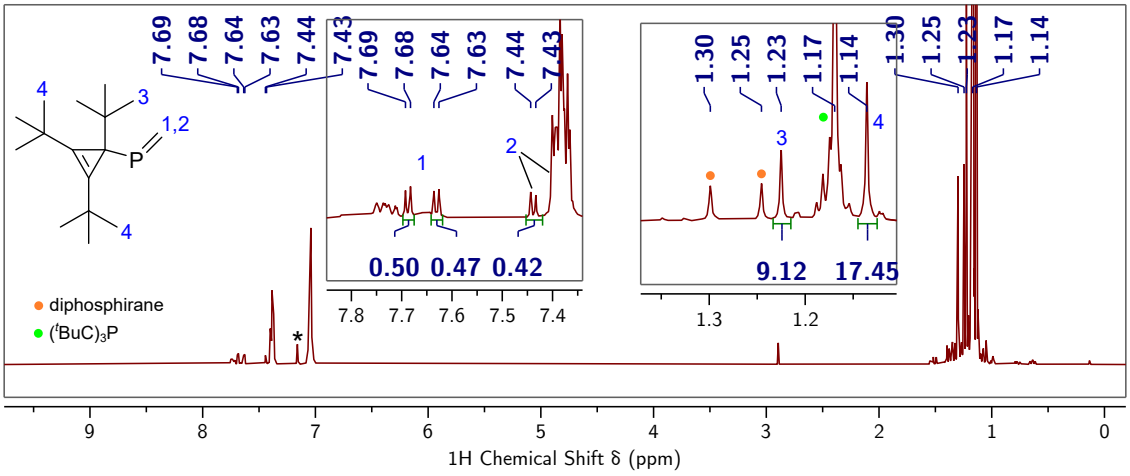

Figure S.10: ^{1}H NMR (500 MHz, benzene-d_6, 25 °C) spectrum of **4** and trace **1**. Insets show zoomed-in regions of the NMR spectrum. * marks benzene-d_6.

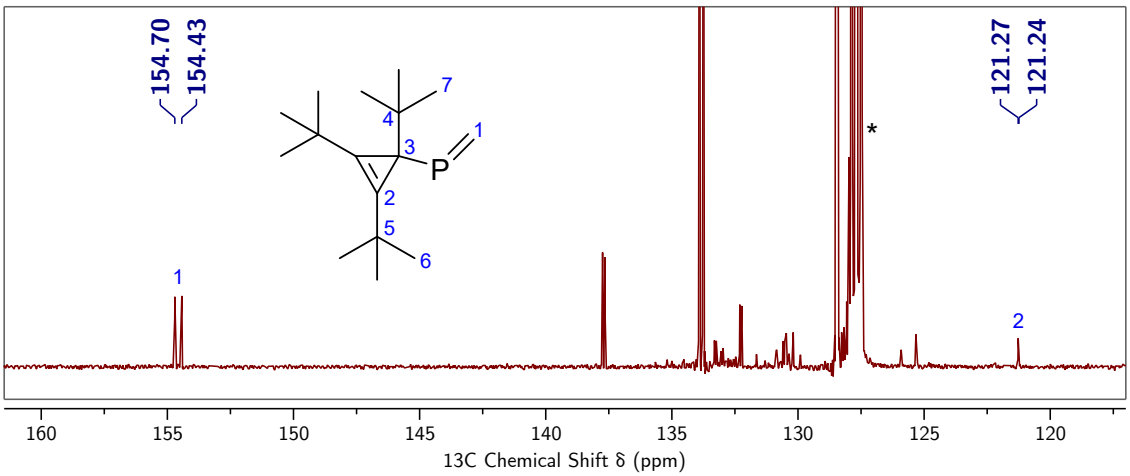

Figure S.11: $^{13}C\{^1H\}$ NMR (126 MHz, benzene-d_6, 25 °C) spectrum of **4**. * marks benzene-d_6.

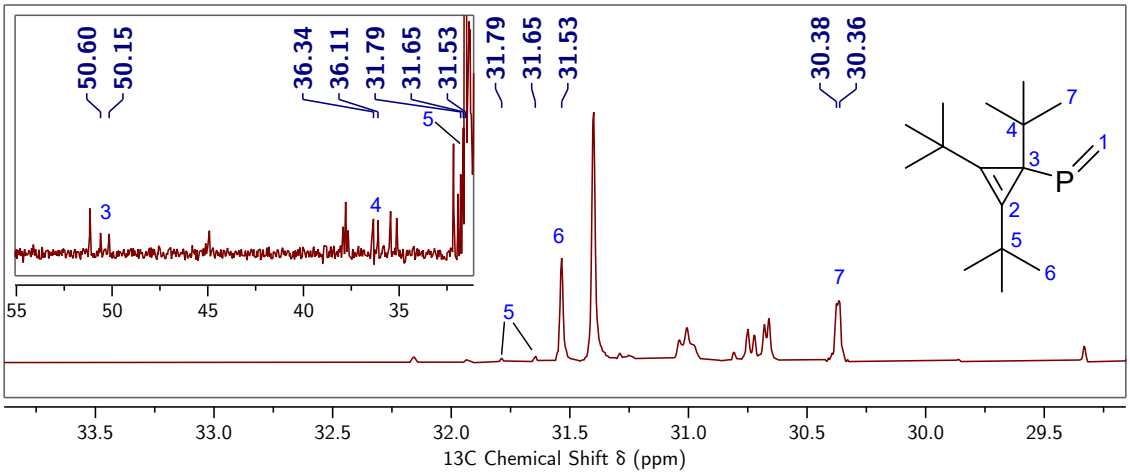

Figure S.12: $^{13}C\{^1H\}$ NMR (126 MHz, benzene-d_6, 25 °C) spectrum of **4**. Inset shows a zoomed-in region of the NMR spectrum.

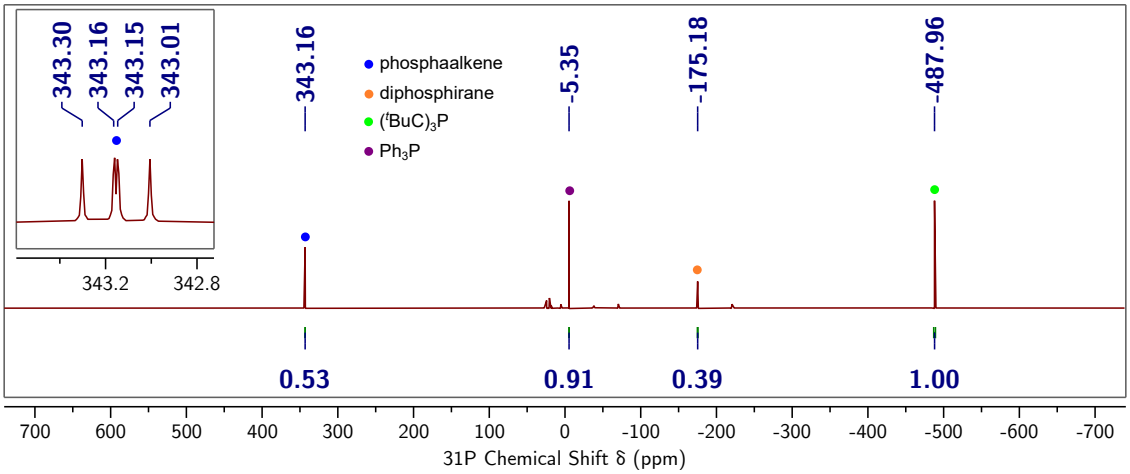

Figure S.13: $^{31}P\{^{1}H\}$ NMR (203 MHz, benzene-d_6, 25 °C) spectrum of **4**. Inset shows the corresponding proton-coupled ^{31}P NMR spectrum.

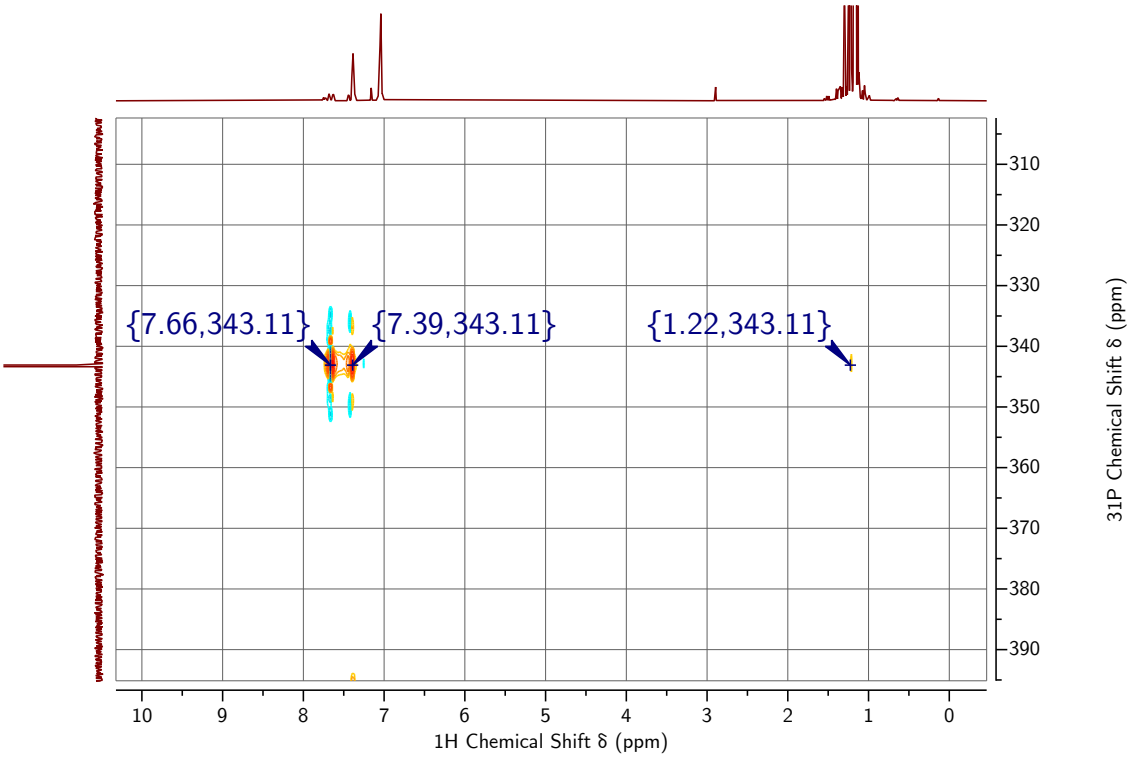

Figure S.14: ^{1}H, ^{31}P-HMQC NMR (500 MHz, benzene-d_6, 25 °C) spectrum of **4**.

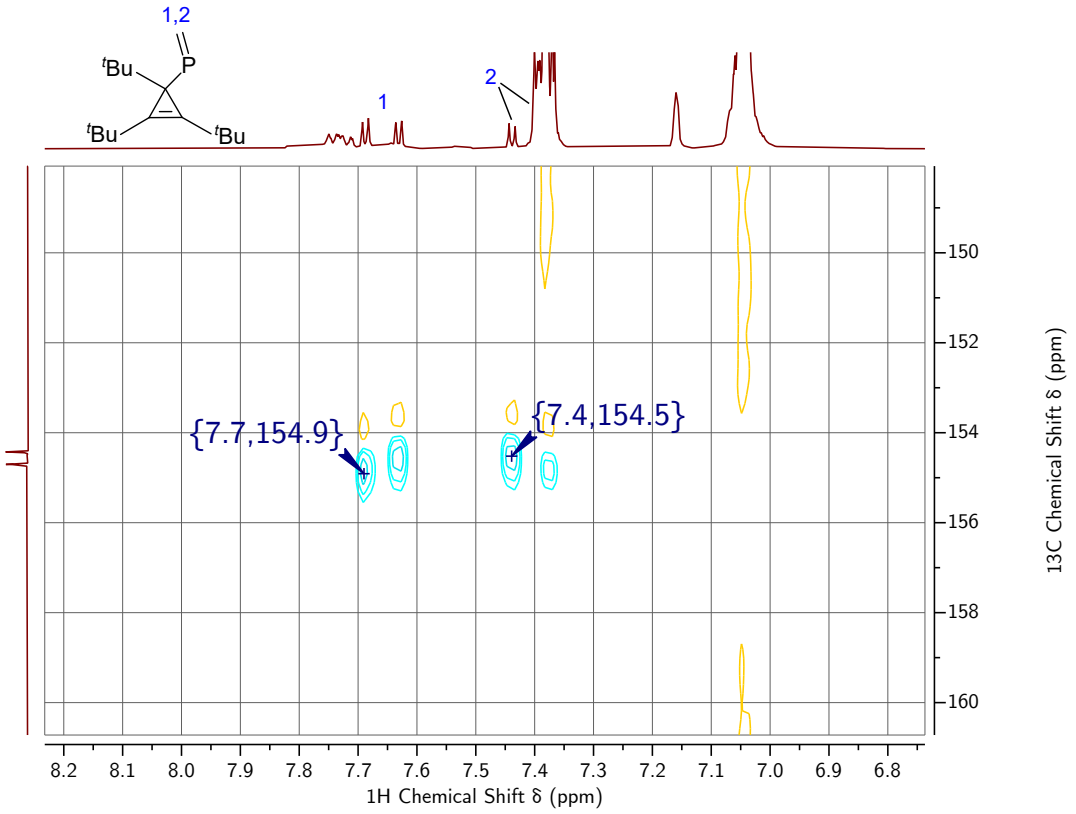

Figure S.15: ^{1}H, ^{13}C-HSQC NMR (500 MHz, benzene-d_6, 25 °C) spectrum of **4**.

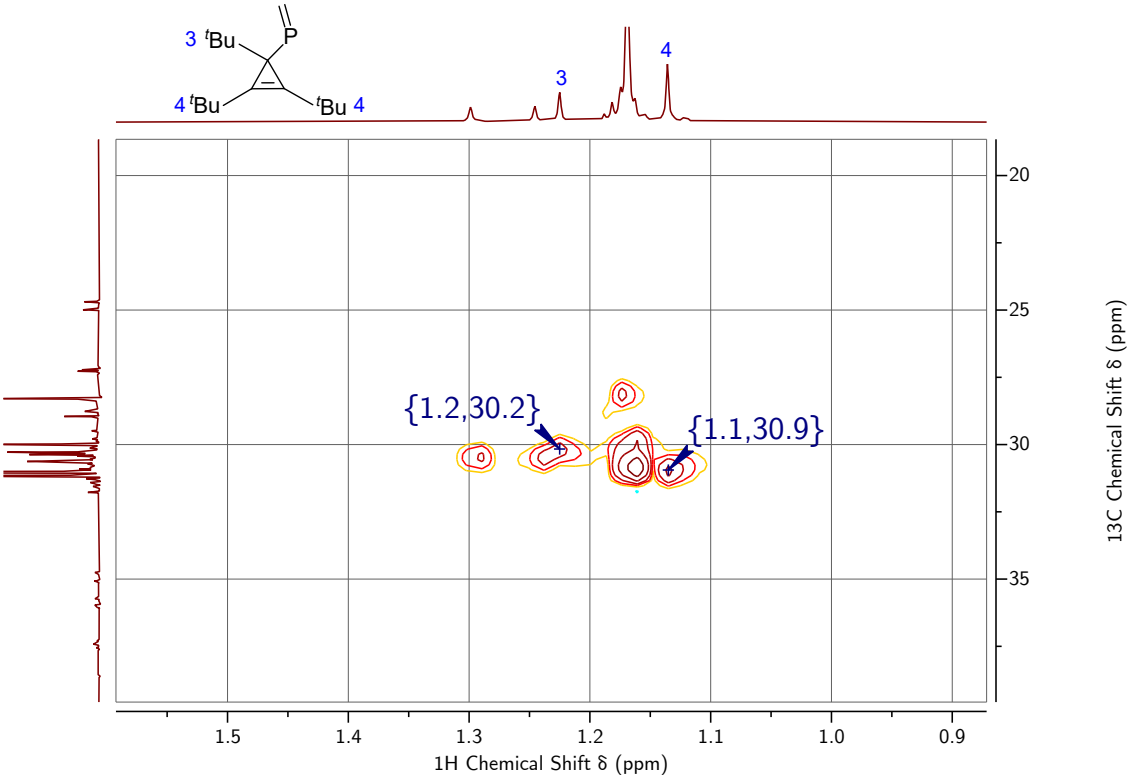

Figure S.16: ^{1}H, ^{13}C-HSQC NMR (500 MHz, benzene-d_6, 25 °C) spectrum of **4**.

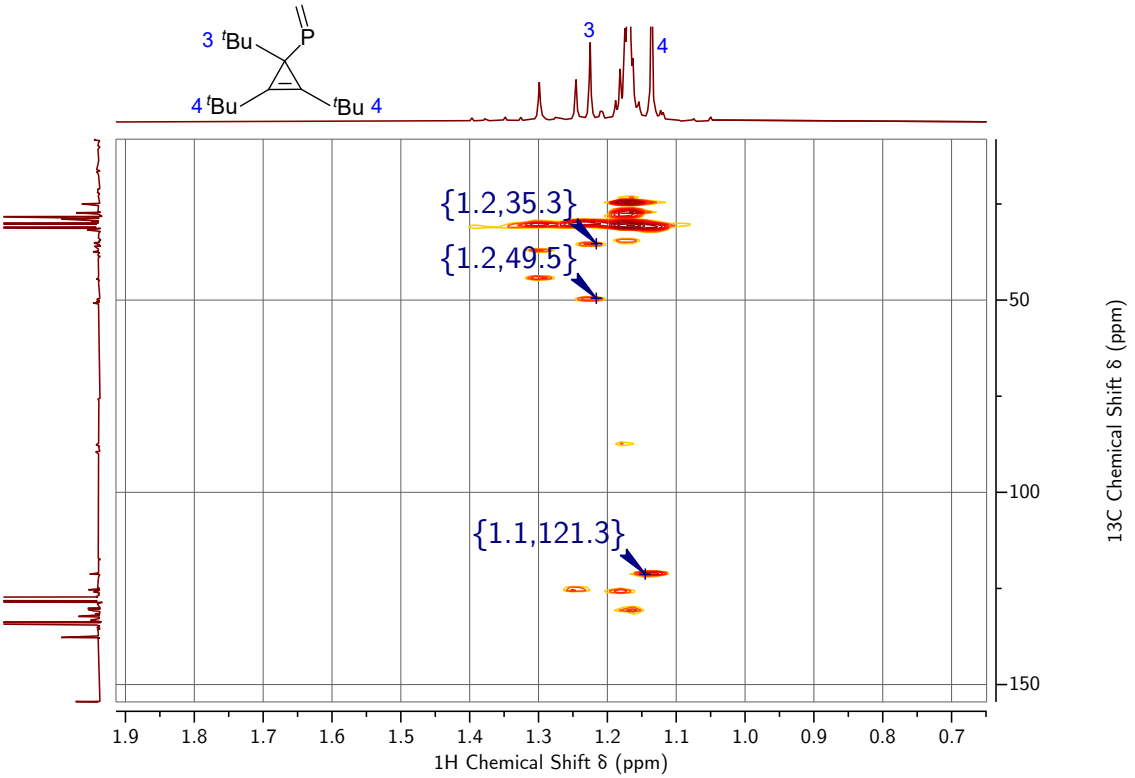

Figure S.17: ^{1}H, ^{13}C-HMBC NMR (500 MHz, benzene-d_6, 25 °C) spectrum of **4**.

S.1.3.2 Treatment of 1 with $Ph_3P{=}CMe_2$

To a THF (0.7 mL) solution of **1** (10 mg, 0.042 mmol, 1.0 equiv) was added $Ph_3P{=}CMe_2$ (13 mg, 0.042 mmol, 1.0 equiv). The solution was then transferred to a J Young tube and placed in a preheated 80 °C oil bath for 26 h. Afterwards, the tube was removed from the bath and its contents were analyzed by $^{31}P\{^1H\}$ NMR spectroscopy (Fig. S.18). A resonance centered at 246.86 ppm has been tentatively assigned to the desired phosphaalkene $(^tBuC)_3P{=}CMe_2$. A major resonance at −15.65 ppm, corresponding to an unidentified product, was also observed.

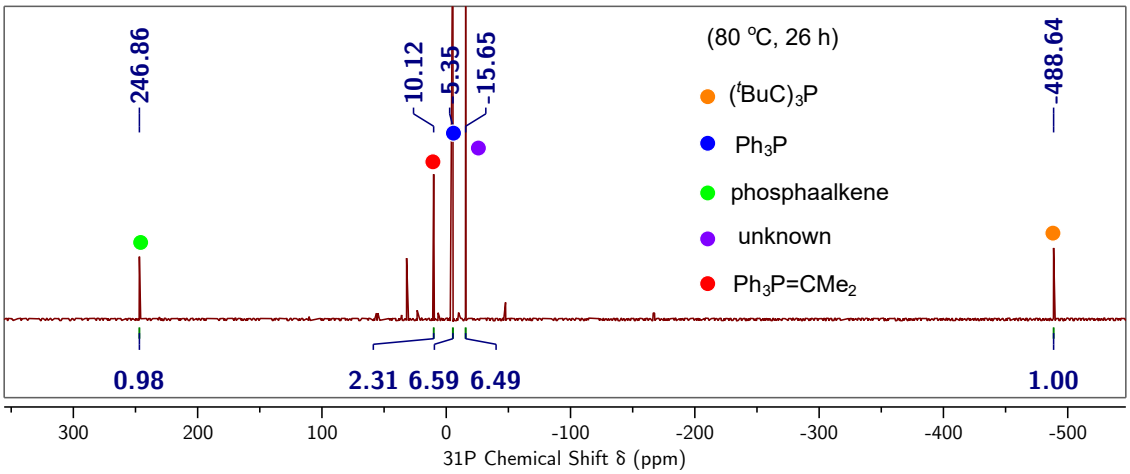

Figure S.18: $^{31}P\{^1H\}$ NMR (162 MHz, THF, 25 °C) spectrum of the crude reaction mixture.

S.1.4 Synthesis of 6-Ph from 1, Ni(COD)$_2$, ^{i}Pr$_3$P, and Styrene

To a stirring solution of Ni(COD)$_2$ (0.029 g, 0.11 mmol, 0.10 equiv) in tetrahydrofuran (9 mL) was added ^{i}Pr$_3$P (0.017 g, 0.11 mmol, 0.10 equiv) and styrene (1.09 g, 10.5 mmol, 10 equiv). To this solution was added a solution of **1** (0.250 g, 1.05 mmol, 1.0 equiv) in tetrahydrofuran (1 mL) dropwise. The brown solution stirred for 90 min and then all volatile materials were removed from the reaction mixture under reduced pressure over 16 h. The brown solids were taken up in pentane (8 mL) and added to charcoal (1.50 g). The slurry stirred for 15 min and was then filtered through a medium sintered frit. The charcoal was washed with additional pentane (2 × 12 mL) and all volatile materials were removed from the combined filtrates under reduced pressure. The beige solids were taken up in tetramethylsilane (1 mL) and placed in a −30 °C freezer overnight. The supernatant was decanted away and the solids were washed with cold tetramethylsilane (0.5 mL). The beige solids were identified as **6**-Ph (0.189 g, 0.553 mmol, 53%), and a second crop (0.019 g, 0.055 mmol; cumulative 0.608 mmol, 58%) was obtained by concentrating the supernatant, setting it in the −30 °C freezer overnight, and collecting the precipitate. Elem. Anal. Calc'd(found) for $C_{23}H_{35}P$: C 80.66(81.00), H 10.30(10.42). ^{1}H NMR (400 MHz, chloroform-*d*, 25 °C, Fig. S.19) δ 7.20 (t, J = 7.6 Hz, 2H), 7.08 (t, J = 7.3 Hz, 1H), 7.02 (d, J = 7.2 Hz, 2H), 2.12 (ddd, J = 10.1, 7.5, 2.6 Hz, 1H), 1.27 (d, $^5J_{PH}$ = 3.5 Hz, 18H), 1.25 (m, 1H), 1.12 (m, 1H), 1.09 (s, 9H) ppm. ^{13}C{^{1}H} NMR (101 MHz, chloroform-*d*, 25 °C, Fig. S.44) δ 143.89 (d, $^2J_{PC}$ = 8.3 Hz), 128.38, 126.08 (d, $^3J_{PC}$ = 4.5 Hz), 125.72 (d, $^2J_{PC}$ = 51.3 Hz), 125.07, 46.26 (d, $^1J_{PC}$ = 54.5 Hz), 37.58 (d, $^2J_{PC}$ = 31.9 Hz), 31.31 (d, $^3J_{PC}$ = 9.8 Hz), 31.22 (d, $^4J_{PC}$ = 39.1 Hz), 30.67 (d, $^3J_{PC}$ = 8.8 Hz), 26.42 (d, $^1J_{PC}$ = 40.0 Hz), 15.45 (d, $^1J_{PC}$ = 43.1 Hz) ppm. ^{31}P{^{1}H} NMR (162 MHz, chloroform-*d*, 25 °C, Fig. S.21) δ −170.4 (d, $^2J_{PH}$ = 19.6 Hz) ppm.

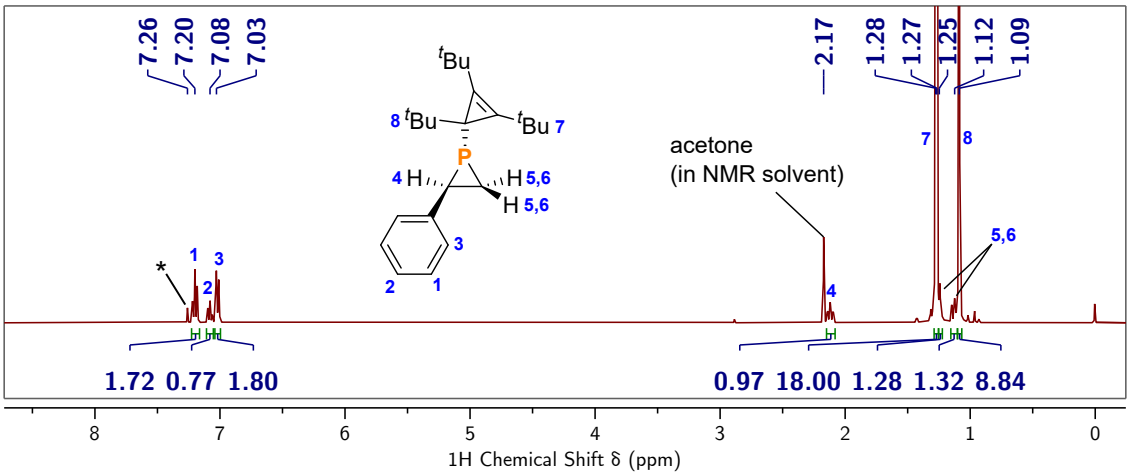

Figure S.19: ^{1}H NMR (400 MHz, chloroform-*d*, 25 °C) spectrum of **6**-Ph. * marks chloroform-*d*.

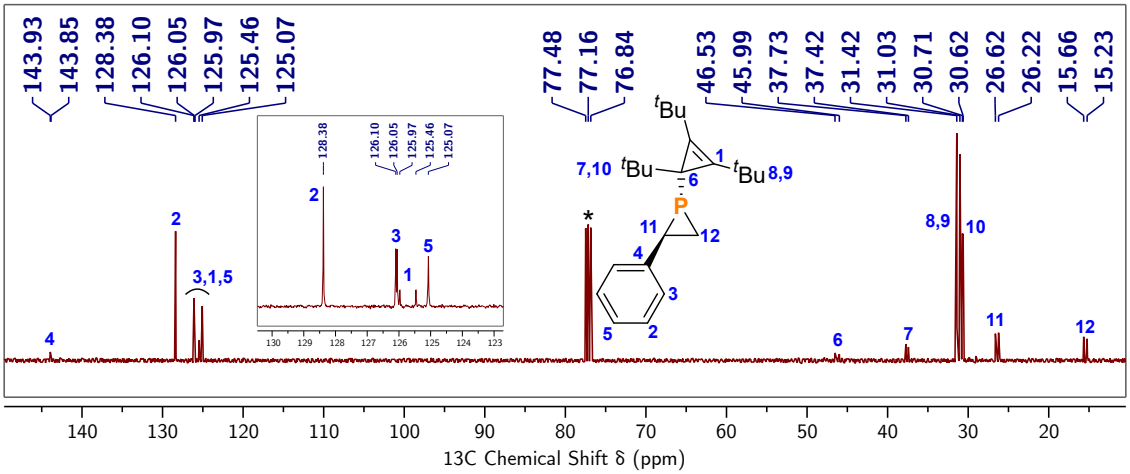

Figure S.20: ^{13}C{^{1}H} NMR (101 MHz, chloroform-*d*, 25 °C) spectrum of **6**-Ph. Inset shows a zoomed-in region of the NMR spectrum. * marks chloroform-*d*.

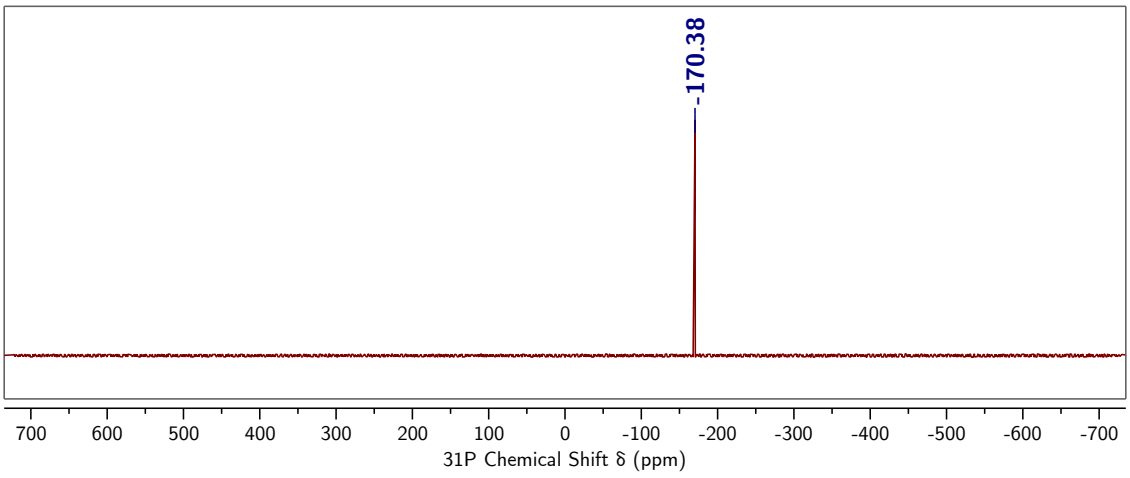

Figure S.21: ^{31}P{^{1}H} NMR (162 MHz, chloroform-*d*, 25 °C) spectrum of **6**-Ph.

S.1.4.1 Ligand Screening

A typical setup involved the addition of **1** (10 mg, 0.042 mmol, 1.0 equiv) to a stirring solution of $Ni(COD)_2$ (2.3 mg, 0.0084 mmol, 0.20 equiv), styrene (44 mg, 0.42 mmol, 10 equiv), and ligand (monodentate ligand: 0.017 mmol, 0.40 equiv; bidentate ligand: 0.0084 mmol, 0.20 equiv) in THF (1 mL). After 30-60 min, an aliquot was removed for NMR analysis. A list of ligands tested for catalysis is given in Table S.1 and $^{31}P\{^{1}H\}$ NMR spectra of the crude reaction mixtures are depicted in Fig. S.22-S.31.

Table S.1: Ligands Screened for Phosphiranation Activity. Abbrevations: IPr*, 1,3-bis(2,6-bis(diphenylmethyl)-4-methylphenyl)imidazo-2-ylidene; DCPE, 1,2-bis(dicyclohexylphosphino)ethane; *rac*-BINAP, (±)-2,2'-bis(diphenylphosphino)-1,1'-binaphthyl; DPPE, 1,2-bis(diphenylphosphino)ethane.

Ligand	Phosphinidene Transfer	Conversion to Phosphirane	NMR Spectrum
$^{i}Pr_3P$	Yes	High	Fig. S.22
None	No	N/A	Fig. S.23
Cy_3P	Yes	High	Fig. S.24
Et_3P	Yes	Moderate	Fig. S.25
$^{t}Bu_3P$	No	N/A	Fig. S.26
Ph_3P	Yes	Low	Fig. S.27
IPr*	No	N/A	Fig. S.28
DCPE	No	N/A	Fig. S.29
rac-BINAP	No	N/A	Fig. S.30
DPPE	No	N/A	Fig. S.31

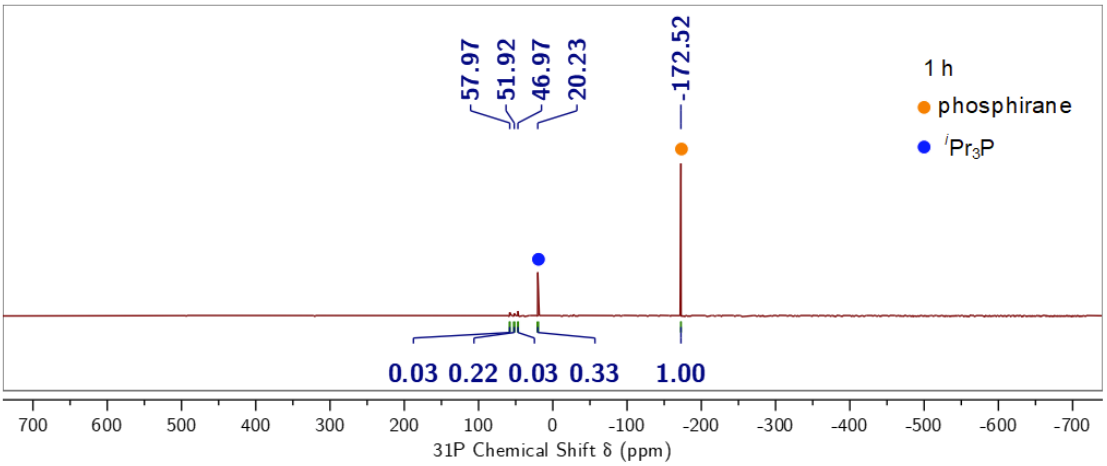

Figure S.22: $^{31}P\{^{1}H\}$ NMR (162 MHz, THF, 25 °C) spectrum of the crude reaction mixture when $^{i}Pr_3P$ is used as a ligand.

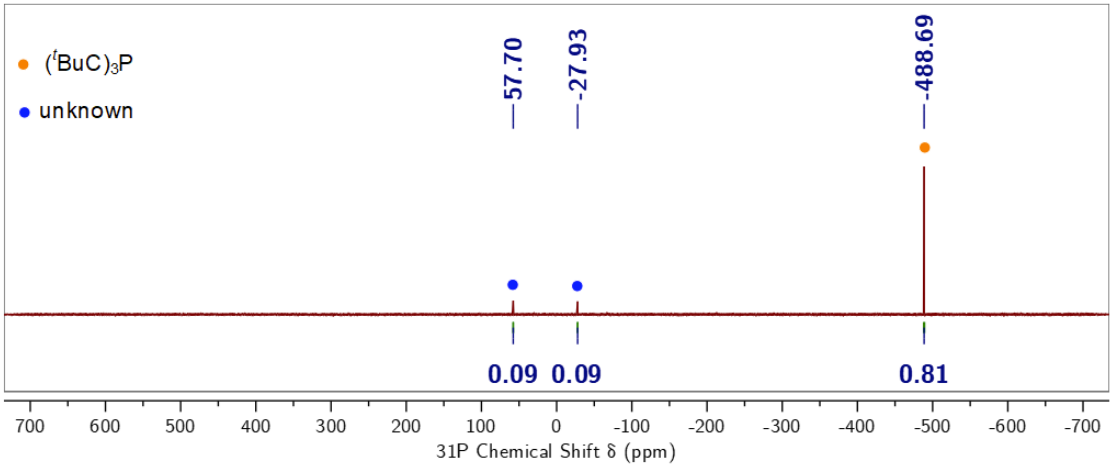

Figure S.23: $^{31}P\{^{1}H\}$ NMR (162 MHz, THF, 25 °C) spectrum of the crude reaction mixture when no ligand is used.

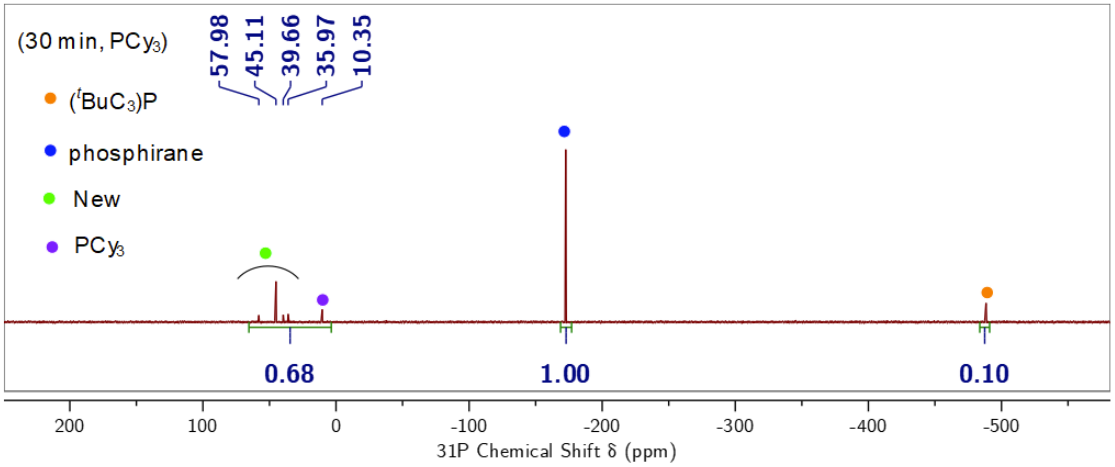

Figure S.24: $^{31}P\{^{1}H\}$ NMR (162 MHz, THF, 25 °C) spectrum of the crude reaction mixture when Cy_3P is used as a ligand.

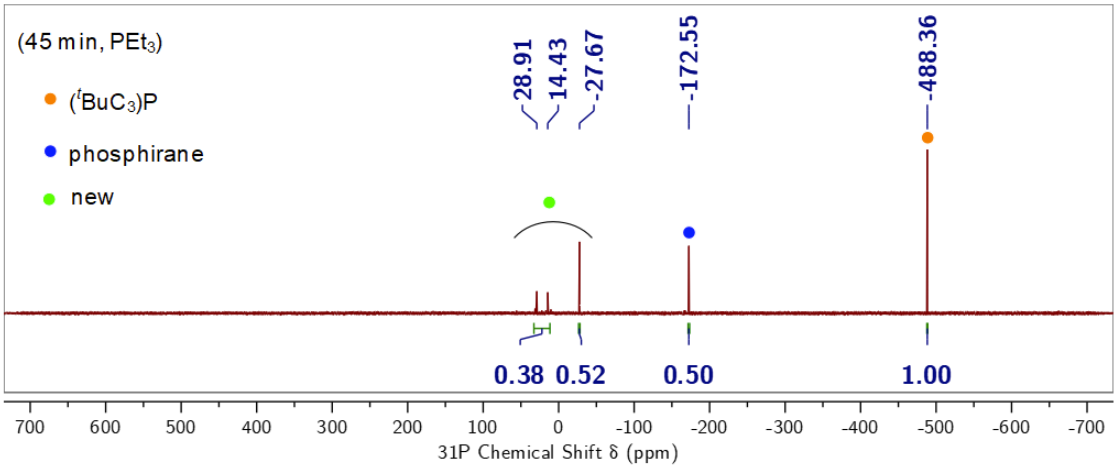

Figure S.25: $^{31}P\{^{1}H\}$ NMR (162 MHz, THF, 25 °C) spectrum of the crude reaction mixture when Et_3P is used as a ligand.

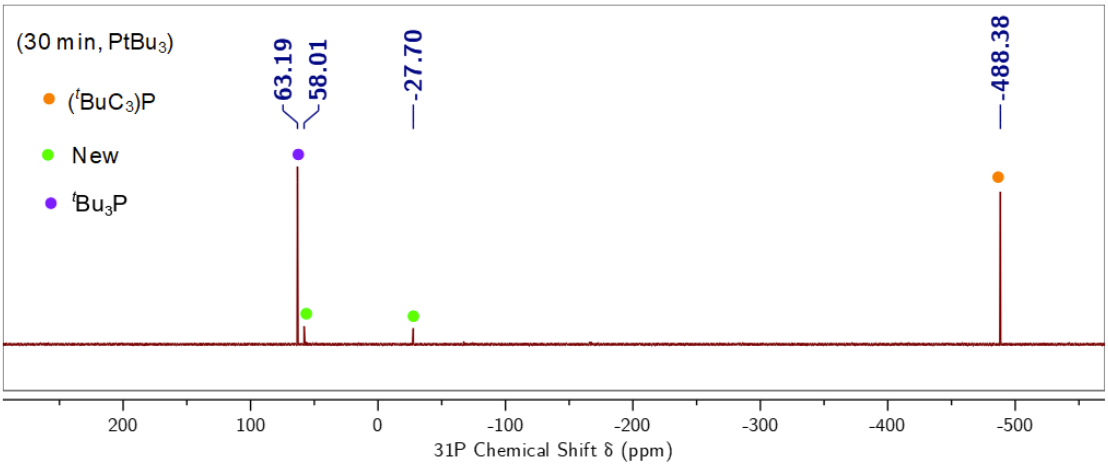

Figure S.26: $^{31}P\{^{1}H\}$ NMR (162 MHz, THF, 25 °C) spectrum of the crude reaction mixture when $^{t}Bu_3P$ is used as a ligand.

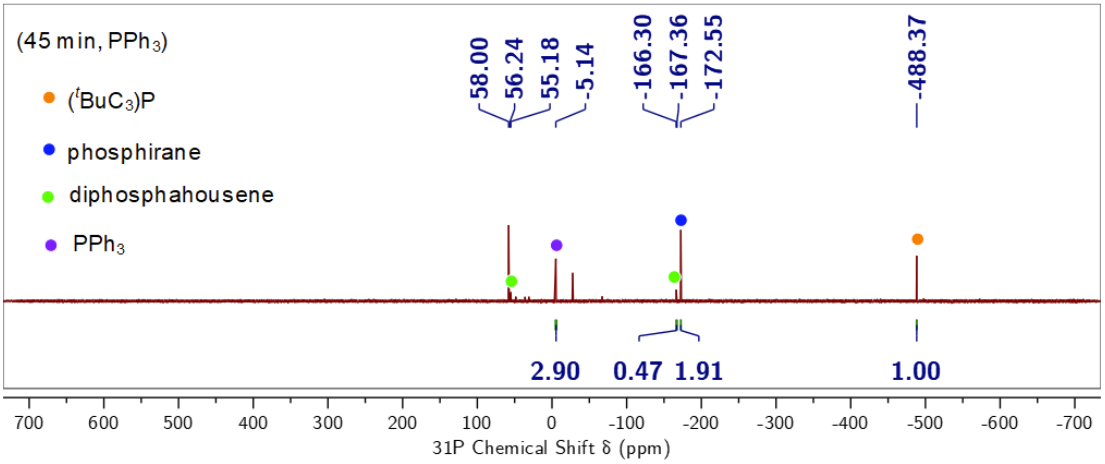

Figure S.27: $^{31}P\{^{1}H\}$ NMR (162 MHz, THF, 25 °C) spectrum of the crude reaction mixture when Ph_3P is used as a ligand.

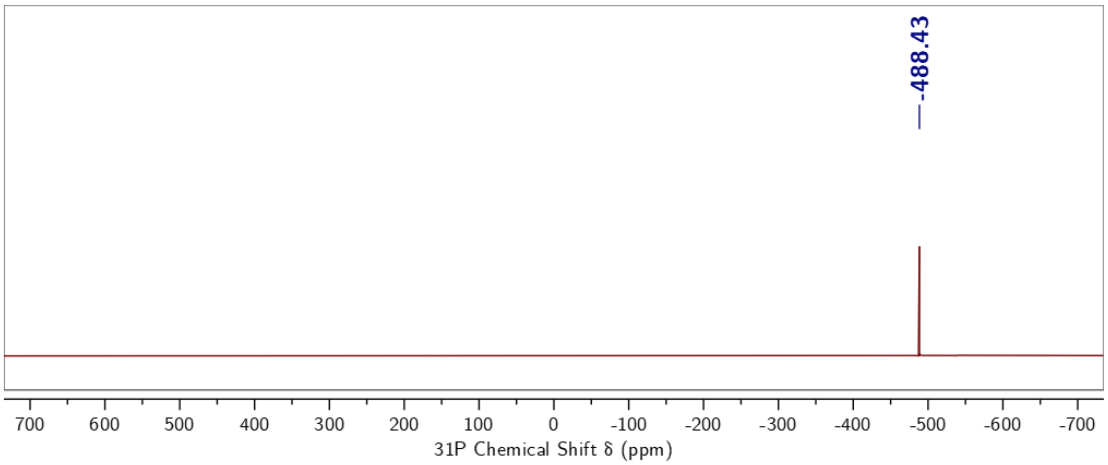

Figure S.28: $^{31}P\{^{1}H\}$ NMR (162 MHz, THF, 25 °C) spectrum of the crude reaction mixture when IPr* is used as a ligand.

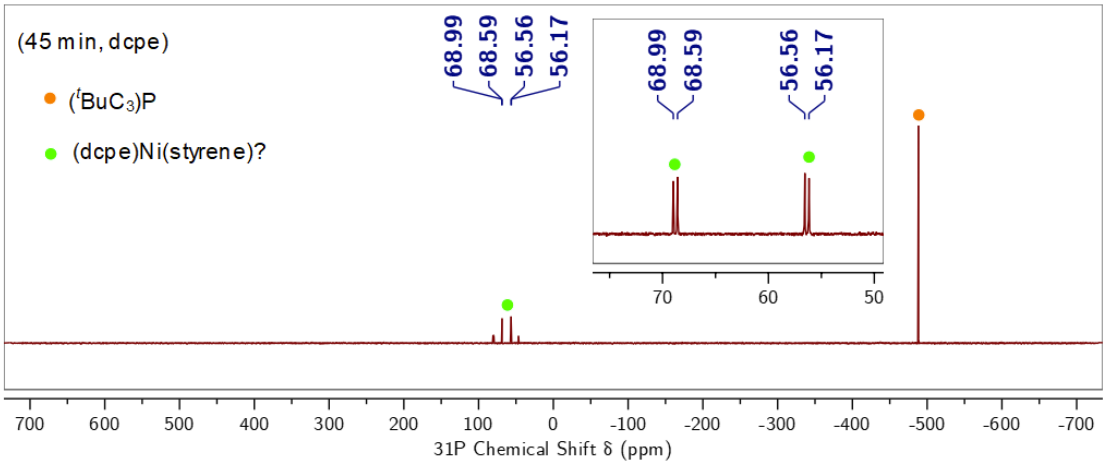

Figure S.29: $^{31}P\{^{1}H\}$ NMR (162 MHz, THF, 25 °C) spectrum of the crude reaction mixture when DCPE is used as a ligand. Inset shows a zoomed-in region of the NMR spectrum.

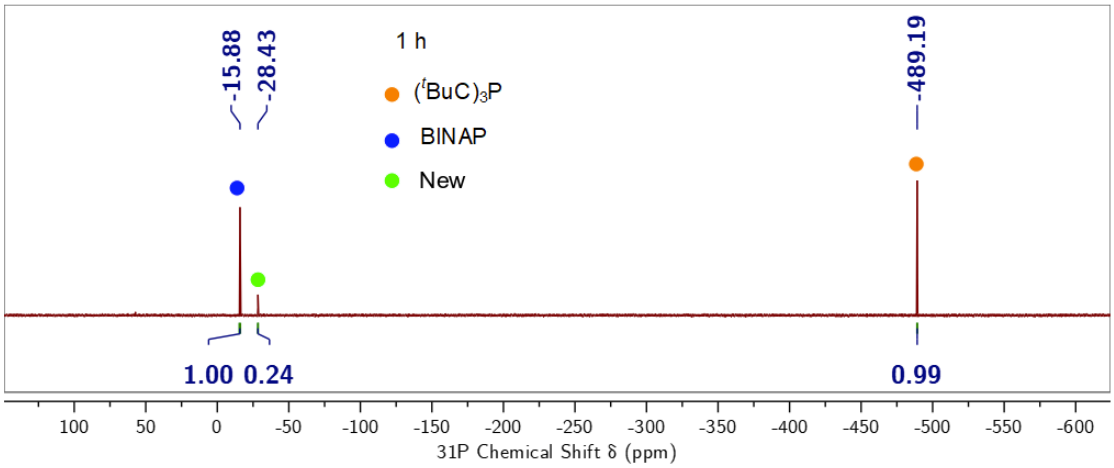

Figure S.30: $^{31}P\{^{1}H\}$ NMR (162 MHz, THF, 25 °C) spectrum of the crude reaction mixture when BINAP is used as a ligand.

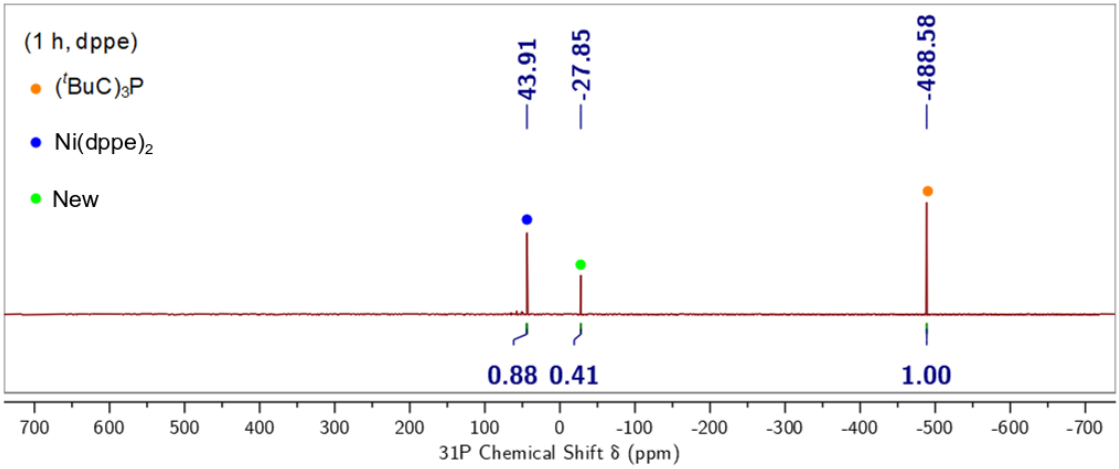

Figure S.31: $^{31}P\{^{1}H\}$ NMR (162 MHz, THF, 25 °C) spectrum of the crude reaction mixture when DPPE is used as a ligand.

S.1.4.2 Quantification of Conversion using an Internal Standard

A stock solution of $Ni(COD)_2$ (0.058 g, 0.21 mmol) and $^{i}Pr_3P$ (0.034 g, 0.21 mmol) was prepared in THF (5 mL). This solution (0.5 mL) was transferred to a vial containing a stir bar, THF (1.5 mL), and styrene (0.218 g, 2.1 mmol, 10 equiv). Compound **1** (0.050 g, 0.21 mmol, 1.0 equiv) was added to the mixture, and the solution was set to stir for 90 min. Afterwards, acenaphthene (0.016 g, 0.21 mmol, 1.0 equiv) was added and an aliquot (0.5 mL) was transferred to a new vial. All volatile materials were removed from the aliquot under reduced pressure and the resulting residue was taken up in benzene-d_6 (0.7 mL) for NMR analysis. Spin-lattice decay constants (T_1) were measured using an inversion recovery pulse sequence and T_1 times of 3 s and 2 s were found for the ethylene proton resonance of acenapthene (2.99 ppm in benzene-d_6) and the benzylic proton resonance of **6**-Ph (2.23 ppm in benzene-d_6), respectively. The relaxation delay was set to 30 s to obtain a quantitative ^{1}H NMR spectrum. The ^{1}H NMR spectrum revealed 84% conversion to **6**-Ph (Fig. S.32).

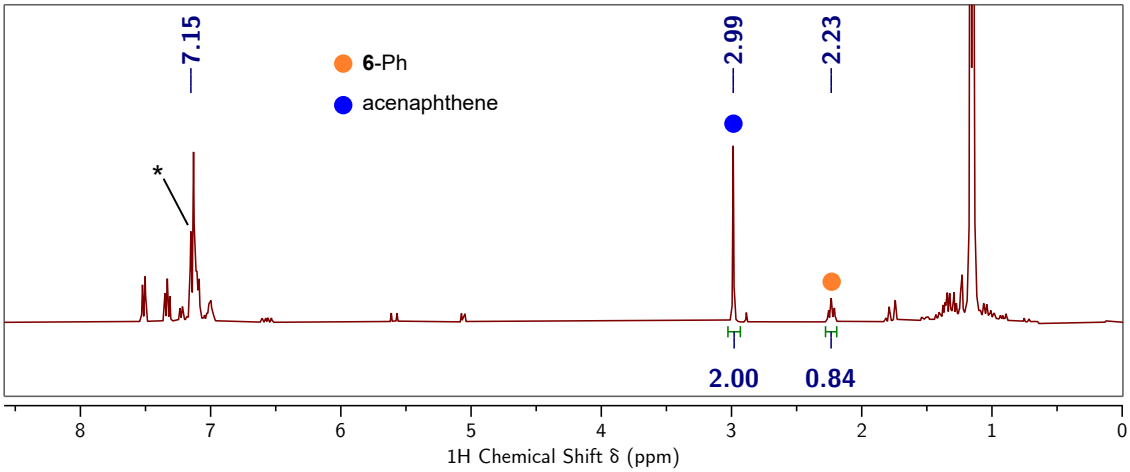

Figure S.32: Quantitative ^{1}H NMR (400 MHz, benzene-d_6, 25 °C) spectrum of the crude reaction mixture. * marks benzene-d_6.

S.1.4.3 Catalysis using Ni($^{4\text{-tBu}}$stb)$_3$ as the Ni(0) Source

To a solution of Ni($^{4\text{-tBu}}$stb)$_3$[11] (20 mg, 0.021 mmol, 0.1 equiv) in THF (2 mL) was added ^{i}Pr$_3$P (3 mg, 0.02 mmol, 0.1 equiv) and styrene (218 mg, 2.10 mmol, 10 equiv). After the solution stirred for 1 min, compound **1** (0.050 g, 0.21 mmol, 1.0 equiv) was added. After the reaction mixture stirred for 45 min, an aliquot was removed for NMR analysis (Fig. S.33). After 90 min, all volatile materials were removed from the crude mixture under reduced pressure. Benzene-d_6 (0.7 mL) and acenaphthene (0.016 g, 0.21 mmol, 1.0 equiv) were added to the dark brown residue, and after the solution was stirred for 1 min, it was transferred to an NMR tube for NMR analysis. The relaxation delay was set to 30 s to obtain a quantitative ^{1}H NMR spectrum and 55% conversion to **6**-Ph was observed (Fig. S.34).

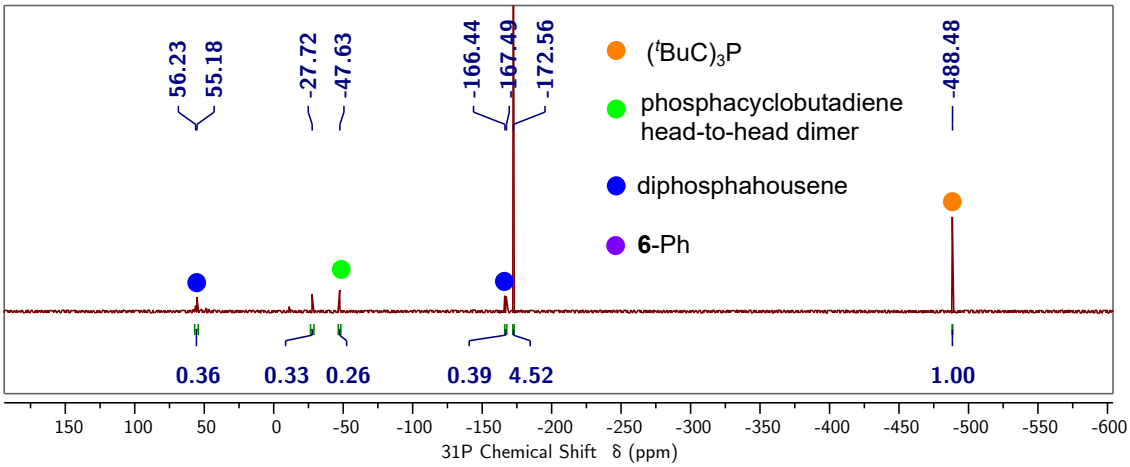

Figure S.33: ^{31}P{^{1}H} NMR (162 MHz, THF, 25 °C) spectrum of the crude reaction mixture after 45 min.

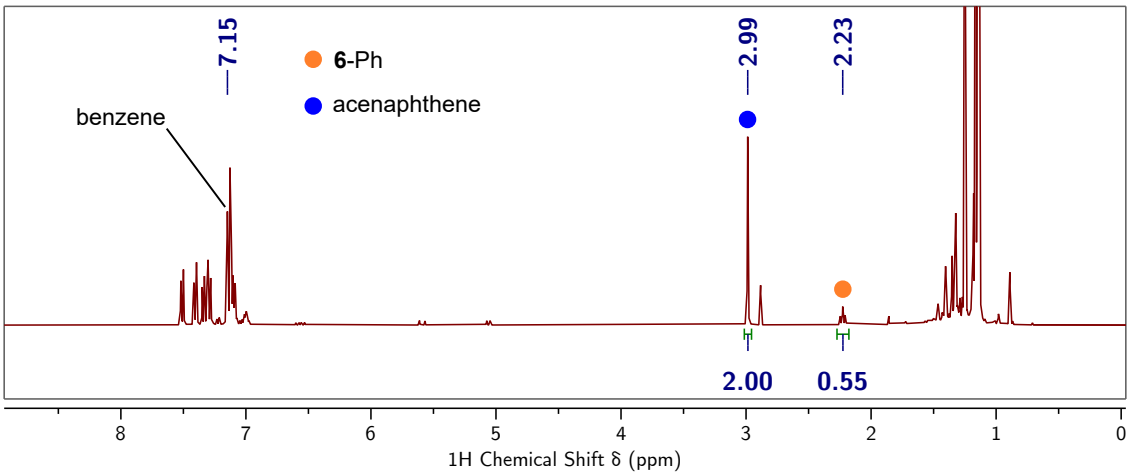

Figure S.34: Quantitative ^{1}H NMR (400 MHz, benzene-d_6, 25 °C) spectrum of the crude reaction mixture.

S.1.4.4 Monitoring Phosphinidene Transfer by Low Temperature NMR Spectroscopy

A stock solution of $Ni(COD)_2$ (0.029 g, 0.11 mmol, 1 equiv), $^{i}Pr_3P$ (0.017 g, 0.11 mmol, 1 equiv), and styrene (0.009 g, 0.1 mmol, 1 equiv) was prepared in THF (2.5 mL, 2.8 g). This solution (0.5 mL) was transferred to a vial containing a few drops of THF-d_8, and the resulting solution was frozen in the coldwell of the glovebox. Upon thawing, the solution was combined with **1** (0.004 g, 0.1 mmol, 1 equiv) and immediately transferred to a J Young tube that was precooled in the coldwell of the box. The tube containing the orange-brown solution was removed from the box and submerged in liquid nitrogen. The tube was then loaded into the precooled (−45 °C) probe of the NMR spectrometer. No signals corresponding to a nickel phosphinidene or a metallacycle intermediate were observed after 1 h at −45 °C (Fig. S.35); therefore, the probe was warmed to −25 °C and a $^{31}P\{^{1}H\}$ NMR spectrum was collected after the sample sat for 30 min (Fig. S.36). Afterwards, the sample was transferred to an NMR spectrometer with the probe set to 25 °C and, after 30 min, a $^{31}P\{^{1}H\}$ NMR spectrum was collected (Fig. S.37).

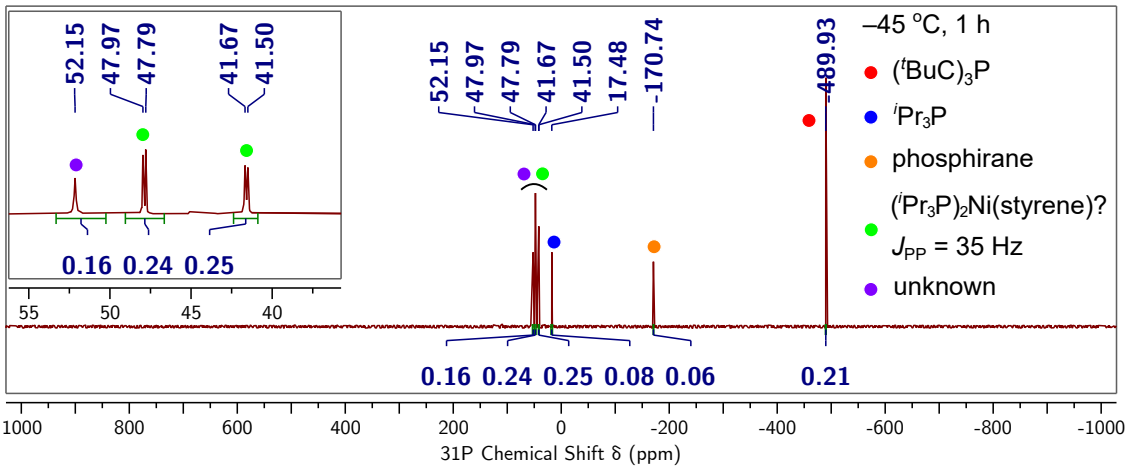

Figure S.35: Low temperature $^{31}P\{^{1}H\}$ NMR (203 MHz, THF, −45 °C) spectrum of the NMR sample after 1 h at −45 °C. Inset shows a zoomed-in region of the NMR spectrum.

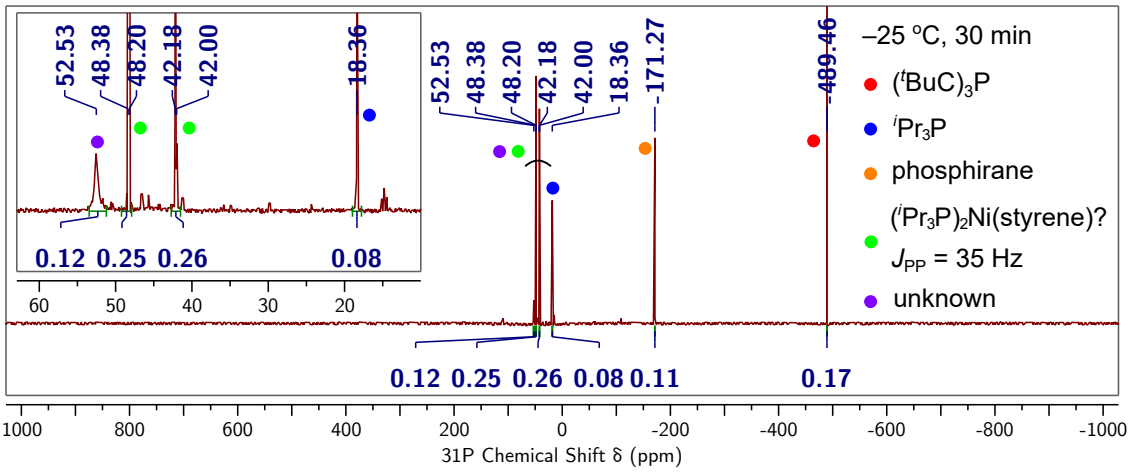

Figure S.36: Low temperature $^{31}P\{^1H\}$ NMR (203 MHz, THF, −25 °C) spectrum of the NMR sample after 30 min at −25 °C. Inset shows a zoomed-in region of the NMR spectrum.

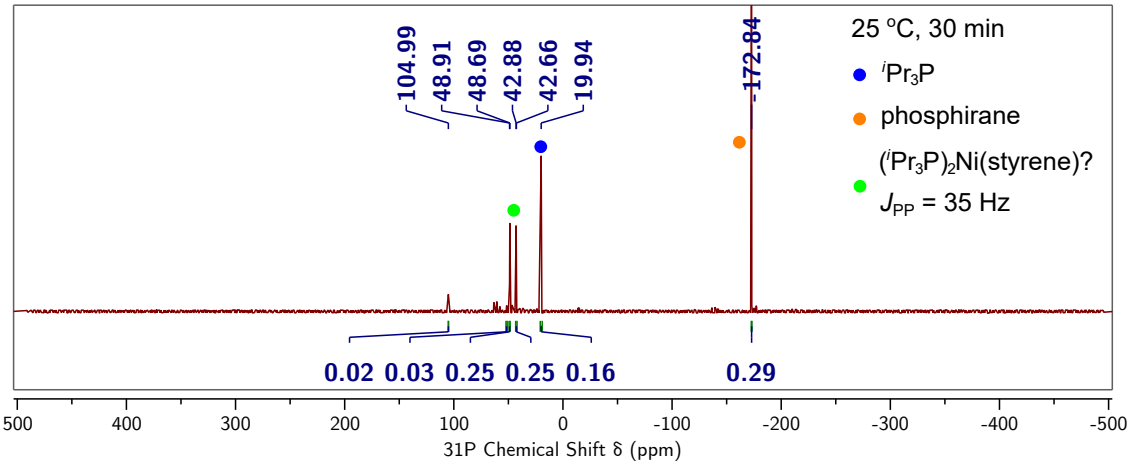

Figure S.37: $^{31}P\{^1H\}$ NMR (162 MHz, THF, 25 °C) spectrum of the NMR sample after 30 min at room temperature.

S.1.4.5 Treatment of 1 with $^{i}Pr_3P$, and Styrene

To a stirring THF (0.7 mL) solution of $^{i}Pr_3P$ (3 mg, 0.02 mmol, 0.4 equiv) and styrene (44 mg, 0.42 mmol, 10 equiv) was added $(^{t}BuC)_3P$ (10 mg, 0.04 mmol, 1 equiv). After the colorless solution stirred for 3 h, it was transferred to an NMR tube for NMR analysis. No reaction was observed (Fig. S.38).

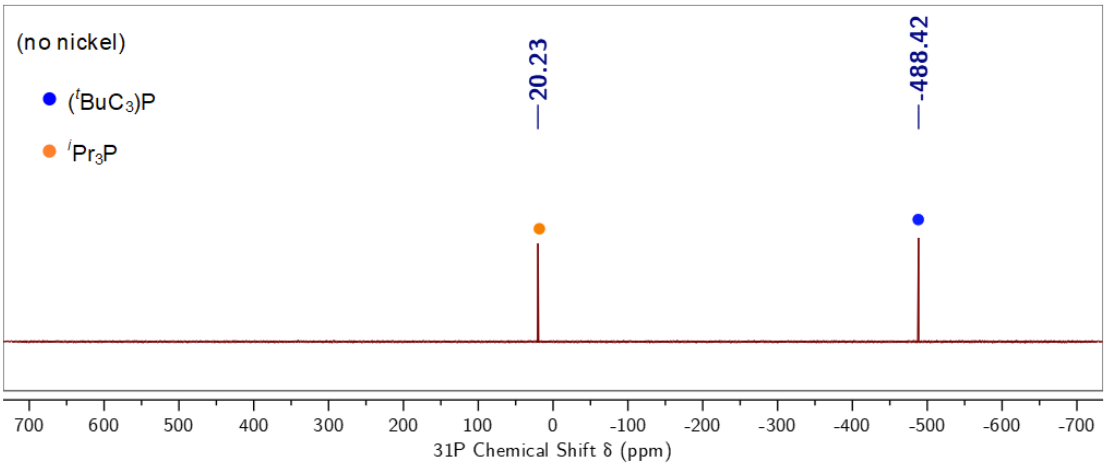

Figure S.38: $^{31}P\{^{1}H\}$ NMR (162 MHz, THF, 25 °C) spectrum of the crude reaction mixture.

S.1.4.6 *cis*-β-Deuterostyrene as a Substrate in Catalysis

To a stirring suspension of $Ni(COD)_2$ (4.6 mg, 0.017 mmol, 0.20 equiv) in THF (2 mL) was added $^{i}Pr_3P$ (2.7 mg, 0.017 mmol, 0.20 equiv) and *cis*-β-deuterostyrene (88 mg, 0.84 mmol, 10 equiv). Note that the *cis*-β-deuterostyrene used was contaminated with unlabeled styrene (ca. 6%).[9] After the yellow solution stirred for ca. 30 s, compound **1** (20 mg, 0.084 mmol, 1.0 equiv) was added. After 45 min, benzene-d_6 (1 drop, ca. 5 mg) was added to the brown reaction mixture and an aliquot was removed for NMR analysis (Fig. S.39). A single resonance corresponding to deuterium-incorporated phosphirane was observed in the ^{2}H NMR spectrum. Additionally, the bulk *cis*-β-deuterostyrene in solution did not undergo scrambling to form *trans*-β-deuterostyrene. Volatile materials were removed from the remaining solution under reduced pressure and the resulting brown residue was taken

up in THF (0.7 mL) and benzene-d_6 (1 drop, ca. 5 mg). The NMR spectra are depicted in Fig. S.40-S.42.

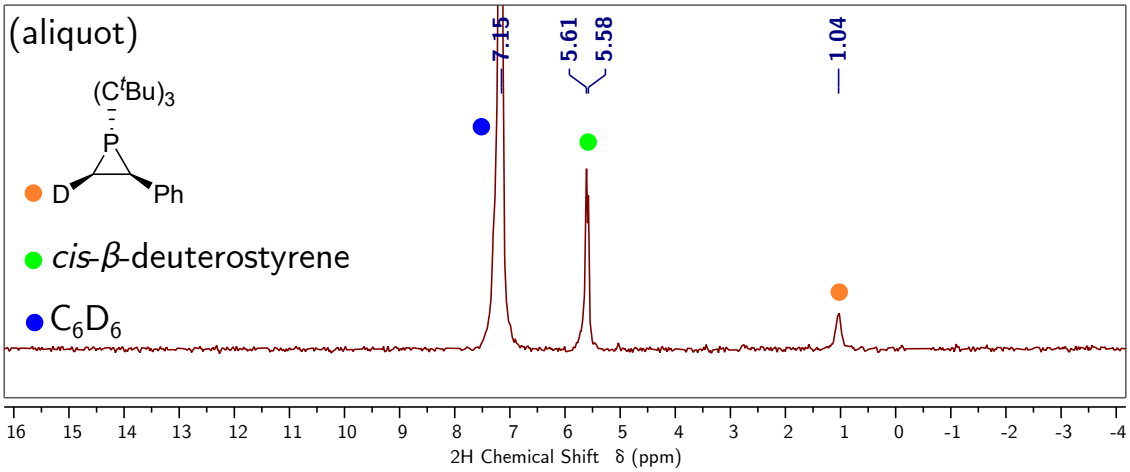

Figure S.39: ^{2}H NMR (77 MHz, THF, 25 °C) spectrum of the crude reaction mixture.

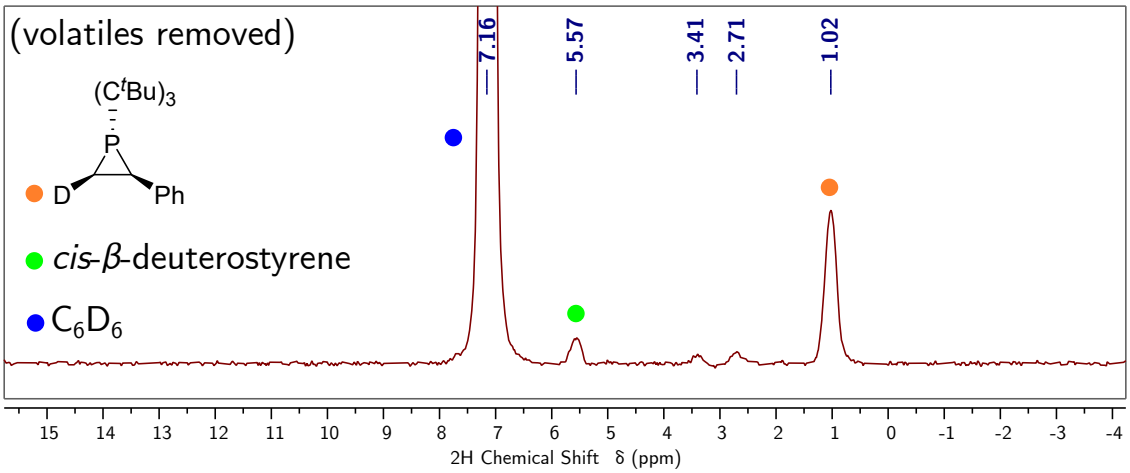

Figure S.40: ^{2}H NMR (61 MHz, THF, 25 °C) spectrum of the crude reaction mixture after removing volatile materials under reduced pressure.

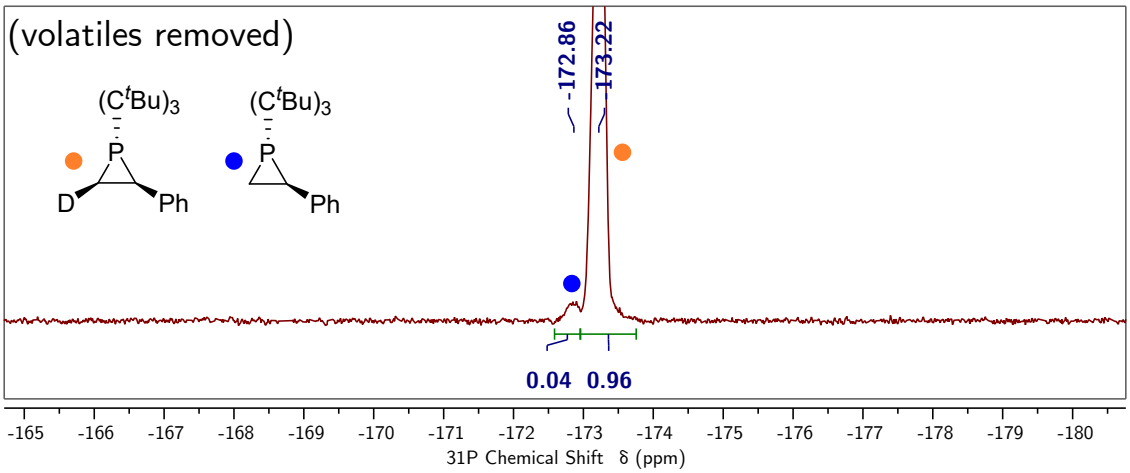

Figure S.41: $^{31}P\{^1H\}$ NMR (162 MHz, THF, 25 °C) spectrum of the crude reaction mixture after removing volatile materials under reduced pressure.

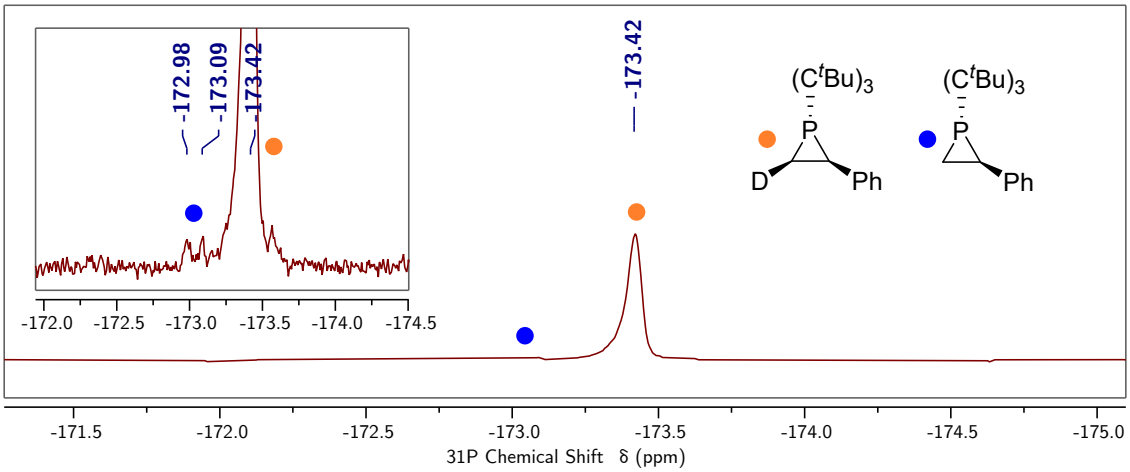

Figure S.42: ^{31}P NMR (203 MHz, THF, 25 °C) spectrum of the crude reaction mixture after removing volatile materials under reduced pressure. Inset shows a zoomed-in region of the NMR spectrum.

S.1.5 Synthesis of 6-H from 1, Ni(COD)$_2$, ^{i}Pr$_3$P, and Ethylene

A solution of Ni(COD)$_2$ (0.023 g, 0.0084 mmol, 0.10 equiv) and ^{i}Pr$_3$P (0.014 g, 0.0084 mmol, 0.10 equiv) in tetrahydrofuran (6 mL) was prepared. The solution was transferred to a 25 mL Schlenk tube and removed from the glovebox. The solution was degassed by three freeze-pump-thaw cycles, allowed to warm to room temperature, and backfilled with ethylene (ca. 1 atm). In the glovebox, a solution of **1** (0.200 g, 0.840 mmol, 1.0 equiv) in THF (1 mL) was prepared and taken up in a 1 mL plastic syringe. The syringe was removed from the box, and its contents were added to the Schlenk tube under positive ethylene pressure dropwise. After the brown solution stirred for 90 min, the tube was brought back into the glovebox where its contents were transferred to a vial. All volatile materials were removed from the solution under reduced pressure, and the resulting brown oil was taken up in pentane (6 mL). Charcoal (1.5 g) was added to the pentane solution, and the slurry stirred for 15 min. The slurry was passed through a medium sintered frit, and the charcoal was washed with additional pentane (2 × 5 mL). All volatile materials were removed from the combined colorless filtrates under reduced pressure. The resulting waxy solids were transferred to a micro sublimator (photograph shown in Fig. S.46) and removed from the glovebox. The sublimator was placed under dynamic vacuum (ca. 200 mTorr) and heated to 70 °C with the coldfinger cooled to 5 °C. Over 30 min, colorless solids coated the coldfinger of the sublimator. The apparatus was brought back into the glovebox where the solids were transferred to a vial. Phosphirane **6**-H was isolated as a colorless, waxy material (0.138 g, 0.527 mmol, 63%). Elem. Anal. Calc'd(found) for $C_{17}H_{31}P$: C 76.64(76.85), H 11.73(11.40). ^{1}H NMR (400 MHz, benzene-d_6, 25 °C, Fig. S.43) δ 1.21 (s, 9H), 1.12 (s, 18H), 0.73 (m, 2H), 0.54 (m, 2H) ppm. ^{13}C{^{1}H} NMR (101 MHz, benzene-d_6, 25 °C, Fig. S.44) δ 125.64, 45.17 (d, $^1J_{PC}$ = 53.5 Hz), 37.71 (d, $^2J_{PC}$ = 32.1 Hz), 31.38, 30.89 (d, $^3J_{PC}$ = 9.2 Hz), 6.11 (d, $^1J_{PC}$ = 41.5 Hz) ppm. ^{31}P{^{1}H} NMR (162 MHz, benzene-d_6, 25 °C, Fig. S.45) δ −220.6 ($^2J_{PH}$ = 17.2 Hz) ppm.

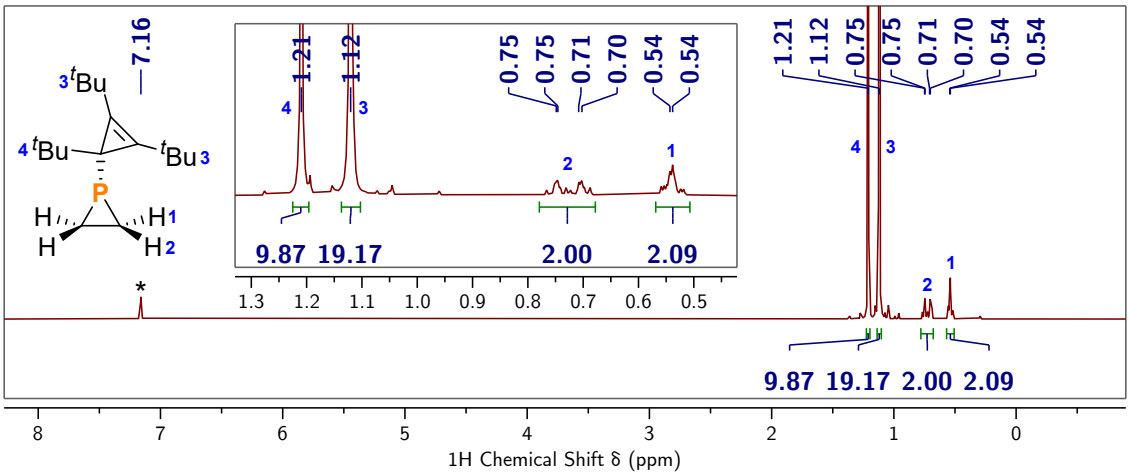

Figure S.43: ^{1}H NMR (400 MHz, benzene-d_6, 25 °C) spectrum of **6**-H. Inset shows a zoomed-in region of the NMR spectrum. * marks benzene-d_6.

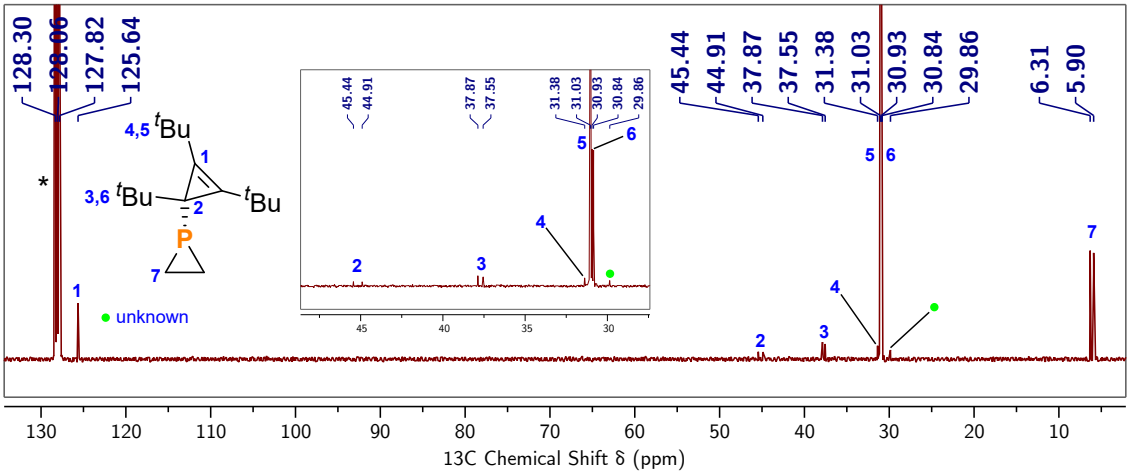

Figure S.44: ^{13}C{^{1}H} NMR (101 MHz, benzene-d_6, 25 °C) spectrum of **6**-H. Inset shows a zoomed-in region of the NMR spectrum. * marks benzene-d_6.

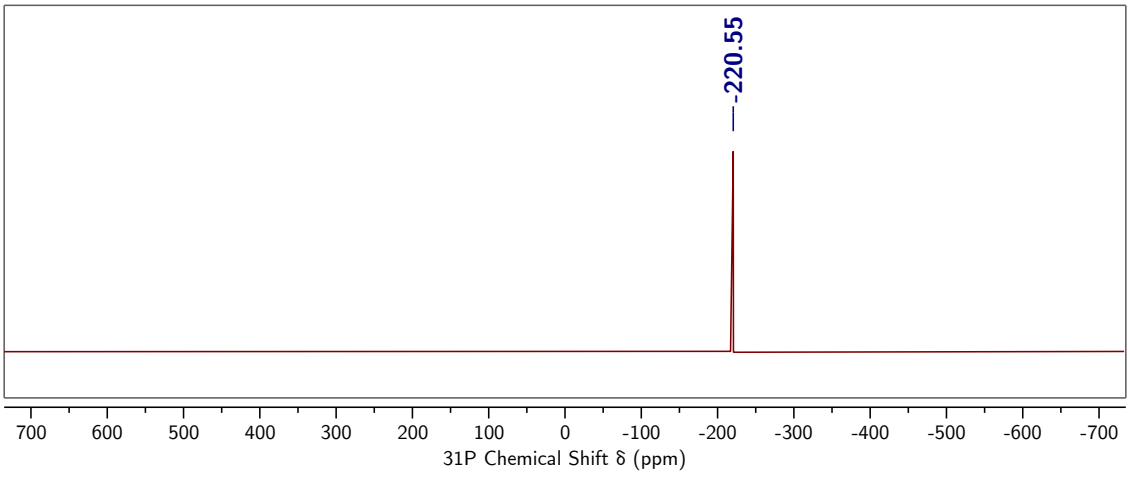

Figure S.45: ^{31}P{^{1}H} NMR (162 MHz, benzene-d_6, 25 °C) spectrum of **6**-H.

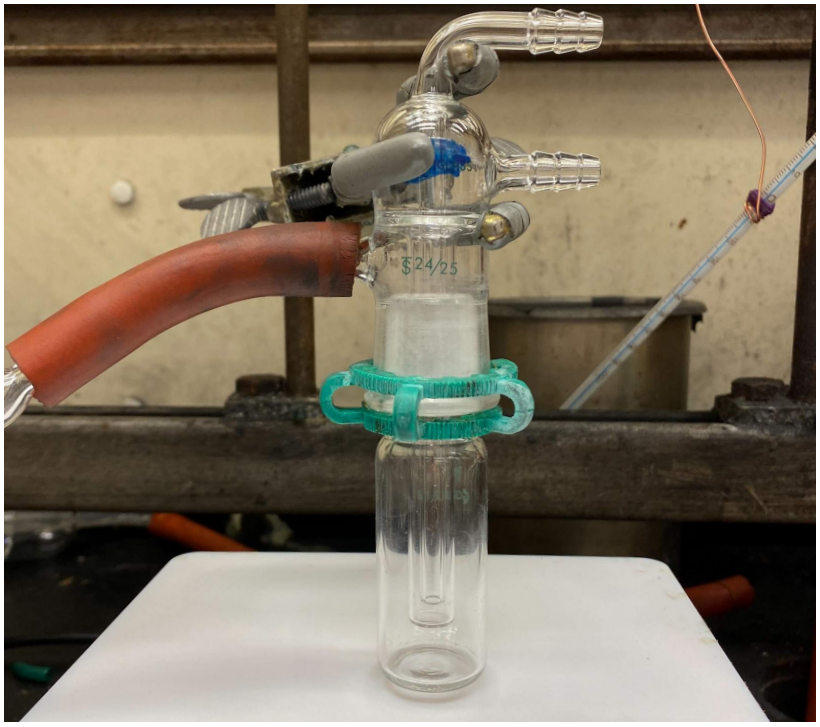

Figure S.46: Photograph of the sublimator.

S.1.6 Synthesis of 6-^{t}Bu from 1, Ni(COD)$_2$, ^{i}Pr$_3$P, and Neohexene

To a stirring solution of Ni(COD)$_2$ (0.017 g, 0.0063 mmol, 0.10 equiv) in tetrahydrofuran (9 mL) was added ^{i}Pr$_3$P (0.010 g, 0.0063 mmol, 0.10 equiv) and neohexene (0.529 g, 6.30 mmol, 10 equiv). To this solution was added a solution of **1** (0.150 g, 0.630 mmol, 1.0 equiv) in tetrahydrofuran (1 mL) dropwise. The brown solution stirred for 90 min and then all volatile materials were removed from the reaction mixture under reduced pressure. Pentane (10 mL) and charcoal (1 g) were added to the resulting brown residue and the slurry was stirred for 15 min. The mixture was passed through a medium sintered frit (15 mL) and the plug of charcoal was washed with pentane (2 × 10 mL). The combined colorless filtrates were brought to constant mass under reduced pressure. The resulting colorless oil was transferred to a round bottom flask (5 mL) connected to a Hickman distillation head. The distillation apparatus (photograph shown in Fig. S.54) was removed from the box and placed under reduced pressure (ca. 100 mTorr). The flask was heated to 100 °C and the phosphirane was distilled with the aid of a heat gun. Afterwards, the apparatus was brought back into the glovebox where the oil collected in the Hickman head was transferred to a vial using pentane. Compound **6**-^{t}Bu was isolated as a colorless oil (0.103 g, 0.320 mmol, 51%) after removing the pentane under reduced pressure. NMR assignments for **6**-^{t}Bu were made using 2D NMR techniques ^{1}H,^{13}C-HSQC and ^{1}H,^{13}C HMBC (Fig. S.51-S.53). While **6**-^{t}Bu was not observed by DART HRMS, [^{t}Bu$_3$C$_3$]$^+$ ([M]$^+$ Calc'd for $C_{15}H_{27}$ 207.21128; Found 207.21156) was observed. ^{1}H NMR (500 MHz, benzene-d_6, 25 °C, Fig. S.47) δ 1.20 (s, 9H), 1.16 (s, 18H), 1.11 (td, J = 7.8, 3.8 Hz, 1H), 0.99 (s, 9H), 0.74 (dt, J = 19.5, 7.3 Hz, 1H), 0.52 (dd, J = 10.2, 6.9 Hz, 1H) ppm. ^{13}C{^{1}H} NMR (126 MHz, benzene-d_6, 25 °C, Fig. S.48 and S.49) δ 126.74, 125.05, 45.24 (d, $^1J_{PC}$ = 52.6 Hz), 37.91 (d, $^2J_{PC}$ = 31.4 Hz), 36.38 (d, $^1J_{PC}$ = 43.3 Hz), 31.43, 31.32 (d, $^2J_{PC}$ = 7.7 Hz), 30.90 (d, $^3J_{PC}$ = 11.8 Hz), 30.91, 30.85, 30.71, 29.71 (d, $^3J_{PC}$ = 5.0 Hz), 9.84 (d, $^1J_{PC}$ = 38.5 Hz) ppm. ^{31}P{^{1}H} NMR (162 MHz, benzene-d_6, 25 °C, Fig. S.50) δ −205.4 ($^2J_{PH}$ = 20.0 Hz) ppm.

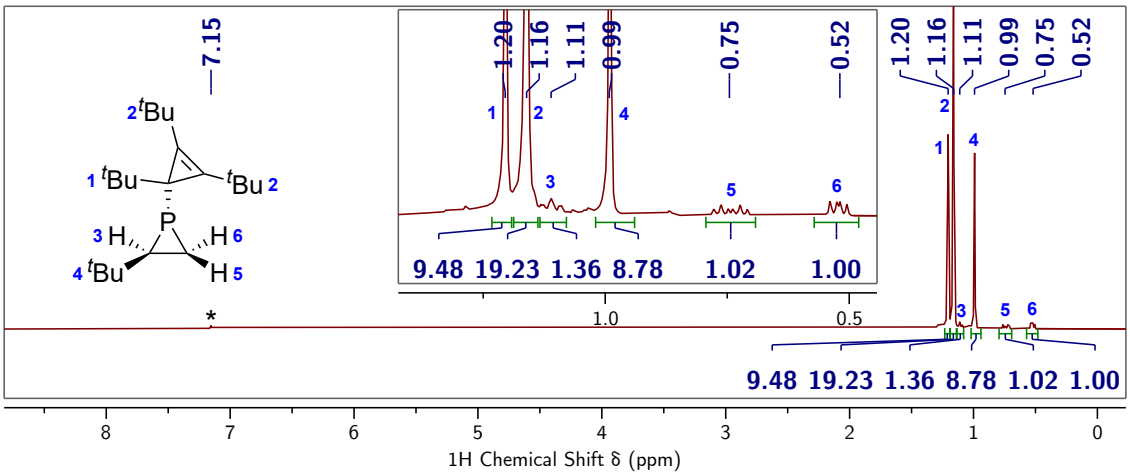

Figure S.47: ^{1}H NMR (500 MHz, benzene-d_6, 25 °C) spectrum of **6**-^{t}Bu. Inset shows a zoomed-in region of the NMR spectrum. * marks benzene-d_6.

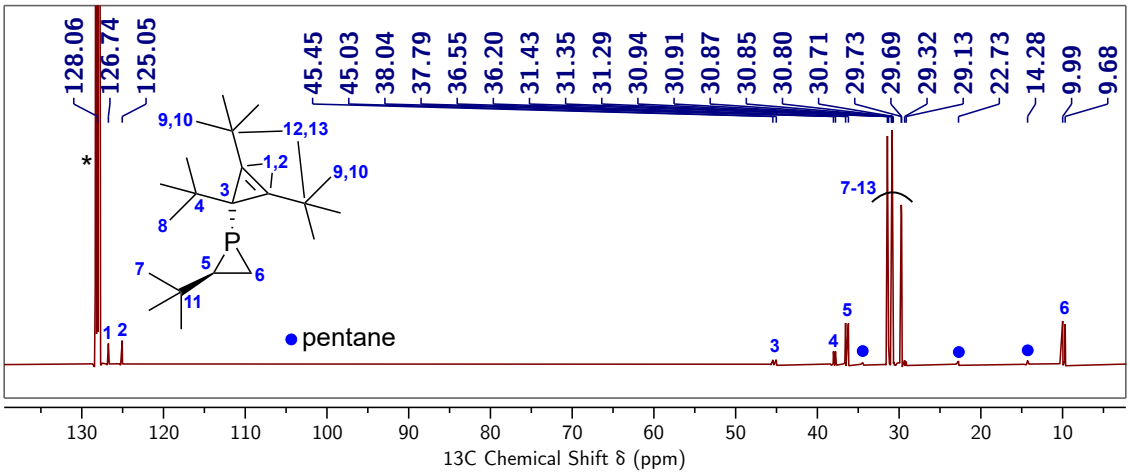

Figure S.48: ^{13}C{^{1}H} NMR (126 MHz, benzene-d_6, 25 °C) spectrum of **6**-^{t}Bu. * marks benzene-d_6.

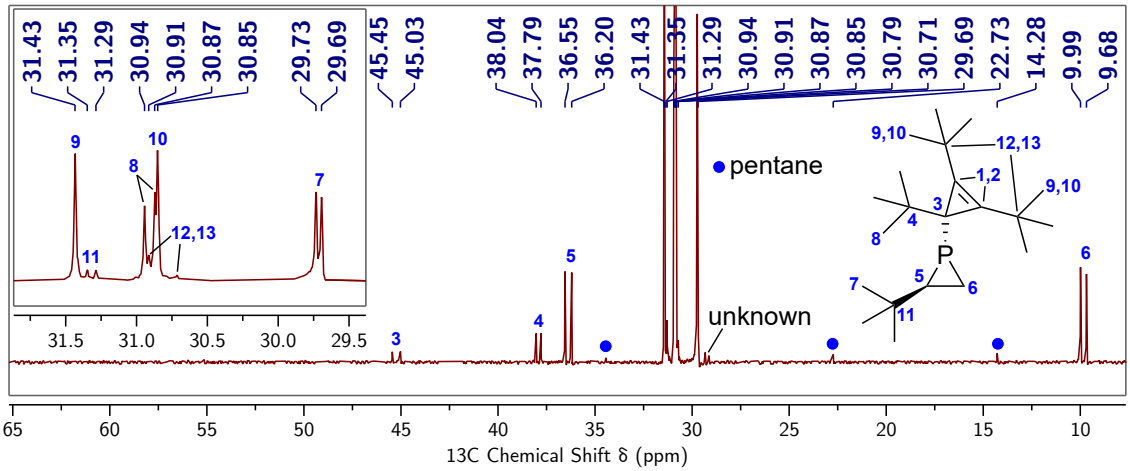

Figure S.49: $^{13}C\{^{1}H\}$ NMR (126 MHz, benzene-d_6, 25 °C) spectrum of **6**-^{t}Bu. Inset shows a zoomed-in region of the NMR spectrum.

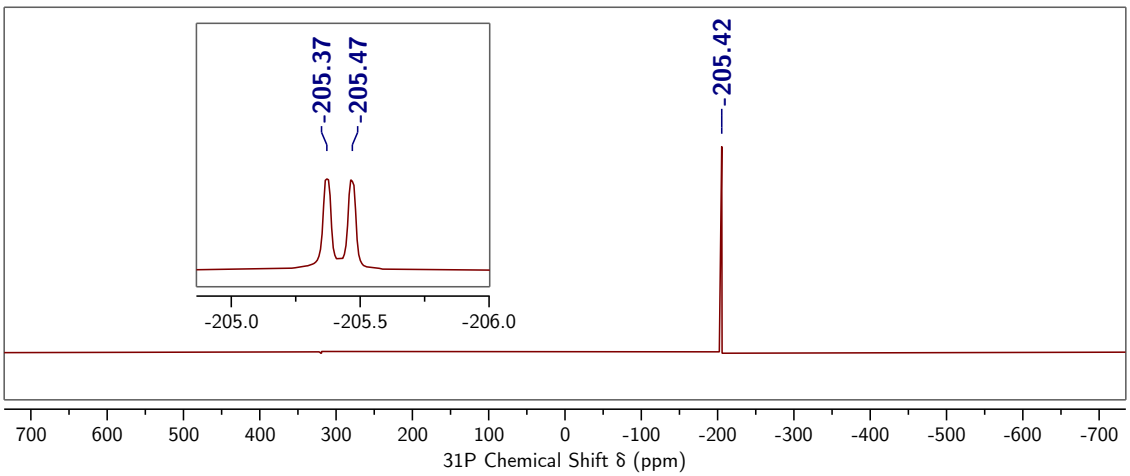

Figure S.50: $^{31}P\{^{1}H\}$ NMR (162 MHz, benzene-d_6, 25 °C) spectrum of **6**-^{t}Bu. Inset shows the corresponding proton-coupled ^{31}P NMR spectrum.

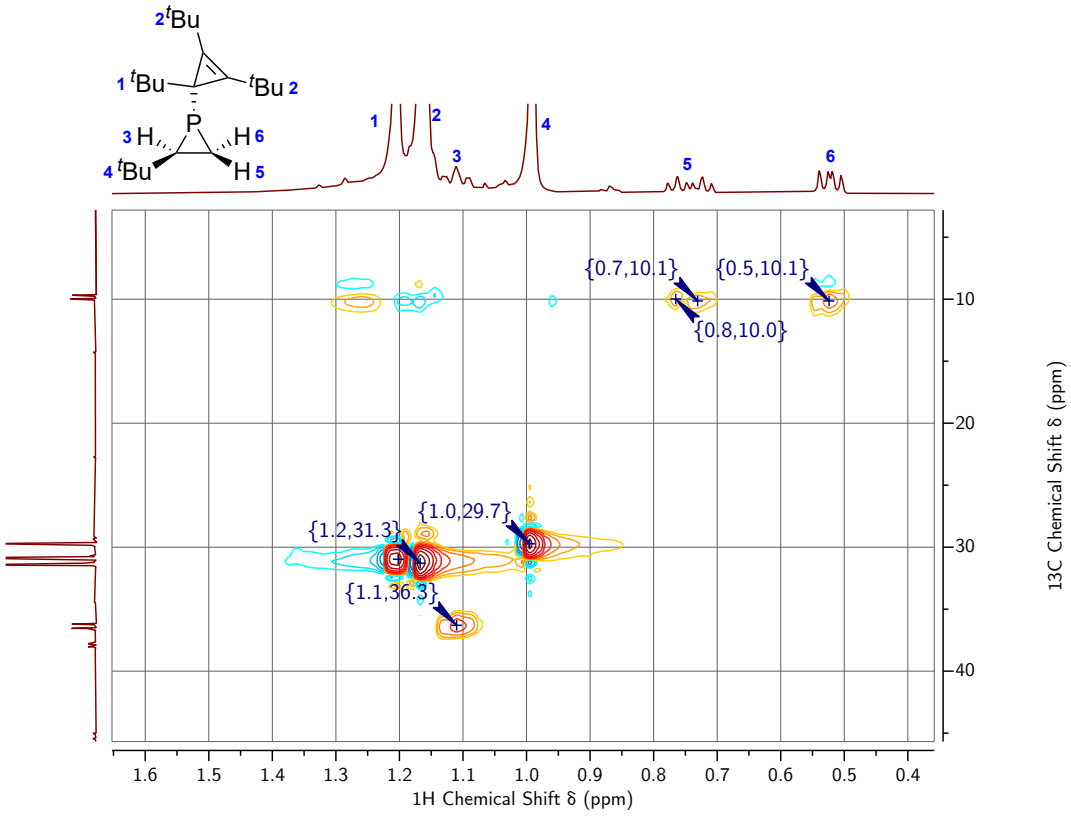

Figure S.51: ^{1}H, ^{13}C-HSQC NMR (500 MHz, benzene-d_6, 25 °C) spectrum of **6**-^{t}Bu.

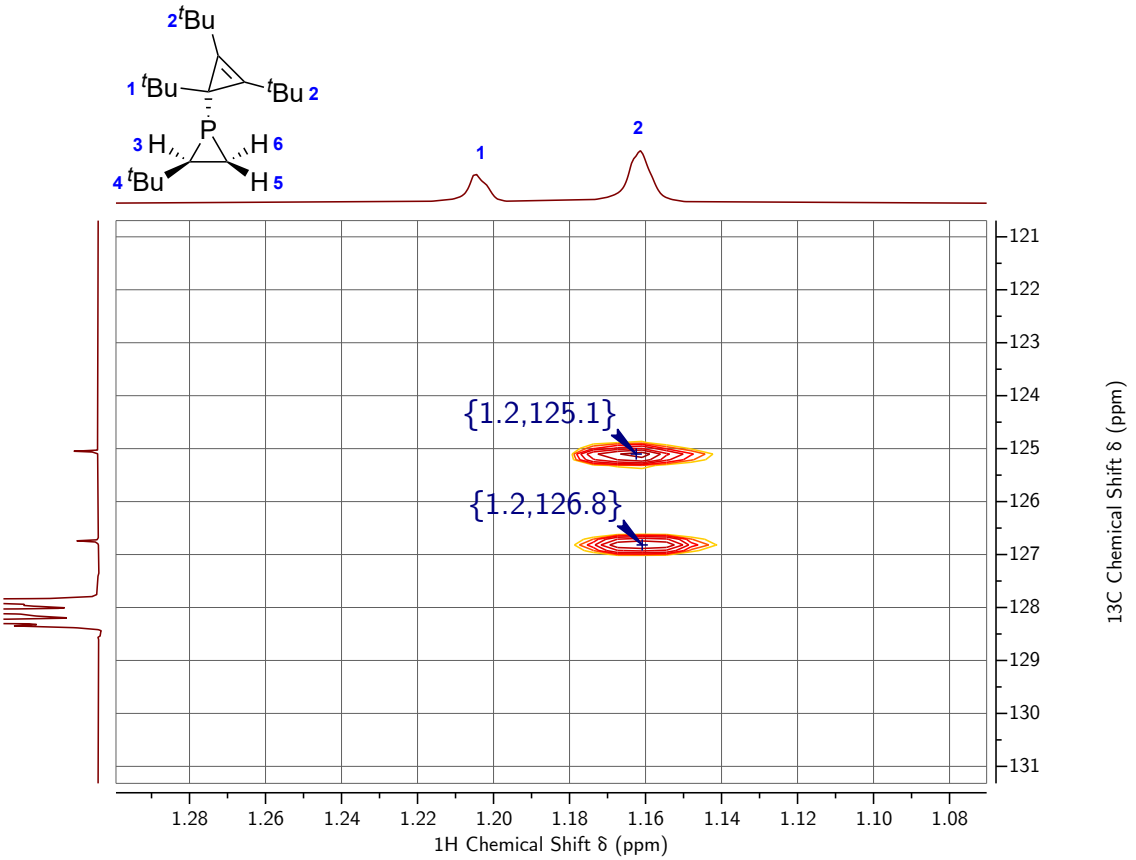

Figure S.52: ^{1}H, ^{13}C-HMBC NMR (500 MHz, benzene-d_6, 25 °C) spectrum of **6**-^{t}Bu.

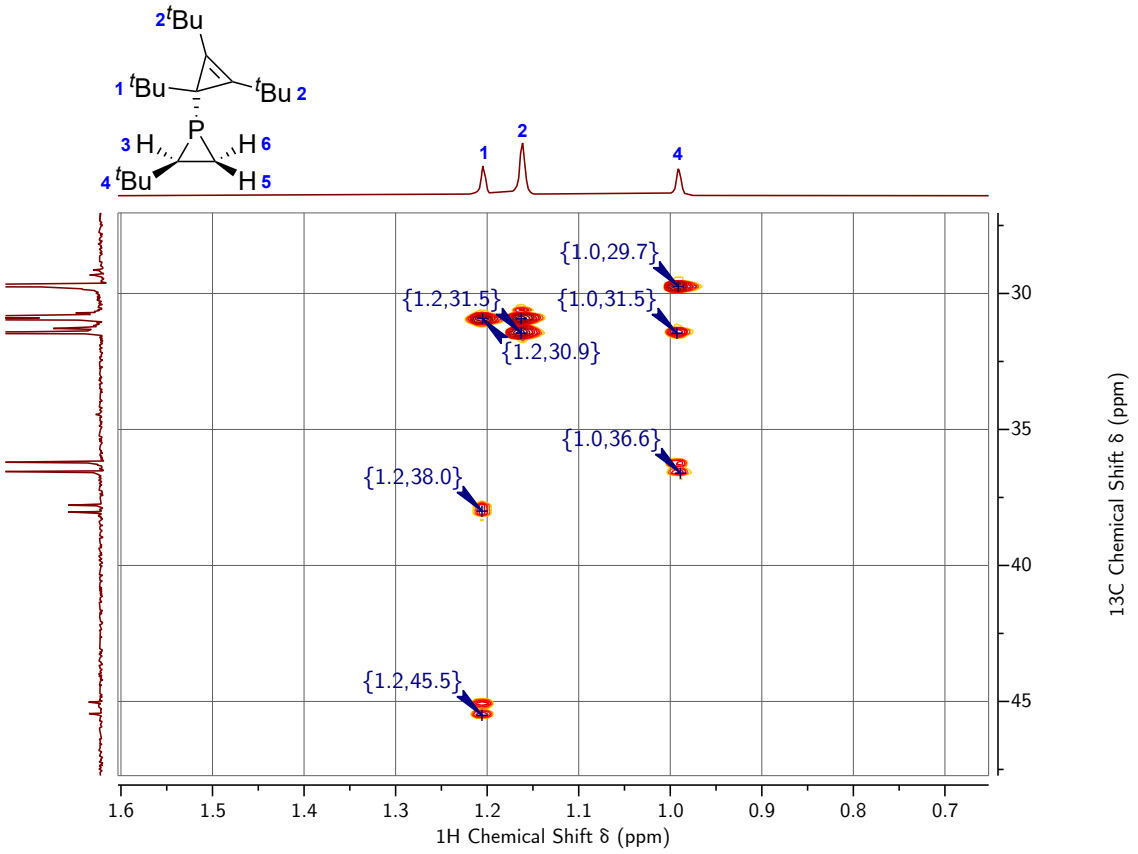

Figure S.53: ^{1}H, ^{13}C-HMBC NMR (500 MHz, benzene-d_6, 25 °C) spectrum of **6**-^{t}Bu.

Figure S.54: Photograph of the distillation apparatus.

S.1.7 Synthesis of 7 from 1, $Ni(COD)_2$, $^iPr_3P$, and 1,3-Cyclohexadiene

To a stirring solution of $Ni(COD)_2$ (0.012 g, 0.042 mmol, 0.10 equiv) in tetrahydrofuran (4 mL) was added $^iPr_3P$ (0.007 g, 0.04 mmol, 0.1 equiv) and 1,3-cyclohexadiene (0.336 g, 4.20 mmol, 10 equiv). To this solution was added a solution of **1** (0.100 g, 0.420 mmol, 1.0 equiv) in tetrahydrofuran (1 mL) dropwise. The brown solution stirred for 90 min and then all volatile materials were removed from the reaction mixture under reduced pressure. The brown oil was taken up in pentane (6 mL) and added to charcoal (0.300 g). The slurry stirred for 5 min and was then filtered through a medium sintered frit. The charcoal was washed with additional pentane (6 mL) and all volatile materials were removed from the combined filtrates under reduced pressure. The pale brown oil was transferred to a round bottom flask (10 mL) connected to a Hickman distillation head using a minimal amount of pentane. The apparatus was removed from the glovebox, placed under dynamic vacuum (ca. 150 mTorr), and set in a preheated 100 °C oil bath. The material distilled into the Hickman head with the aid of a heat gun. The apparatus was allowed to cool to room temperature and was then brought back into the glovebox, where the yellow oil collected in the Hickman head was transferred to a vial using tetramethylsilane. After removing all volatile materials from the vial under reduced pressure, compound **7** was isolated as a pale yellow oil (0.087 g, 0.27 mmol, 64%). Elem. Anal. Calc'd(found) for $C_{21}H_{35}P$: C 79.20(78.95), H 11.08(10.85). ^1H NMR (500 MHz, benzene-d_6, 25 °C, Fig. S.55) δ 6.28 (m, 1H), 5.49 (m, 1H), 2.16 (m, 1H), 2.07 (m, 1H), 1.96 (m, 1H), 1.81 (m, 1H), 1.70 (dd, J = 9.4, 5.4 Hz, 1H), 1.59 (m, 1H), 1.16 (s, 9H), 1.12 (d, $^5J_{PH}$ = 5.8 Hz, 18H) ppm. $^{13}C\{^1H\}$ NMR (126 MHz, benzene-d_6, 25 °C, Fig. S.56) δ 127.30 (d, J_{PC} = 8.7 Hz), 126.08 (d, $^3J_{PC}$ = 18.4 Hz), 123.92 (d, J_{PC} = 5.0 Hz), 44.82 (d, $^1J_{PC}$ = 57.3 Hz), 37.75 (d, $^2J_{PC}$ = 30.8 Hz), 31.31 (d, $^3J_{PC}$ = 26.7 Hz), 31.11 (d, $^4J_{PC}$ = 13.7 Hz), 30.82 (d, $^3J_{PC}$ = 8.9 Hz), 25.42 (d, J_{PC} = 44.1 Hz), 23.53 (d, J_{PC} = 37.7 Hz), 22.45 (d, J_{PC} = 5.2 Hz), 20.65 (d, J_{PC} = 16.0 Hz) ppm. $^{31}P\{^1H\}$ NMR (203 MHz, benzene-d_6, 25 °C, Fig. S.57) δ −171.91 (d, $^3J_{PH}$ = 17.0 Hz) ppm.

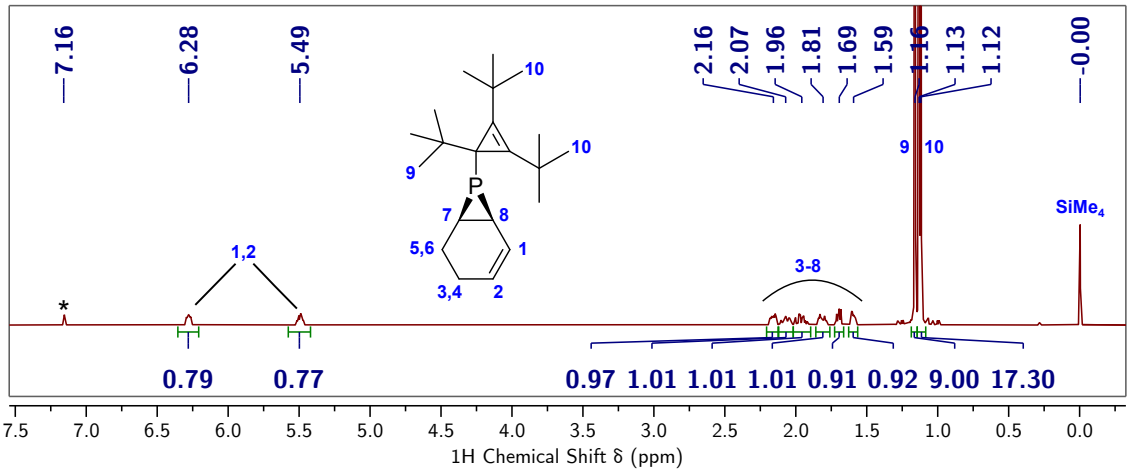

Figure S.55: ^{1}H NMR (500 MHz, benzene-d_6, 25 °C) spectrum of **7** and residual tetramethylsilane. * marks benzene-d_6.

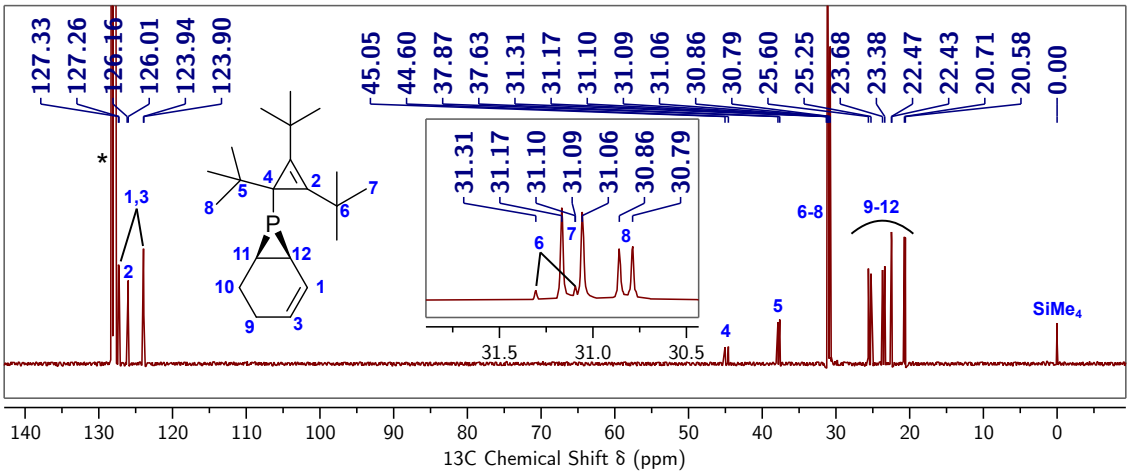

Figure S.56: ^{13}C{^{1}H} NMR (126 MHz, benzene-d_6, 25 °C) spectrum of **7** and residual tetramethylsilane. Inset shows a zoomed-in region of the NMR spectrum. * marks benzene-d_6.

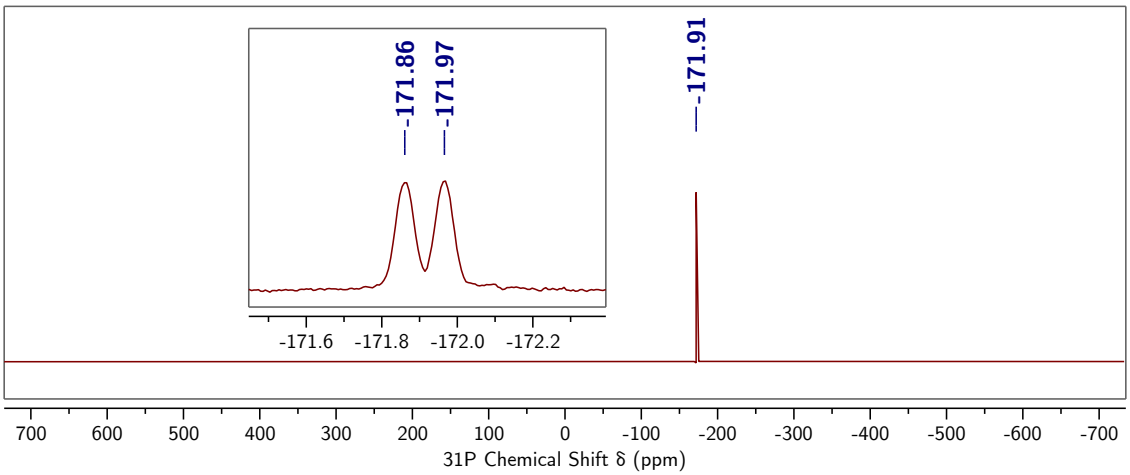

Figure S.57: $^{31}P\{^{1}H\}$ NMR (203 MHz, benzene-d_6, 25 °C) spectrum of **7**. Inset shows the corresponding proton-coupled ^{31}P NMR spectrum.

S.1.7.1 Thermal Stability of 7 in Mesitylene

Compound **7** (5 mg) was dissolved in mesitylene (0.7 mL) and the solution was transferred to a J Young tube. The tube was placed in a preheated 140 °C oil bath and after 90 min a $^{31}P\{^{1}H\}$ NMR spectrum was collected (Fig. S.58). No reaction was observed.

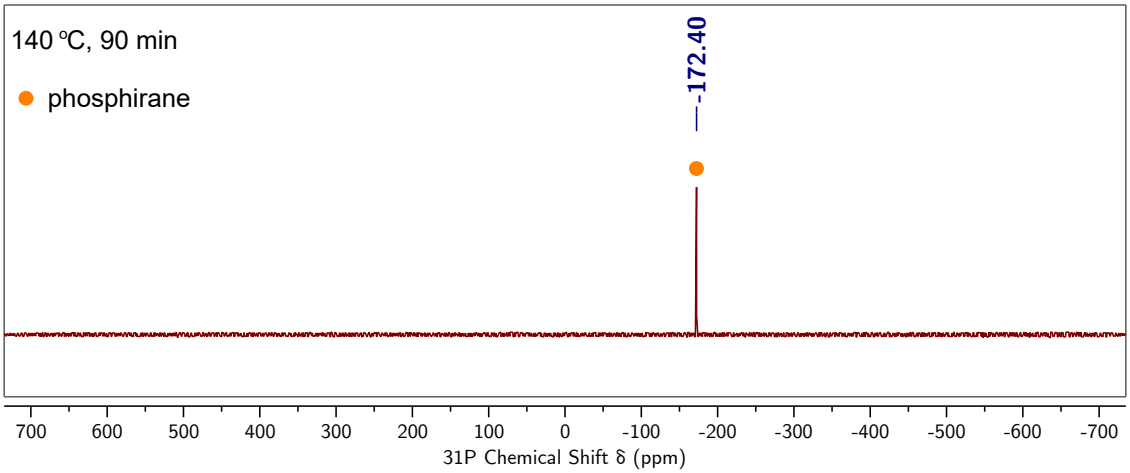

Figure S.58: $^{31}P\{^{1}H\}$ NMR (162 MHz, mesitylene, 25 °C) spectrum of **7** in mesitylene after 90 min at 140 °C.

S.1.8 Attempted Phosphinidene Transfer to Benzene

To a stirring solution of $Ni(COD)_2$ (0.006 g, 0.02 mmol, 0.2 equiv) and $^{i}Pr_3P$ (0.003 g, 0.02 mmol, 0.2 equiv) in benzene (1 mL) was added **1** (0.025 g, 0.11 mmol, 1 equiv). After the mixture stirred for 45 min, an aliquot was transferred to an NMR tube for NMR analysis. No phosphinidene transfer to benzene was observed (Fig. S.59). Instead, phosphatetrahedrane dimers and phosphinidene transfer to 1,5-cyclooctadiene were observed.

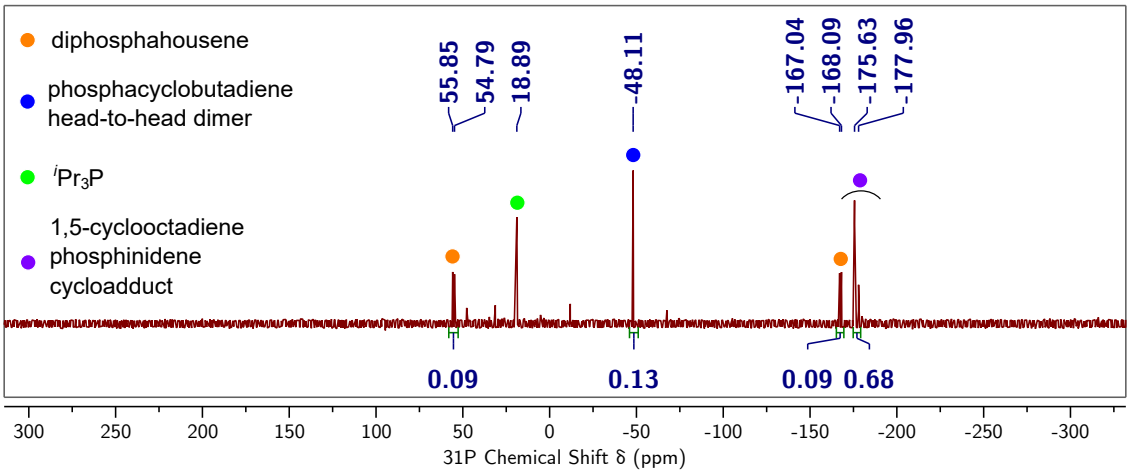

Figure S.59: $^{31}P\{^{1}H\}$ NMR (162 MHz, benzene, 25 °C) spectrum of the crude reaction mixture 45 min after treating $(^{t}BuC)_3P$ with benzene under catalytic conditions.

S.1.9 Attempted Phosphinidene Transfer to Ferrocene

To a stirring solution of $Ni(COD)_2$ (0.006 g, 0.02 mmol, 0.2 equiv) and $^{i}Pr_3P$ (0.003 g, 0.02 mmol, 0.2 equiv) in THF (2 mL) was added ferrocene (0.097 g, 0.53 mmol, 5 equiv). After the mixture stirred for 1 min, **1** (0.025 g, 0.11 mmol, 1 equiv) was added. After the solution stirred for 45 min, an aliquot was transferred to an NMR tube for NMR analysis. No phosphinidene transfer to ferrocene was observed (Fig. S.60). Instead, phosphatetrahedrane dimers and phosphinidene transfer to 1,5-cyclooctadiene were observed.

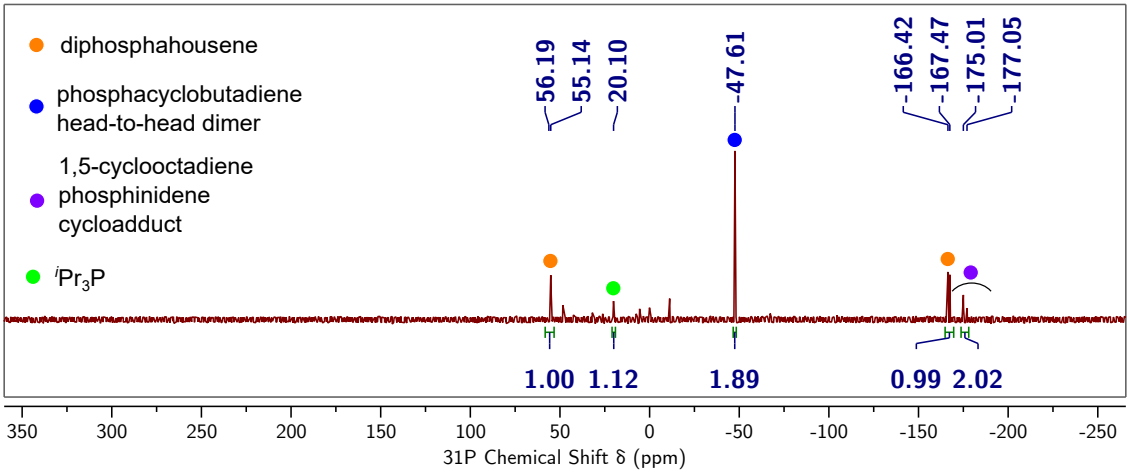

Figure S.60: $^{31}P\{^{1}H\}$ NMR (162 MHz, THF, 25 °C) spectrum of the crude reaction mixture 45 min after treating $(^{t}BuC)_3P$ with ferrocene under catalytic conditions.

S.1.10 Attempted Phosphinidene Transfer to 1,1-Difluoro-2-vinyl-cyclopropane (Radical Clock)

To a stirring solution of $Ni(COD)_2$ (0.006 g, 0.02 mmol, 0.2 equiv) and $^{i}Pr_3P$ (0.003 g, 0.02 mmol, 0.2 equiv) in THF (2 mL) was added 1,1-difluoro-2-vinyl-cyclopropane (0.055 g, 0.53 mmol, 5 equiv). After the red solution stirred for 1 min, compound **1** (0.025 g, 0.11 mmol, 1 equiv) was added. After 45 min, an aliquot of the orange solution was transferred to an NMR tube for NMR analysis. The reaction mixture contains a significant amount of unreacted **1** (Fig. S.61). $^{19}F\{^{1}H\}$ NMR spectroscopy revealed partial decomposition of 1,1-difluoro-2-vinyl-cyclopropane (Fig. S.62). Partial decomposition of 1,1-difluoro-2-vinyl-cyclopropane was also observed when this reaction was repeated in the absence of **1** (Fig. S.63)

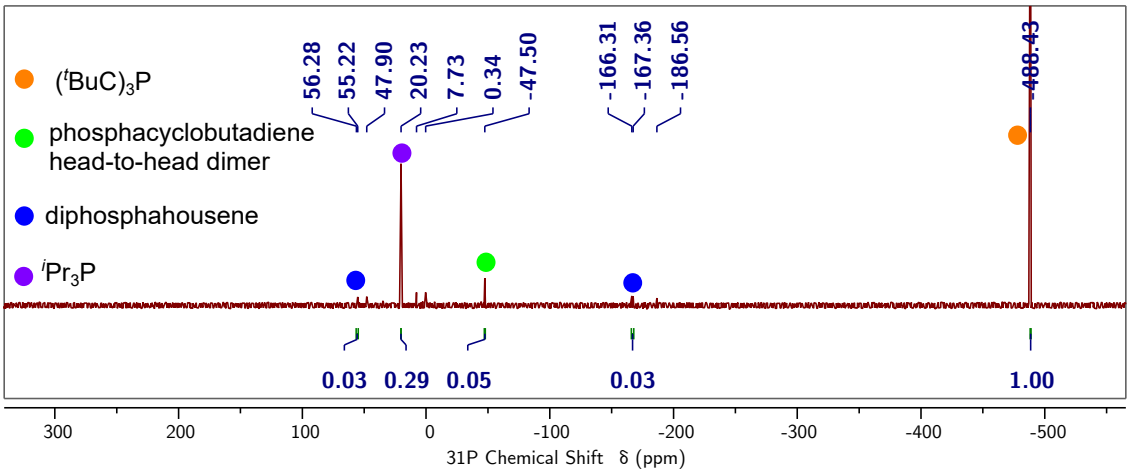

Figure S.61: $^{31}P\{^{1}H\}$ NMR (162 MHz, THF, 25 °C) spectrum of the crude reaction mixture 45 min after treating (^{t}BuC)$_3$P with 1,1-difluoro-2-vinyl-cyclopropane under catalytic conditions.

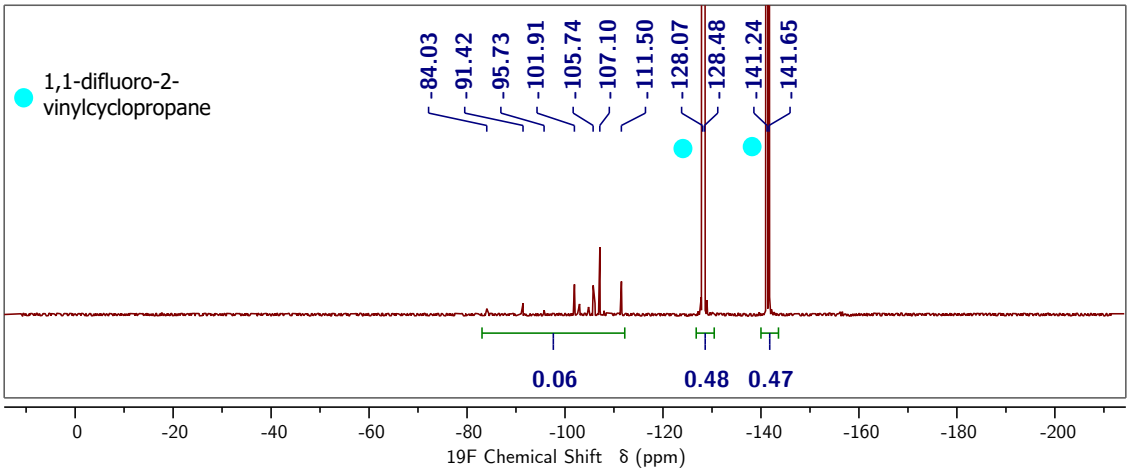

Figure S.62: $^{19}F\{^{1}H\}$ NMR (377 MHz, THF, 25 °C) spectrum of the crude reaction mixture 45 min after treating $(^{t}BuC)_3P$ with 1,1-difluoro-2-vinyl-cyclopropane under catalytic conditions.

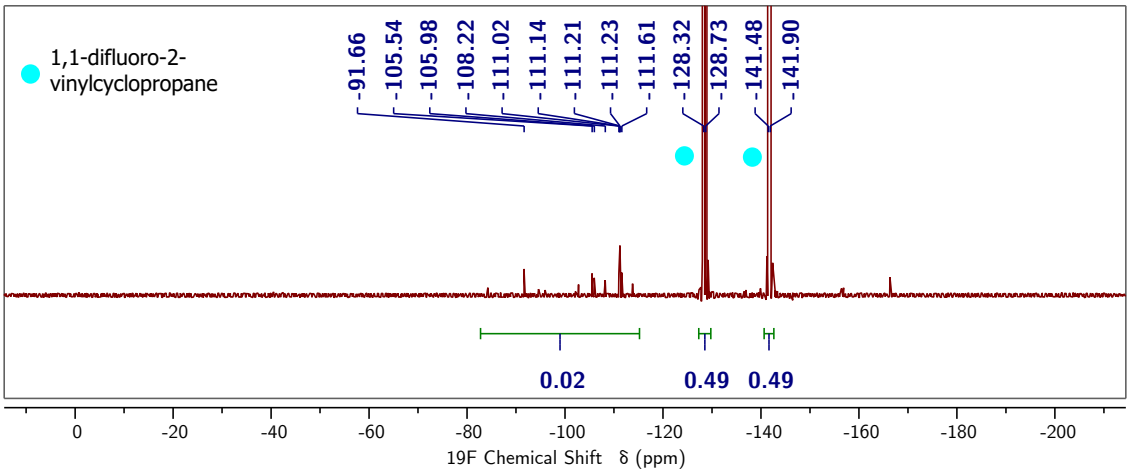

Figure S.63: $^{19}F\{^{1}H\}$ NMR (377 MHz, THF, 25 °C) spectrum of the crude reaction mixture 30 min after combining 1,1-difluoro-2-vinyl-cyclopropane with $Ni(COD)_2$ and $^{i}Pr_3P$.

S.1.11 Generation of Phosphirane and Isolation of 8·W(CO)$_5$

To a stirring solution of **6**-H (0.040 g, 0.15 mmol, 1.0 equiv) in THF (2 mL) was added a solution of HOTf (0.027 g, 0.18 mmol, 1.2 equiv) in THF (1 mL) dropwise. After the cloudy solution stirred for 5 min, it was passed through a glass pipette plugged with glass microfiber filter paper. NMR spectra of the filtrate revealed clean formation of phosphirane (**8**, Fig. S.64) and match reported spectra of the molecule.[12] Additionally, the colorless solids collected on the filter paper correspond to [^{t}Bu$_3$C$_3$]OTf, as assessed by NMR spectroscopy (Fig. S.65-S.67). [^{t}Bu$_3$C$_3$]OTf was also prepared by combining [^{t}Bu$_3$C$_3$]BF$_4$ with trimethylsilyl triflate and its synthesis and characterization are described in section S.1.13. A stirbar was added to the colorless filtrate and a freshly prepared THF solution of (CO)$_5$W(THF) (6 mL, 0.025 M, 1 equiv; see section S.1.11.1) was added with stirring. After the yellow solution stirred for 30 min, it was concentrated to ca. 0.1 mL under reduced pressure. The yellow solution was diluted with pentane (1 mL) and passed through a pipette plugged with glass microfiber filter paper and a two-inch plug of silica. The plug was washed with additional pentane (2 mL) and the combined filtrates were brought to constant mass under reduced pressure. The resulting white solids were transferred to a sublimator and heated (60 °C) under reduced pressure (ca. 150 mTorr). The sublimator was brought back into the glovebox where the coldfinger was washed with a minimal amount of pentane (0.5 mL) and all volatile materials were removed from the pentane solution under reduced pressure, providing a mixture of **8**·W(CO)$_5$ and trace W(CO)$_6$ as a colorless solid (0.025 g, 0.065 mmol, 43%). NMR spectra of **8**·W(CO)$_5$ (Fig. S.68-S.70) match reported spectra of the molecule.[13,14] Attempts to separate **8**·W(CO)$_5$ from W(CO)$_6$ by sublimation were unsuccessful.

NMR data for **8**: ^{31}P{^{1}H} NMR (162 MHz, THF, 25 °C, Fig. S.64) δ −310.62 (dtt, J_{PH} = 157.5, 16.5, and 2.8 Hz) ppm.

NMR data for **8**·W(CO)$_5$: ^{1}H NMR (500 MHz, chloroform-*d*, 25 °C, Fig. S.68) δ 1.99 (dm, $^1J_{PH}$ = 350.2 Hz, 1H), 1.68 (m, 2H), 1.13 (m, 2H) ppm. ^{13}C{^{1}H} NMR (126 MHz, chloroform-*d*, 25 °C, Fig. S.69) δ 197.18 (d, $^2J_{PC}$ = 32.2 Hz), 195.04 (d, $^2J_{PC}$ = 8.3 Hz),

3.41 (d, $^{1}J_{PC}$ = 10.3 Hz) $^{31}P\{^{1}H\}$ NMR (162 MHz, chloroform-*d*, 25 °C, Fig. S.70) δ −253.2 ($^{1}J_{WP}$ = 255.1 Hz) ppm.

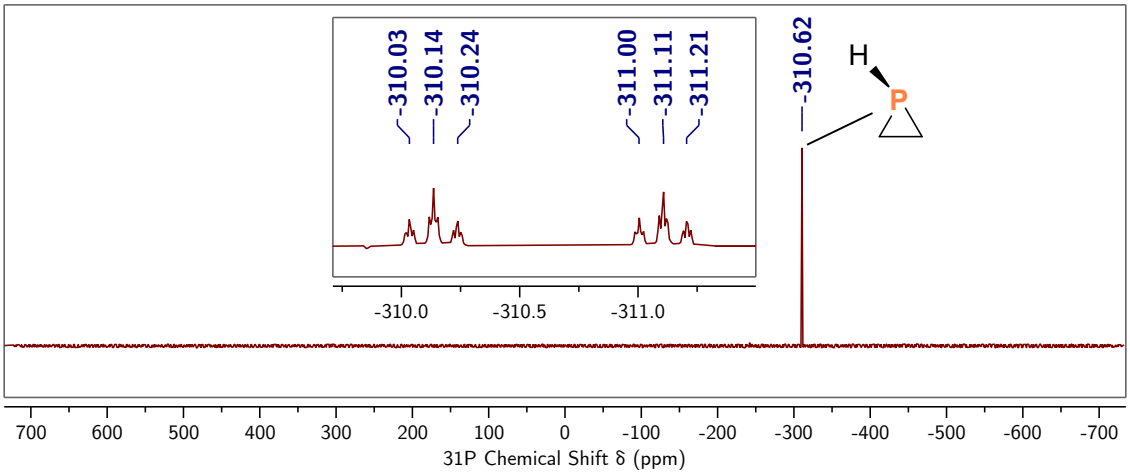

Figure S.64: $^{31}P\{^{1}H\}$ NMR (162 MHz, THF, 25 °C) spectrum of **8**. Inset shows the corresponding proton-coupled ^{31}P NMR spectrum.

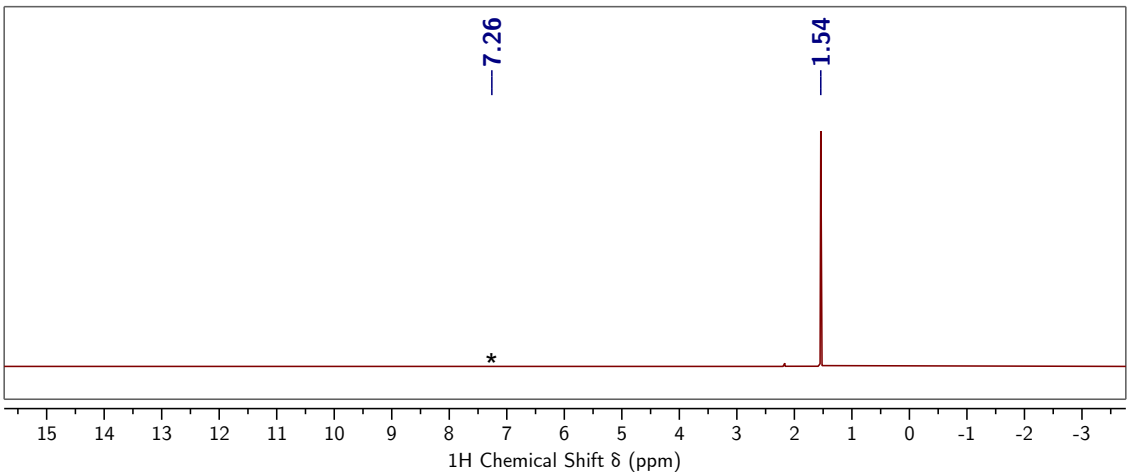

Figure S.65: ^{1}H NMR (400 MHz, chloroform-*d*, 25 °C) spectrum of [$^{t}Bu_3C_3$]OTf. * marks chloroform-*d*.

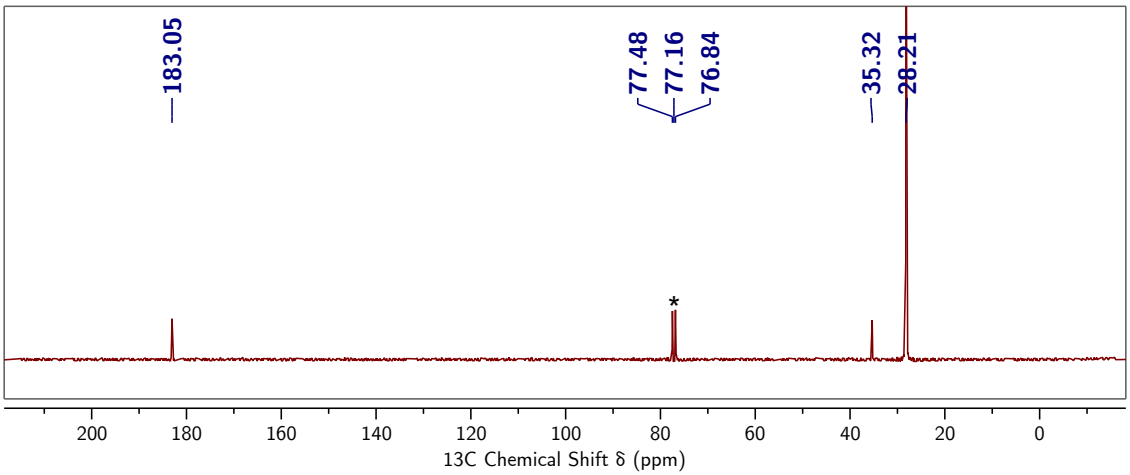

Figure S.66: $^{13}C\{^{1}H\}$ NMR (101 MHz, chloroform-*d*, 25 °C) spectrum of $[^{t}Bu_3C_3]OTf$. * marks chloroform-*d*.

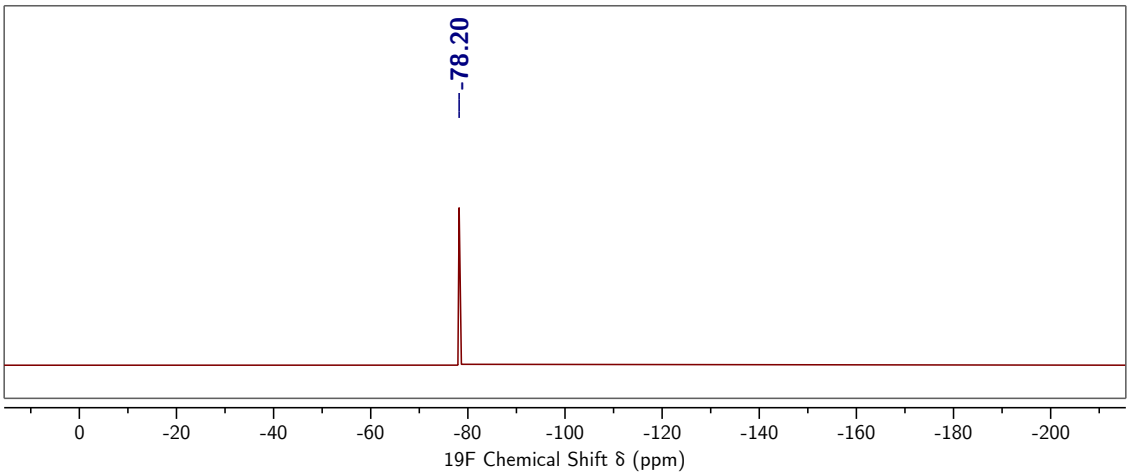

Figure S.67: $^{19}F\{^{1}H\}$ NMR (471 MHz, chloroform-*d*, 25 °C) spectrum of $[^{t}Bu_3C_3]OTf$.

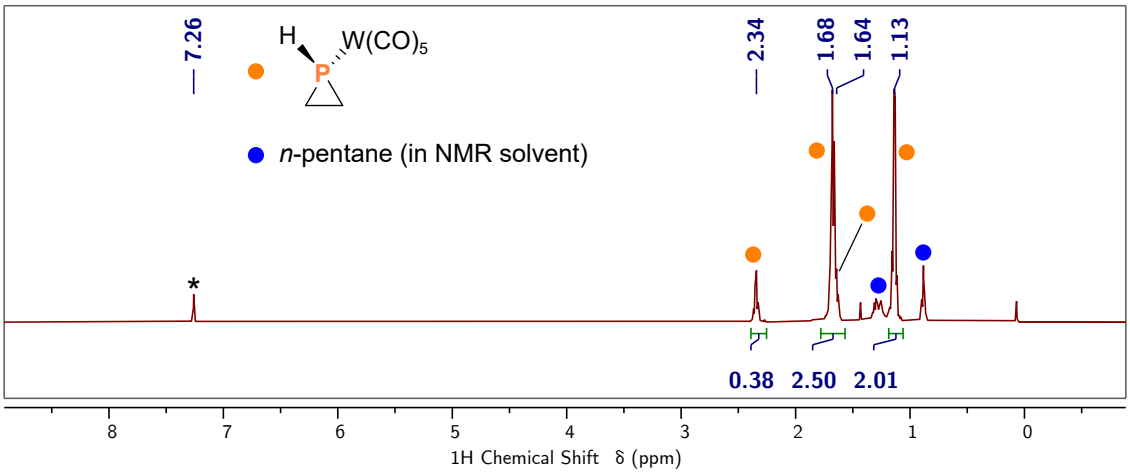

Figure S.68: ^{1}H NMR (500 MHz, chloroform-*d*, 25 °C) spectrum of **8**·$W(CO)_5$. * marks chloroform-*d*.

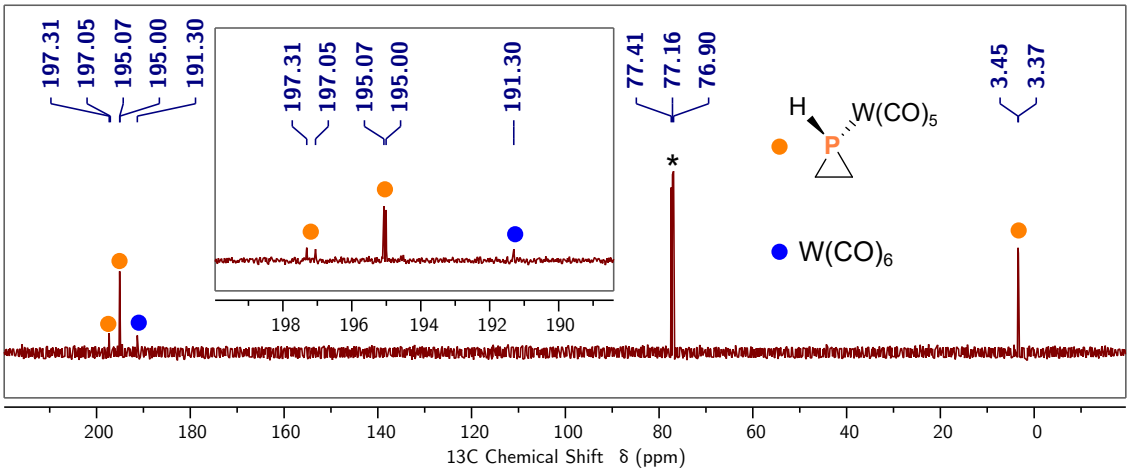

Figure S.69: $^{13}C\{^1H\}$ NMR (101 MHz, chloroform-*d*, 25 °C) spectrum of **8**·W(CO)$_5$ and trace W(CO)$_6$. Inset shows a zoomed-in region of the NMR spectrum. * marks chloroform-*d*.

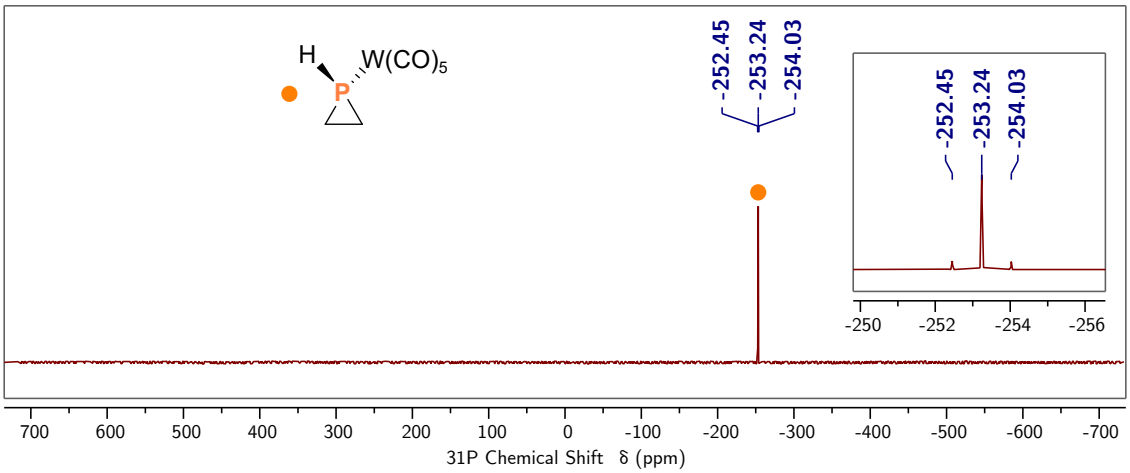

Figure S.70: $^{31}P\{^1H\}$ NMR (162 MHz, chloroform-*d*, 25 °C) spectrum of **8**·W(CO)$_5$. Inset shows a zoomed-in region of the NMR spectrum.

S.1.11.1 Preparation of (THF)W(CO)$_5$

A solution of tungsten hexacarbonyl (0.052 g, 0.15 mmol) in THF (6 mL) was prepared and transferred to a Schlenk flask (100 mL). The solution was degassed by three freeze-pump-thaw cycles and irradiated with UV light for 2 h. The yellow solution was degassed, using the same method, and irradiated for an additional 20 h. The solution was used immediately afterwards.

S.1.11.2 Quantification of Conversion to 8 using an Internal Standard

Prior to running this experiment, spin-lattice decay constants (T_1) were measured using an inversion recovery pulse sequence and T_1 times of approximately 1.8 s, 1.8 s, and 3.2 s were found for the phosphorus nucleus of Ph_3P (−5.45 ppm in THF), **6**-H (−221.70 ppm in THF), and **8** (−310.78 ppm in THF), respectively (Fig. S.73). Therefore, all $^{31}P\{^1H\}$ NMR spectra were recorded with the relaxation delay set to 30 s to obtain quantitative $^{31}P\{^1H\}$ NMR spectra. Compound **6**-H (0.020 g, 0.076 mmol, 1.0 equiv) was dissolved in THF (1 mL) and the solution was transferred to a J Young tube containing flame-sealed capillary charged with a solution of triphenylphosphine (0.52 M) and chromium(III) acetylacetonate (0.015 M), which functions as a paramagnetic relaxation agent.[15] The tube was sealed and an initial $^{31}P\{^1H\}$ NMR spectrum was collected (Fig. S.71). The tube was brought back into the glovebox where HOTf (0.014 g, 0.091 mmol, 1.2 equiv) was added to the solution. The tube was sealed and shaken, resulting in the rapid precipitation of [^{t}Bu$_3$C$_3$]OTf. After the sample sat for 10 min, a $^{31}P\{^1H\}$ NMR spectrum was collected (Fig. S.72). The $^{31}P\{^1H\}$ NMR spectrum shows 92% conversion to **8**.

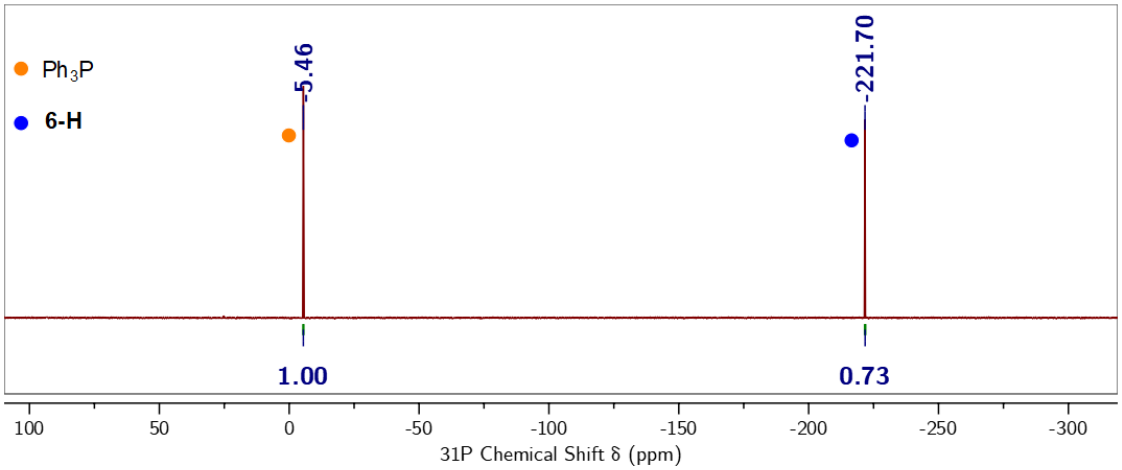

Figure S.71: Quantitative $^{31}P\{^{1}H\}$ NMR (162 MHz, THF, 25 °C) spectrum before the addition of HOTf.

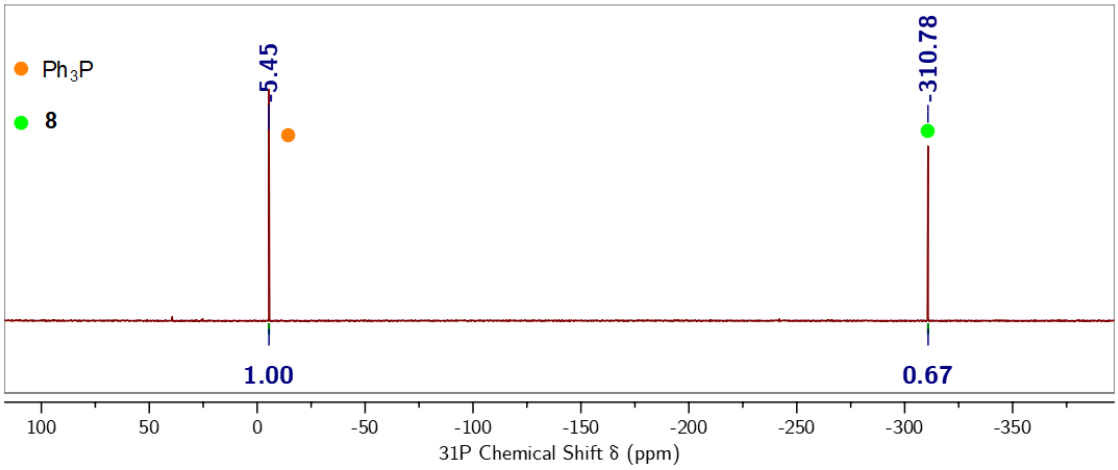

Figure S.72: Quantitative $^{31}P\{^{1}H\}$ NMR (162 MHz, THF, 25 °C) spectrum 10 min after the addition of HOTf.

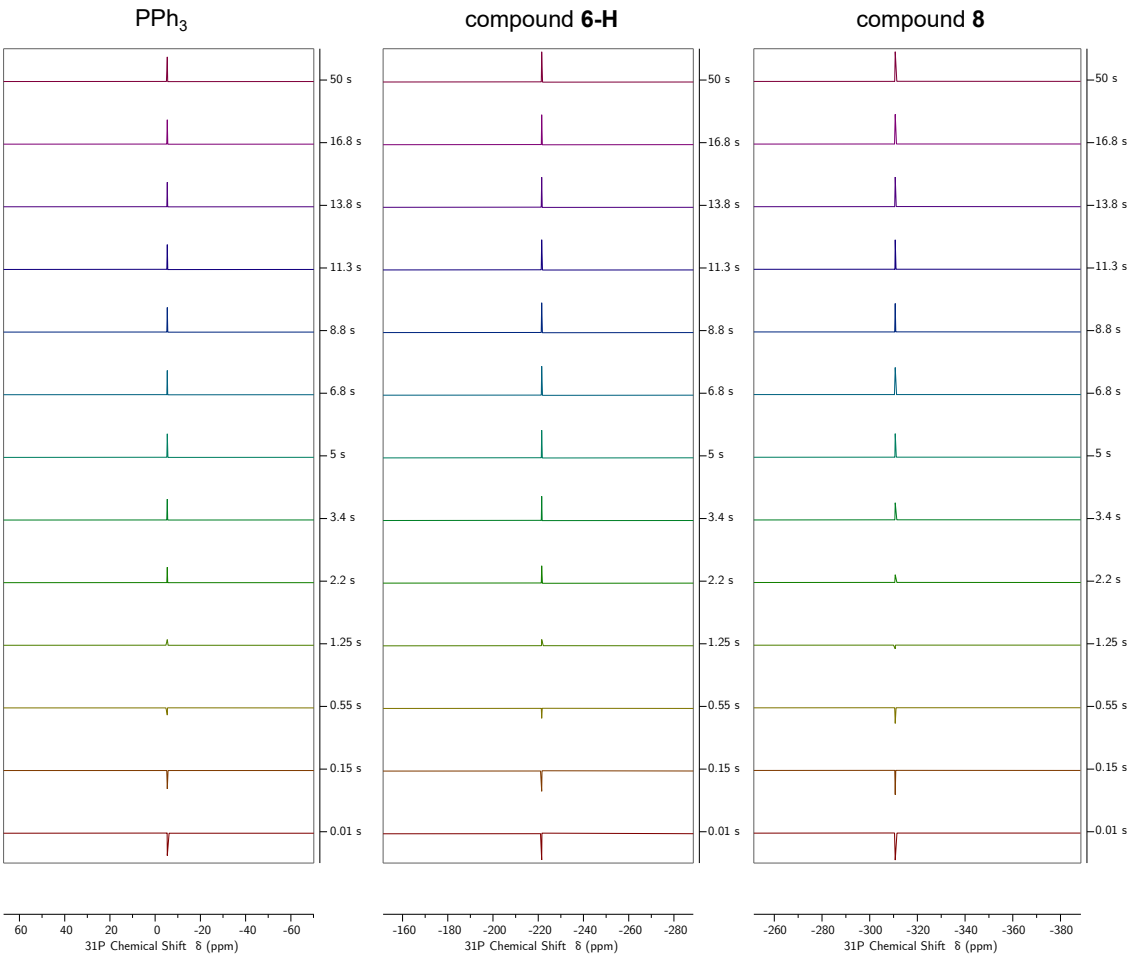

Figure S.73: Array of $^{31}P\{^{1}H\}$ NMR spectra of the species studied by the inversion recovery experiment.

S.1.12 Treatment of 6-Ph with HOTf

All $^{31}P\{^{1}H\}$ NMR spectra were recorded with the relaxation delay set to 30 s, allowing us to quantify conversion by integration of the products' resonances against that of Ph_3P. Compound **6**-Ph (0.026 g, 0.076 mmol, 1.0 equiv) was dissolved in THF (1 mL) and the solution was transferred to a J Young tube containing flame-sealed capillary charged with a solution of triphenylphosphine (0.52 M) and chromium(III) acetylacetonate (0.015 M). The tube was sealed and an initial $^{31}P\{^{1}H\}$ NMR spectrum was collected (Fig. S.74). The tube was brought back into the glovebox where HOTf (0.014 g, 0.091 mmol, 1.2 equiv) was added to the solution. The tube was sealed and shaken, resulting in the rapid precipitation of $[^{t}Bu_3C_3]OTf$. After the sample sat for 10 min, a $^{31}P\{^{1}H\}$ NMR spectrum was collected (Fig. S.75). Deprotection of **6**-Ph proceeds quantitatively, resulting in the two isomers (*cis*-**9** and *trans*-**9**) depicted in Fig. S.75. Our assignments are supported by the ^{31}P NMR spectra depicted in Fig. S.76 and S.77.

NMR data for *cis*-**9**: ^{31}P NMR (162 MHz, THF, 25 °C, Fig. S.76) δ −235.80 (dt, J_{PH} = 160.3, 15.8 Hz) ppm

NMR data for *trans*-**9**: ^{31}P NMR (162 MHz, chloroform-*d*, 25 °C, Fig. S.77) δ −269.42 (dd, J_{PH} = 157.9, 19.4 Hz) ppm.

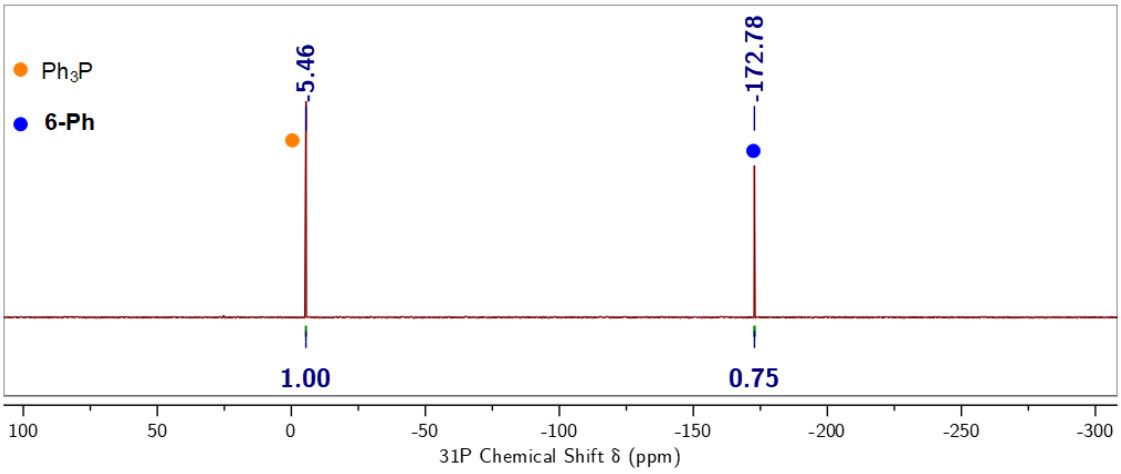

Figure S.74: $^{31}P\{^{1}H\}$ NMR (162 MHz, THF, 25 °C) spectrum before the addition of HOTf. The relaxation delay was set to 30 s.

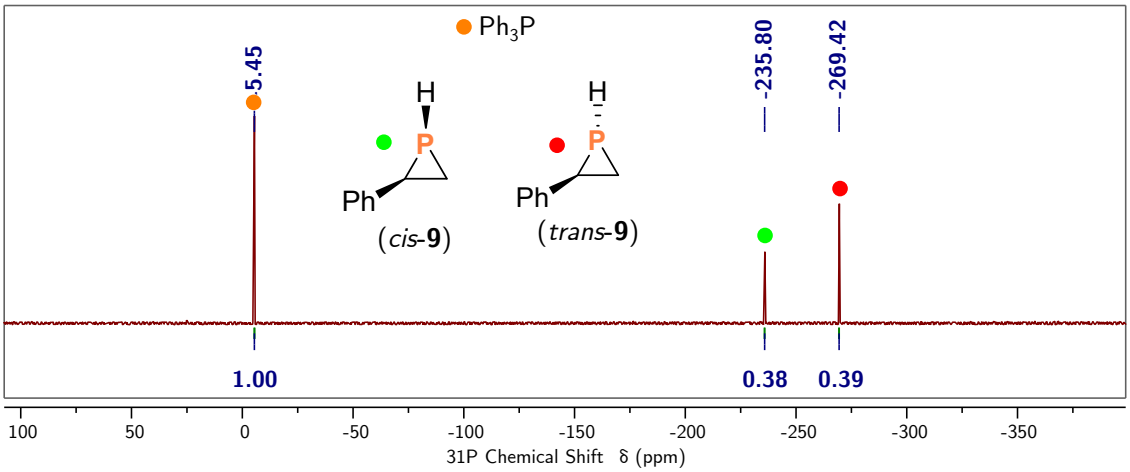

Figure S.75: Quantitative $^{31}P\{^{1}H\}$ NMR (162 MHz, THF, 25 °C) spectrum 10 min after the addition of HOTf. The relaxation delay was set to 30 s.

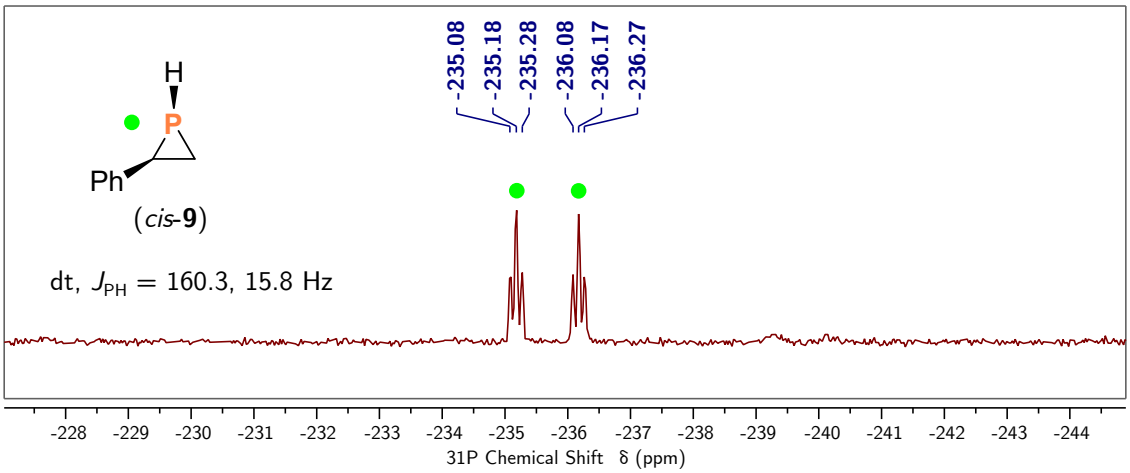

Figure S.76: ^{31}P NMR (162 MHz, THF, 25 °C) spectrum *cis*-**9**.

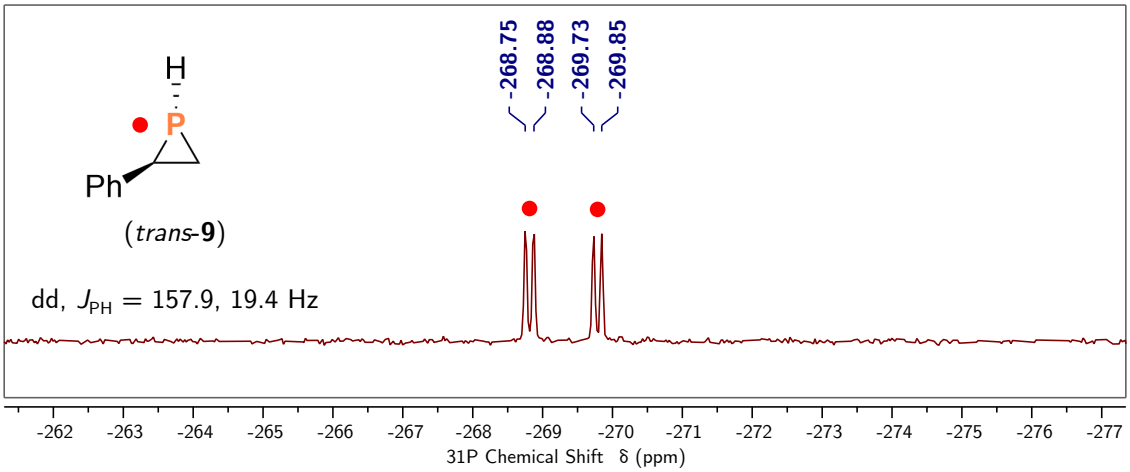

Figure S.77: ^{31}P NMR (162 MHz, THF, 25 °C) spectrum of *trans*-**9**.

S.1.13 Synthesis of [^{t}Bu$_3$C$_3$]OTf

To a stirring dichloromethane (4 mL) solution of [^{t}Bu$_3$C$_3$]BF$_4$ (0.100 g, 0.340 mmol, 1.0 equiv) was added a dichloromethane (2 mL) solution of trimethylsilyl triflate (0.076 g, 0.34 mmol, 1.0 equiv) dropwise. After the solution stirred for 30 min, all volatile materials were removed under reduced pressure. The resulting colorless solids were triturated with diethyl ether (2 × 4 mL). Crystallization from a solution of dichloromethane (1 mL) layered with diethyl ether (3 mL) afforded colorless crystals of [^{t}Bu$_3$C$_3$]OTf (0.056 g, 0.18 mmol, 53%). Elem. Anal. Calc'd(found) for $C_{16}H_{27}F_3O_3S$: C 53.91(54.01), H 7.64(7.63). ^{1}H NMR (400 MHz, chloroform-*d*, 25 °C, Fig. S.78) δ 1.56 ppm. ^{13}C{^{1}H} NMR (101 MHz, chloroform-*d*, 25 °C, Fig. S.79) δ 182.89, 35.35, 28.31 ppm. ^{19}F{^{1}H} NMR (377 MHz, chloroform-*d*, 25 °C, Fig. S.80) δ 78.37 ppm.

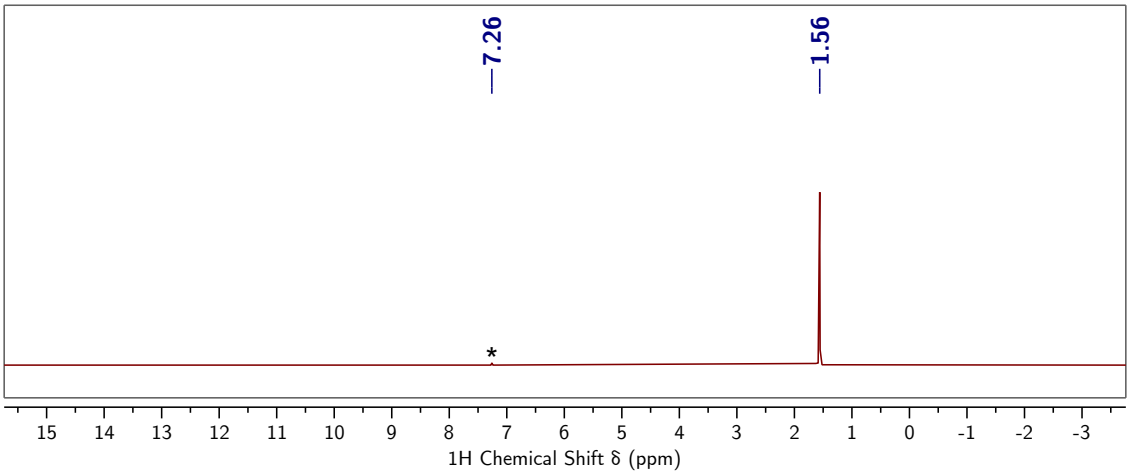

Figure S.78: ^{1}H NMR (400 MHz, chloroform-*d*, 25 °C) spectrum of [^{t}Bu$_3$C$_3$]OTf. * marks chloroform-*d*.

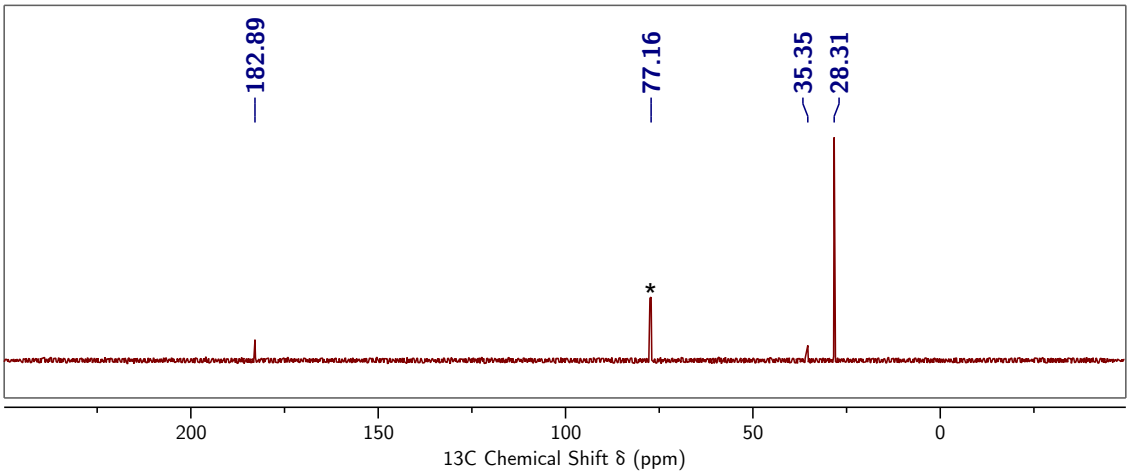

Figure S.79: $^{13}C\{^1H\}$ NMR (101 MHz, chloroform-*d*, 25 °C) spectrum of [^{t}Bu$_3$C$_3$]OTf. * marks chloroform-*d*.

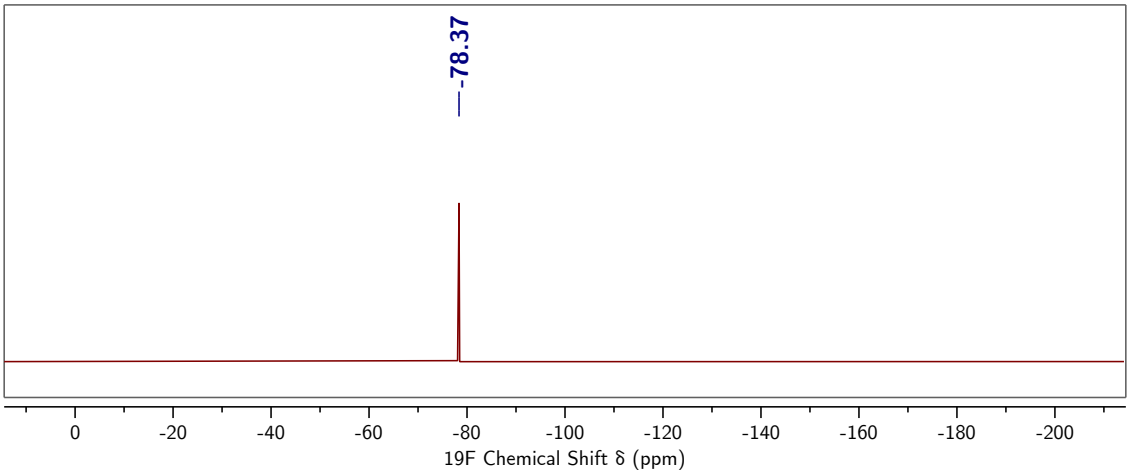

Figure S.80: $^{19}F\{^1H\}$ NMR (377 MHz, chloroform-*d*, 25 °C) spectrum of [^{t}Bu$_3$C$_3$]OTf.

S.2 X-Ray Diffraction Studies

Low-temperature (100 K) diffraction data were collected on a Bruker-AXS X8 Kappa Duo diffractometer with $I\mu S$ micro-sources, coupled to a Photon 3 CPAD detector using Mo K_α radiation ($\lambda = 0.71073$ Å) for the structures of **3** and **6**-Ph and a Smart APEX2 CCD detector using Cu K_α radiation ($\lambda = 1.54178$ Å) for the structure of **5**, performing ϕ- and ω-scans. The structures were solved by dual-space methods using SHELXT[16] and refined against F^2 on all data by full-matrix least squares with SHELXL-2017[17] following established refinement strategies.[18] All non-hydrogen atoms were refined anisotropically. All hydrogen atoms were included into the model at geometrically calculated positions and refined using a riding model. The isotropic displacement parameters of all hydrogen atoms were fixed to 1.2 times the U-value of the atoms they are linked to (1.5 times for methyl groups). Details of the data quality and a summary of the residual values of the refinement are listed in tables S.2-S.4. Further details can be found in the form of .cif files available from the CCDC.

Compound **3** crystallizes in the monoclinic space group $P2_1$ with one molecule of **3** in the asymmetric unit. The molecule exhibits no disorder. Compound **5** crystallizes in the tetragonal space group $P4_2/n$ with one molecule of **5** in the asymmetric unit. The structure was disordered over three positions and refined with the help of similarity restraints on 1−2 and 1−3 positions and displacement parameters. The disorder ratios were refined freely and converged at 0.566(0.001), 0.186(0.001), and 0.247(0.001), respectively. The twin law that corresponds to a 180° rotation about the crystallographic a-axis was applied and the twin ratio refined to 0.496(1). Compound **6**-Ph crystallizes in the triclinic space group $P\bar{1}$ with one molecule of **6**-Ph in the asymmetric unit. The crystal was twinned; therefore, the orientation matrices for three components were determined using CELL_NOW[19] and the twin ratios refined to 0.37(1) and 0.21(2). The molecule exhibits no disorder.

Table S.2: Crystallographic Data for **3**

Reciprocal Net code / CCDC	P8_20084 / 2102704
Empirical formula, FW (g/mol)	$C_{36}H_{68}N_3PSi_3$, 658.17
Color / Morphology	Red / Block
Crystal size (mm^3)	$0.215 \times 0.180 \times 0.125$
Temperature (K)	100(2)
Wavelength (Å)	0.71073
Crystal system, Space group	Monoclinic, $P2_1$
Unit cell dimensions (Å, °)	$a = 9.3621(2)$, $\alpha = 90$
	$b = 19.3974(4)$, $\beta = 90.5410(10)$
	$c = 11.2144(3)$, $\gamma = 90$
Volume ($Å^3$)	2036.45(8)
Z	2
Density (calc., g/cm^3)	1.073
Absorption coefficient (mm^{-1})	0.182
$F(000)$	724
Theta range for data collection (°)	1.816 to 33.210
Index ranges	$-14 \leq h \leq 14$, $-29 \leq k \leq 29$,
	$-17 \leq l \leq 17$
Reflections collected	123448
Independent reflections, R_{int}	15631, 0.0346
Completeness to $\theta_{\max}$ (%)	100.0
Absorption correction	Semi-empirical from equivalents
Refinement method	Full-matrix least-squares on F^2
Data / Restraints / Parameters	15631 / 1 / 409
Goodness-of-fit[a]	1.050
Final R indices[b] $[I > 2\sigma(I)]$	$R_1 = 0.0237$, $wR_2 = 0.0614$
R indices[b] (all data)	$R_1 = 0.0258$, $wR_2 = 0.0630$
Largest diff. peak and hole ($e \cdot Å^{-3}$)	0.247 and −0.170

[a] GooF $= \sqrt{\frac{\Sigma[w(F_o^2 - F_c^2)^2]}{(n-p)}}$ [b] $R_1 = \frac{\Sigma||F_o| - |F_c||}{\Sigma|F_o|}$; $wR_2 = \sqrt{\frac{\Sigma[w(F_o^2 - F_c^2)^2}{\Sigma[w(F_o^2)^2]}}$; $w = \frac{1}{\sigma^2(F_o^2) + (aP)^2 + bP}$; $P = \frac{2F_c^2 + \max(F_o^2, 0)}{3}$

Table S.3: Crystallographic Data for **5**

Reciprocal Net code / CCDC	X8_21017 / 2118437
Empirical formula, FW (g/mol)	$C_{30.94}H_{56}P_2$, 489.98
Color / Morphology	Colorless / Needle
Crystal size (mm^3)	$0.350 \times 0.050 \times 0.045$
Temperature (K)	100(2)
Wavelength (Å)	1.54178
Crystal system, Space group	Tetragonal, $P4_2/n$
Unit cell dimensions (Å, °)	$a = 26.7457(5)$, $\alpha = 90$
	$b = 26.7457(5)$, $\beta = 90$
	$c = 9.0128(3)$, $\gamma = 90$
Volume ($Å^3$)	6447.1(3)
Z	8
Density (calc., g/cm^3)	1.010
Absorption coefficient (mm^{-1})	1.313
$F(000)$	2173
Theta range for data collection (°)	1.652 to 69.871
Index ranges	$-32 \leq h \leq 29$, $-32 \leq k \leq 28$,
	$-10 \leq l \leq 10$
Reflections collected	57069
Independent reflections, R_{int}	6053, 0.0502
Completeness to $\theta_{\max}$ (%)	99.9
Absorption correction	Semi-empirical from equivalents
Refinement method	Full-matrix least-squares on F^2
Data / Restraints / Parameters	6053 / 3772 / 950
Goodness-of-fit[a]	1.065
Final R indices[b] $[I > 2\sigma(I)]$	$R_1 = 0.0450$, $wR_2 = 0.1195$
R indices[b] (all data)	$R_1 = 0.0497$, $wR_2 = 0.1234$
Largest diff. peak and hole ($e \cdot Å^{-3}$)	0.202 and −0.137

[a] GooF $= \sqrt{\frac{\Sigma[w(F_o^2-F_c^2)^2]}{(n-p)}}$ [b] $R_1 = \frac{\Sigma||F_o|-|F_c||}{\Sigma|F_o|}$; $wR_2 = \sqrt{\frac{\Sigma[w(F_o^2-F_c^2)^2}{\Sigma[w(F_o^2)^2]}}$; $w = \frac{1}{\sigma^2(F_o^2)+(aP)^2+bP}$; $P = \frac{2F_c^2+\max(F_o^2,0)}{3}$

Table S.4: Crystallographic Data for **6**-Ph

Reciprocal Net code / CCDC	P8_21103 / 2102709
Empirical formula, FW (g/mol)	$C_{23}H_{35}P$, 342.48
Color / Morphology	Colorless / Blade
Crystal size (mm^3)	$0.150 \times 0.050 \times 0.030$
Temperature (K)	100(2)
Wavelength (Å)	0.71073
Crystal system, Space group	Triclinic, $P\bar{1}$
Unit cell dimensions (Å, °)	$a = 8.7555(9)$, $\alpha = 90.211(3)$
	$b = 8.7781(8)$, $\beta = 101.363(3)$
	$c = 15.8058(18)$, $\gamma = 118.799(3)$
Volume ($Å^3$)	1036.77(19)
Z	2
Density (calc., g/cm^3)	1.097
Absorption coefficient (mm^{-1})	0.134
$F(000)$	376
Theta range for data collection (°)	1.323 to 32.090
Index ranges	$-13 \leq h \leq 12$, $-13 \leq k \leq 13$,
	$0 \leq l \leq 23$
Reflections collected	7230
Independent reflections, R_{int}	7230, 0.0489
Completeness to $\theta_{\max}$ (%)	100.0
Absorption correction	Semi-empirical from equivalents
Refinement method	Full-matrix least-squares on F^2
Data / Restraints / Parameters	7230 / 0 / 228
Goodness-of-fit[a]	1.092
Final R indices[b] $[I > 2\sigma(I)]$	$R_1 = 0.0495$, $wR_2 = 0.1005$
R indices[b] (all data)	$R_1 = 0.0644$, $wR_2 = 0.1080$
Largest diff. peak and hole ($e \cdot Å^{-3}$)	0.736 and −0.327

[a] GooF $= \sqrt{\frac{\Sigma[w(F_o^2 - F_c^2)^2]}{(n-p)}}$ [b] $R_1 = \frac{\Sigma||F_o| - |F_c||}{\Sigma|F_o|}$; $wR_2 = \sqrt{\frac{\Sigma[w(F_o^2 - F_c^2)^2}{\Sigma[w(F_o^2)^2]}}$; $w = \frac{1}{\sigma^2(F_o^2) + (aP)^2 + bP}$; $P = \frac{2F_c^2 + \max(F_o^2, 0)}{3}$

S.3 Computational Details

S.3.1 Bonding Analysis for 3

Calculations were performed with a development version of the ORCA program package based on version 4.2.[20,21] Coordinates for **3** were obtained from a single crystal X-ray diffraction experiment (see section S.2). Intrinsic bond orbitals (IBOs)[22] were generated at the B3LYP-D3(BJ)/def2-TZVP(-f) level of theory[23–25] using the following input file:

```
!B3LYP D3BJ Def2-TZVP(-f) Def2/J RIJCOSX TightSCF Grid4 FinalGrid5 GridX4
%pal nprocs 16 end
%loc LocMet IAOIBO end
%maxcore 8000
*xyzfile 0 1 model.xyz
```

The IBO corresponding to the phosphasilene π bond is depicted in Fig. S.81. Orbital coefficients of 0.78 and 0.18 were found for phosphorus and silicon, respectively.

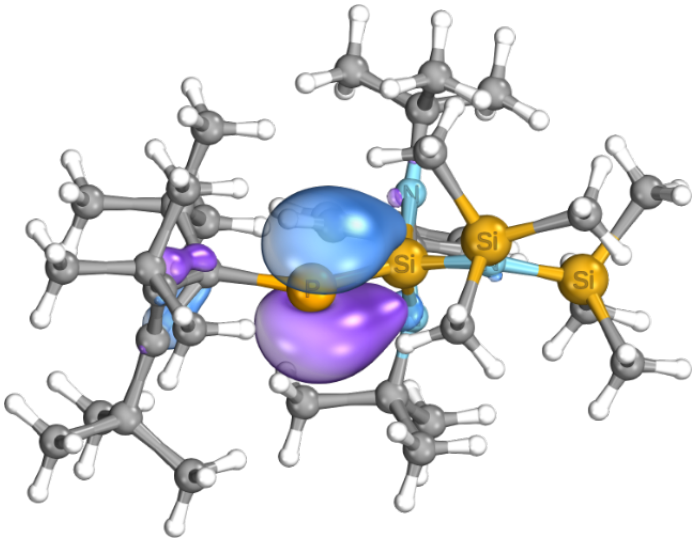

Figure S.81: Intrinsic bond orbital corresponding to the phosphasilene π bond found in **3**.

S.3.2 Mechanism for the Formation of 6-H

Geometry optimization and frequency calculations were performed with the Gaussian 16 Rev C.01 quantum chemistry package.[26] All geometries were optimized at B3LYP-D3(BJ)/def2-TZVP level of theory.[23–25] In all cases, computed electronic energies were corrected for thermal energy to obtain the corresponding free energy (T = 298.15 K). To disclose the nature of all stationary points we computed the corresponding frequencies (Nimag=0 for minima and 1 for transition states). All electronic energies were augmented with higher level DLPNO-CCSD(T)/cc-pVTZ energies.[27–29] These calculations were performed with a development version of the ORCA program package based on version 5.0.[20,21,30] The results are summarized in Fig. S.82. Cartesian coordinates of the optimized geometries are also provided. Displacement vectors for **TS2** are shown in Fig. S.83. Attempts to locate a transition state that connects **Ni·THD** to **Int2** were unsuccessful.

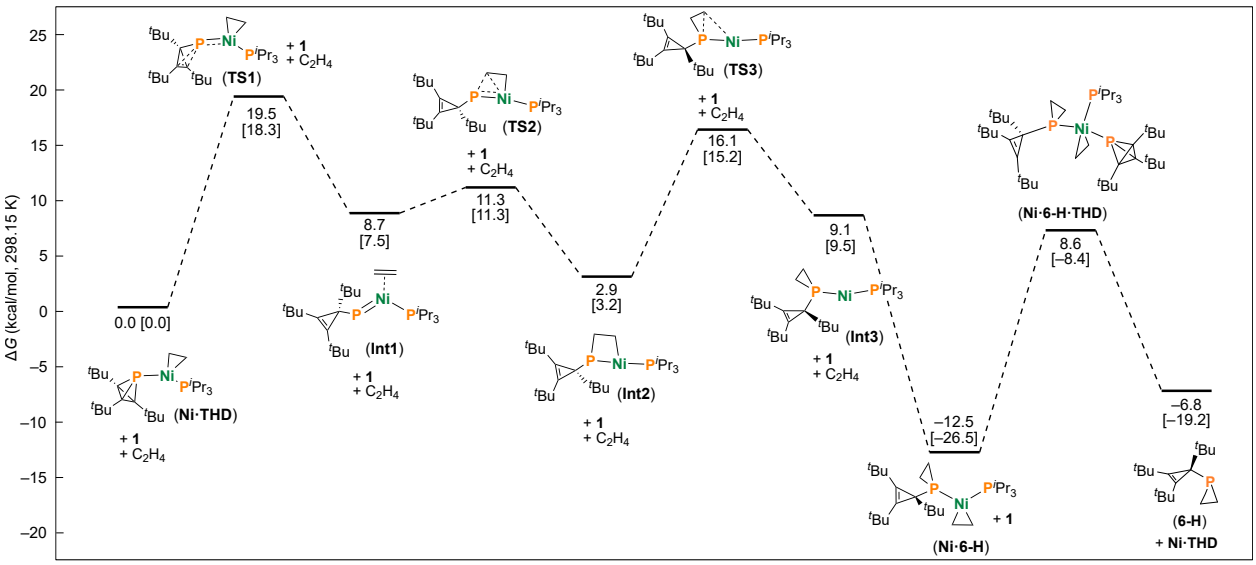

Figure S.82: Calculated stationary points and transition states and their relative free energies (298.15 K) involved in the nickel-catalyzed phosphinidene transfer to ethylene. Enthalpies are given in brackets.

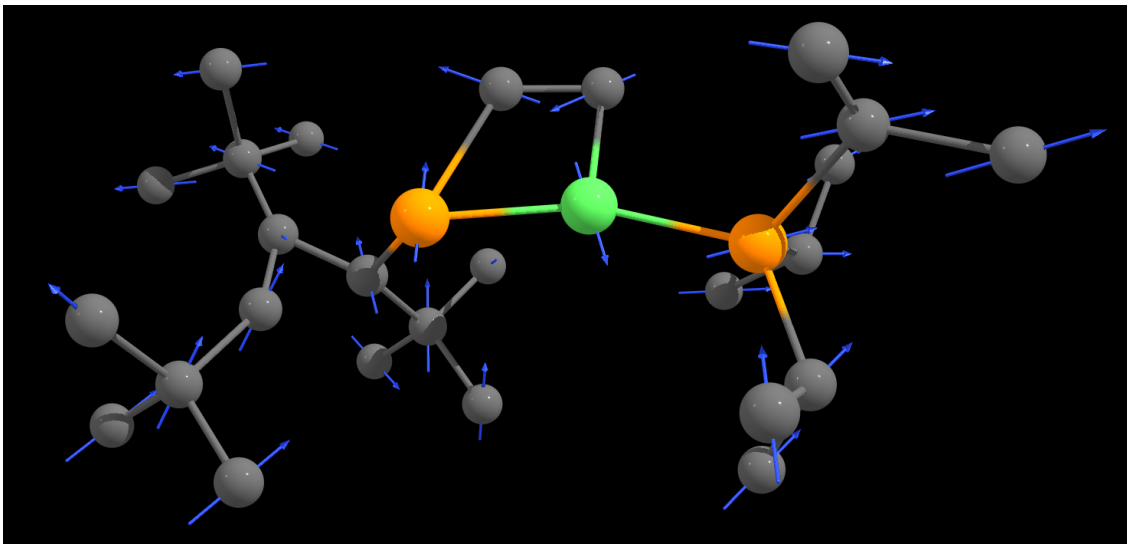

Figure S.83: Displacement vectors for **TS2**. Hydrogen atoms have been omitted for clarity.

References

(1) Pangborn, A. B.; Giardello, M. A.; Grubbs, R. H.; Rosen, R. K.; Timmers, F. J. Safe and Convenient Procedure for Solvent Purification. *Organometallics* **1996**, *15*, 1518–1520.

(2) Williams, D. B. G.; Lawton, M. Drying of Organic Solvents: Quantitative Evaluation of the Efficiency of Several Desiccants. *J. Org. Chem.* **2010**, *75*, 8351–8354.

(3) Riu, M.-L. Y.; Eckhardt, A. K.; Cummins, C. C. Dimerization and Cycloaddition Reactions of Transient Tri-*tert*-butylphosphacyclobutadiene Generated by Lewis Acid Induced Isomerization of Tri-*tert*-butylphosphatetrahedrane. *J. Am. Chem. Soc.* **2021**, *143*, 13005–13009.

(4) Swarnakar, A. K.; McDonald, S. M.; Deutsch, K. C.; Choi, P.; Ferguson, M. J.; McDonald, R.; Rivard, E. Application of the Donor–Acceptor Concept to Intercept Low Oxidation State Group 14 Element Hydrides using a Wittig Reagent as a Lewis Base. *Inorg. Chem.* **2014**, *53*, 8662–8671.

(5) Sen, S. S.; Hey, J.; Herbst-Irmer, R.; Roesky, H. W.; Stalke, D. Striking Stability of a Substituted Silicon(II) Bis(trimethylsilyl)amide and the Facile Si−Me Bond Cleavage without a Transition Metal Catalyst. *J. Am. Chem. Soc.* **2011**, *133*, 12311–12316.

(6) Transue, W. J.; Yang, J.; Nava, M.; Sergeyev, I. V.; Barnum, T. J.; McCarthy, M. C.; Cummins, C. C. Synthetic and Spectroscopic Investigations Enabled by Modular Synthesis of Molecular Phosphaalkyne Precursors. *J. Am. Chem. Soc.* **2018**, *140*, 17985–17991.

(7) Hans, M.; Lorkowski, J.; Demonceau, A.; Delaude, L. Efficient synthetic protocols for the preparation of common N-heterocyclic carbene precursors. *Beilstein J. Org. Chem.* **2015**, *11*, 2318–2325.

(8) Gómez-Suárez, A.; Ramón, R. S.; Songis, O.; Slawin, A. M. Z.; Cazin, C. S. J.; Nolan, S. P. Influence of a Very Bulky N-Heterocyclic Carbene in Gold-Mediated Catalysis. *Organometallics* **2011**, *30*, 5463–5470.

(9) Geeson, M. B.; Transue, W. J.; Cummins, C. C. Organoiron- and Fluoride-Catalyzed Phosphinidene Transfer to Styrenic Olefins in a Stereoselective Synthesis of Unprotected Phosphiranes. *J. Am. Chem. Soc.* **2019**, *141*, 13336–13340.

(10) Fulmer, G. R.; Miller, A. J. M.; Sherden, N. H.; Gottlieb, H. E.; Nudelman, A.; Stoltz, B. M.; Bercaw, J. E.; Goldberg, K. I. NMR Chemical Shifts of Trace Impurities: Common Laboratory Solvents, Organics, and Gases in Deuterated Solvents Relevant to the Organometallic Chemist. *Organometallics* **2010**, *29*, 2176–2179.

(11) Nattmann, L.; Cornella, J. Ni($^{4\text{-tBu}}$stb)$_3$: A Robust 16-Electron Ni(0) Olefin Complex for Catalysis. *Organometallics* **2020**, *39*, 3295–3300.

(12) Goldwhite, H.; Rowsell, D.; Vertal, L. E.; Bowers, M. T.; Cooper, M. A.; Manatt, S. L. Nuclear magnetic resonance of phosphorus compounds: 9—The NMR spectra of phosphirane. *Org. Magn. Reson.* **1983**, *21*, 494–500.

(13) Deschamps, B.; Ricard, L.; Mathey, F. Preliminary chemical and structural study of (1-chlorophosphirane)pentacarbonyltungsten. *Polyhedron* **1989**, *8*, 2671–2676.

(14) Hao, Y.; Zhang, C.; Mei, Y.; Tian, R.; Duan, Z.; Mathey, F. The chemistry of parent phosphiranide in the coordination sphere of tungsten. *Dalton Trans.* **2016**, *45*, 8284–8290.

(15) Levy, G. C.; Komoroski, R. A. Paramagnetic relaxation reagents. Alternatives or complements to lanthanide shift reagents in nuclear magnetic resonance spectral analysis. *J. Am. Chem. Soc.* **1974**, *96*, 678–681.

(16) Sheldrick, G. M. SHELXT – Integrated space-group and crystal-structure determination. *Acta Cryst. A* **2015**, *71*, 3–8.

(17) Sheldrick, G. M. Crystal structure refinement with *SHELXL*. *Acta Cryst. C* **2015**, *71*, 3–8.

(18) Müller, P. Practical suggestions for better crystal structures. *Crystallogr. Rev.* **2009**, *15*, 57–83.

(19) Sheldrick, G. M. *CELL_NOW*; University of Göttingen: Germany, 2008.

(20) Neese, F. The ORCA Program System. *WIREs Comput. Mol. Sci.* **2012**, *2*, 73–78.

(21) Neese, F. Software Update: The ORCA Program System, Version 4.0. *WIREs Comput. Mol. Sci.* **2018**, *8*, e1327.

(22) Knizia, G. Intrinsic Atomic Orbitals: An Unbiased Bridge Between Quantum Theory and Chemical Concepts. *J. Chem. Theory Comput.* **2013**, *9*, 4834–4843.

(23) Becke, A. D.; Johnson, E. R. A Density-Functional Model of the Dispersion Interaction. *J. Chem. Phys.* **2005**, *123*, 154101.

(24) Grimme, S.; Ehrlich, S.; Goerigk, L. Effect of the Damping Function in Dispersion Corrected Density Functional Theory. *J. Comput. Chem.* **2011**, *32*, 1456–1465.

(25) Weigend, F.; Ahlrichs, R. Balanced Basis Sets of Split Valence, Triple Zeta Valence and Quadruple Zeta Valence Quality for H to Rn: Design and Assessment of Accuracy. *Phys. Chem. Chem. Phys.* **2005**, *7*, 3297–3305.

(26) Frisch, M. J. et al. Gaussian 16 Revision C.01. 2016; Gaussian Inc. Wallingford CT.

(27) Riplinger, C.; Sandhoefer, B.; Hansen, A.; Neese, F. Natural Triple Excitations in Local Coupled Cluster Calculations with Pair Natural Orbitals. *J. Chem. Phys.* **2013**, *139*, 134101.

(28) Riplinger, C.; Pinski, P.; Becker, U.; Valeev, E. F.; Neese, F. Sparse Maps−A Systematic Infrastructure for Reduced-Scaling Electronic Structure Methods. II. Linear Scaling Domain Based Pair Natural Orbital Coupled Cluster Theory. *J. Chem. Phys.* **2016**, *144*, 024109.

(29) Dunning, T. H. Gaussian basis sets for use in correlated molecular calculations. I. The atoms boron through neon and hydrogen. *J. Chem. Phys.* **1989**, *90*, 1007–1023.

(30) Neese, F.; Wennmohs, F.; Becker, U.; Riplinger, C. The ORCA Quantum Chemistry Program Package. *J. Chem. Phys.* **2020**, *152*, 224108.